

UNIVERSITY OF OKLAHOMA

GRADUATE COLLEGE

PRODUCTION OF ALKYL-AROMATICS FROM LIGHT OXYGENATES

OVER ZEOLITE CATALYSTS FOR BIO-OIL REFINING

A DISSERTATION

SUBMITTED TO THE GRADUATE FACULTY

in partial fulfillment of the requirements for the

Degree of

DOCTOR OF PHILOSOPHY

By

TRUNG Q. HOANG

Norman, Oklahoma

2010

PRODUCTION OF ALKYL-AROMATICS FROM LIGHT OXYGENATES  
OVER ZEOLITE CATALYSTS FOR BIO-OIL REFINING

A DISSERTATION APPROVED FOR THE  
SCHOOL OF CHEMICAL, BIOLOGICAL AND MATERIALS ENGINEERING

BY

---

Dr. Richard G. Mallinson, Chair

---

Dr. Daniel E. Resasco

---

Dr. Lance L. Lobban

---

Dr. Dimitrios V. Papavassiliou

---

Dr. Robert L. White

© Copyright by TRUNG Q. HOANG 2010  
All Rights Reserved.

## ACKNOWLEDGEMENTS

I would like to thank my parents, Hoang Quang Thuan and Phan Thi Kim Thanh, for loving and supporting me all my life. They are always encouraging me to pursue my dreams. I am indebted to them for their love and I would not be here today without them.

I would also like to thank my wife, Oat for always being on my side and encouraging me to achieve my goals. Without her constant loving support, I could not imagine how I can go through this journey.

Being abroad, I am so grateful and fortunate to have Dr. Mallinson as my advisor in both of my Master's and PhD's program at OU. I can't even begin to express how thankful I am for his constant assistance, encouragement, guidance and the tremendous support and opportunities he provided throughout my studies at OU. I am indebted for his patience, kindness and the motivation he provided to bring this dissertation to fruition.

I would especially like to express my deep appreciation for my Professors, Dr. Resasco and Dr. Lobban for their valuable discussions on my research that helped me gain insights and knowledge on the topics. I would also like to thank Dr. Tawan Sooknoi, Dr. Roberto Galiasso, Dr. Friederike Jentoft, and Dr. Rolf Jentoft for sharing their unique expertise in our group meeting discussion. I would like to thank my

committee members, Dr. Dimitrios Papavasiliou and Dr. Robert White for their valuable time and discussions at my General Exam and my Defense.

I would also like to thank all my fellows and friends at OU. Most of all I would like to thank Trung Pham for being a great friend since my first time I arrived at OKC airport and started a new life at OU. I would like to thank Uncle Larry and Miss Ha for their support our Vietnamese student group. During my time studying at OU, I have known and worked with many excellent students and post-docs that I would like to thank for their help and support: Xinli, Tanate, Grant, Huy, Phuong, Amalia, Veronica, Steven, Anirudh, Kyu, Air, Quincy, Martina, Giulio, Lyon, P'Auan, P'Khwan, Jeab, Meo, Pak, Mink, Sunya, and others.

Lastly, I would like to thank for tremendous helps from OU Chemical Engineering Department Staff: Terry and Vernita for always being there to explain me how to place order chemicals and equipment, Donna for answering and processing my paper works, and most of all, Alan for his excellent assistant for building my reactors, fixing equipment, and providing useful advices.

Thanks again to all of you, who have made my stay here in Norman a wonderful memory that I would never forget.

## TABLE OF CONTENT

### CHAPTER 1

INTRODUCTION .....	1
1.1. Overview .....	1
1.2. Selecting model compound and catalysts.....	5
1.3. Objectives and methodology .....	6
References .....	8

### CHAPTER 2

EXPERIMENTAL.....	11
2.1. Catalyst preparation.....	11
2.2. Catalytic measurement .....	12
2.3. Catalyst characterization .....	15
Acknowledgements .....	16
References .....	16

### CHAPTER 3

A COMPARISON OF THE REACTIVITIES OF PROPANAL AND PROPYLENE ON HZSM-5 .....	17
---	----

Abstract .....	17
3.1. Introduction .....	18
3.2. Experimental .....	20
3.2.1. Catalyst Preparation.....	20
3.2.2. Equipment and Procedures. ....	21
3.2.3. Product analysis.....	22
3.2.4. Characterization.....	22
3.3. Results.....	23
3.3.1. Characterization.....	23
3.3.3. Transient Conversion of Propanal. ....	32
3.3.4. Transient Conversion of Propylene. ....	38
3.4. Discussion .....	38
3.5. Conclusions .....	43
Acknowledgements .....	43
References .....	44
<b>CHAPTER 4</b>	
<b>EFFECTS OF HZSM-5 CRYSTALLITE SIZE ON STABILITY AND AROMATICS</b>	
<b>DISTRIBUTION FROM CONVERSION OF PROPANAL .....</b>	<b>47</b>
Abstract .....	47

4.1. Introduction .....	48
4.2. Experimental .....	49
4.2.1. Catalyst Preparation.....	49
4.2.2. Equipment and Procedures.....	50
4.2.3. Product analysis.....	50
4.3. Characterization .....	51
4.4. Results .....	51
4.4.1. Characterization.....	51
4.4.2. Catalyst activity .....	53
4.5. Discussion .....	59
4.6. Conclusions .....	62
Acknowledgements .....	63
References .....	63

## CHAPTER 5

A COMPARISON OF THE EFFECTS OF CHANNEL STRUCTURE OF ZEOLITES HZSM 5 AND 22 ON CONVERSION OF PROPANAL TO ISOALKENES AND AROMATICS .....	66
Abstract .....	66
5.1. Introduction .....	67



5.2. Experimental .....	69
5.2.1. Catalyst Preparation.....	69
5.2.2. Equipment and Procedures. ....	70
5.2.3. Product analysis.....	70
5.3. Characterization .....	70
5.4. Results .....	72
5.4.1 Characterization.....	72
5.4.2. Catalyst activity .....	72
5.4.3. Coke analysis of HZSM-22 and HZSM-5.....	78
5.4.4. Effect of water on catalyst activity .....	81
5.5. Discussion .....	81
5.6. Conclusions .....	85
Acknowledgements .....	86
References .....	86

## CHAPTER 6

CATALYTIC AROMATIZATION OF GLYCEROL FOR BIOFUELS .....	89
Abstract .....	89
6.1. Introduction .....	90
6.2. Experimental .....	92

6.2.1. Catalyst Preparation.....	92
6.2.2. Equipment and Procedures.....	93
6.3. Results .....	94
6.3.1. Activity and stability of the zeolites.....	94
6.3.2. Glycerol conversion on HZSM-5 & HZSM-22 at different W/F.....	99
6.3.3. Glycerol conversion on Pd/ZnO followed by HZSM-5.....	106
6.3.4. The effect of Zn-HZSM-5.....	110
6.4.1. Dehydration.....	112
6.4.2. Deoxygenation.....	112
6.4.3. Oligomerization.....	113
6.5. Conclusions .....	113
Acknowledgements .....	114
References .....	115
 CHAPTER 7	
CONCLUSIONS.....	118

## LIST OF TABLES

Table 3.1. Total acid density and Si/Al of zeolites	24
Table 3.3. Product distribution of propanal and propylene	28
Table 3.2. Product distribution of propanal and 2-methyl-2-pentene	27
Table 5.1 – Structure properties of HZSM-22 and HZSM-5	82
Table 6.1. Pore structure of zeolite catalysts use	95
Table 6.2. Products observed from glycerol conversion over HNaMOR, H-OMEGA, and HZSM-22 zeolite catalysts at 300 °C and 400 °C, W/F= 0.5h	96
Table 6.3. Products observed from HZSM-5 and HY zeolite catalysts at 300 °C and 400 °C, W/F= 0.5h	96
Table 6.4. Product distribution on different zeolites, T=400 °C, TOS=3 hrs, W/F= 0.5 hr, 300 psi	98
Table 6.5. Liquid product volume on single bed HZSM-5 and two beds PdZnO & HZSM-5, at 300 psi, T=400 °C, TOS=3 hrs, W/F= 0.5 hr	106

## LIST OF FIGURES

Figure 1.1 Global biofuel production from 2000 to 2007	2
Figure 1.2 European biodiesel production from 1998 to 2007	2
Figure 1.3 Annual global production of glycerol from 2002 to 2007	4
Figure 1.4 Example zeolite framework of HZSM-5 (left) and HY (right)	7
Figure 1.5 Illustration of reaction in zeolite.	7
Figure 2.1 Reactor system diagram and picture at atmospheric pressure and aromatic products shown in a vial.	14
Figure 3.1. IPA-TPD profiles propylene evolution of HZSM-5 (45) and HZSM-5 (25)	24
Figure 3.2. W/F series of propanal conversion on HZSM-5 (45) at 400 °C	26
Figure 3.3. W/F series of propylene conversion on HZSM-5 (25) at 500 °C	30
Figure 3.4. Pulse series of propanal on HZSM-5 (45) at different temperatures: a) 400 °C; b) 350 °C; c) 300 °C	33
Figure 3.5. Pulse series of propanal on HZSM-5 (45) at 400 °C	35
Figure 3.6. TPD of propanal on HZSM-5 (45) a) Pulse propanal at isothermal phase 250 °C; b) TPD phase from 250 °C – 600 °C at 10 °C/min ramp rate	37

Figure 3.7. Pulse series of propylene on HZSM-5 (25) a) At 400 °C; b) At 500 °C	39
Figure 3.8. Propose mechanism of TMB formation from propanal aldol trimer	41
Figure 3.9. Proposed pathway of propanal conversion	42
Figure 4.1. SEM of small (a) and large (b) crystallite HZSM-5 (Si/Al= 45)	52
Figure 4.2. Acidity profile of small and large crystallite HZSM-5 (Si/Al=45)	54
Figure 4.3. Effect of crystallite size on catalyst activity at different W/F and TOS at 400 °C	55
Figure 4.4. Effect of crystallite size on product distribution and conversion with TOS at 400 °C	57
Figure 4.5. Product yields versus conversion at 400 °C (combined TOS and W/F data), solid line (small crystallite), dash line (large crystallite)	58
Figure 4.6. Effect of crystallite size on p-xylene ratio as function of conversion for different W/F at TOS= 30 min	60
Figure 4.7. Effect of crystal size on C <sub>9</sub> /(C <sub>8</sub> +C <sub>7</sub> ) ratio as function of conversion for different W/F at TOS= 30 min	60
Figure 5.1. XRD (a) & SEM (b) of synthesized HZSM-22 and HZSM-5	73
Figure 5.2. Acidity profile of HZSM-5 and HZSM-22 (both with Si/Al=45)	73
Figure 5.3. Conversion vs. TOS HZSM-22 & HZSM-5 at 400 °C	75

Figure 5.4. W/F series of HZSM-5 & HZSM-22 at 400 °C and TOS=60 min	76
Figure 5.5. TOS of HZSM-5 & HZSM-22 at 400 °C	77
Figure 5.6. Product distribution as the function of conversion on HZSM-5 & HZSM-22, at 400 °C, with both data from TOS and W/F	79
Figure 5.7. TPO of HZSM-22 at W/F=1h & HZSM-5 at W/F=0.5h, TOS=2h %coke (HZSM-22) = 2.2%, %coke (HZSM-5) = 3.8%, Total coke (HZSM-22) = 1.10 mg/50mg CAT, Total coke (HZSM-5) = 1.98 mg/50mg CAT	80
Figure 5.8. Effect of water with propanal conversion on HZSM-22 & 5	83
Figure 6.1. The product selectivities of glycerol conversion over HZSM-5 as a function of W/F: (a) Polar phase and (b) Non-polar phase. Reaction conditions: T = 400 °C, P = 300 psi, (data taken offline)	100
Figure 6.2. W/F series (a) and TOS (b) of glycerol conversion on HZSM-5, 400 °C, atmospheric pressure (data taken online)	101
Figure 6.3. W/F (a) series and TOS (b) of glycerol conversion on HZSM-22, 400 °C, atmospheric pressure (data taken online)	103
Figure 6.4. TPO of glycerol conversion on HZSM-5 & HZSM-22, 400 °C, atmospheric pressure	105

Figure 6.5. Hydrocarbon product distribution in HZSM-5 and Pd/ZnO&HZSM-5,  
at 400 °C, 300 psi 108

Figure 6.6. (a) Glycerol conversion at various intervals between the samples  
(b) Percentage by volume of hydrocarbon phase at various intervals  
between the sample at 300 psi and 400 °C 109

Figure 6.7. (a) Percentage by volume of aromatics product on HZSM-5 and 5% wt Zn--  
ZSM-5 (b) Aromatic product distribution of HZSM-5 and 5% wt Zn-  
HZSM-5. 111

## ABSTRACT

Upgrading of light oxygenates derived from biomass conversion, such as propanal and glycerol, to more valuable aromatics for biofuels has been demonstrated on zeolite catalysts. Aromatics with a high ratio of  $C_9/(C_8+C_7)$  and little benzene are produced at much higher yield from oxygenates than from olefins at mild conditions over HZSM-5. It is proposed that  $C_9$  aromatics are predominantly produced via acid-catalyzed aldol condensation. This reaction pathway is different from the pathway of propylene and other hydrocarbon aromatization that occurs via a hydrocarbon pool at more severe conditions with major aromatic products  $C_6$  and  $C_7$ . In fact, investigation on the effect of crystallite size HZSM-5 has shown a higher ratio of  $C_9/(C_8+C_7)$  aromatics on small crystallite. This is due to faster removal of products from the shorter diffusion path length. As a result, a longer catalyst lifetime, less isomerization, and less cracking were observed on small crystallites. Beside crystallite size, pore geometry of zeolites was also found to significantly affect aromatic production for both conversion of propanal and glycerol. It is shown that the structure of the HZSM-22, with a one-dimensional and narrower channel system, restricts the formation of aromatics. In contrast, a higher yield of aromatic products is observed over HZSM-5 with its three-dimensional channel system. By increasing channel dimension and connectivity of the channels, increasing catalyst activity was also observed due to more accessible acid sites. It was also found that glycerol is highly active for



dehydration on zeolites to produce high yields of acrolein (propenal), a high value chemical. To maximize aromatics from glycerol conversion, HZSM-5 and HY were found to be effective. A two-bed reactor of Pd/ZnO and HZSM-5 was used to first deoxygenate/hydrogenate glycerol over Pd/ZnO to intermediate oxygenates that can further aromatize on HZSM-5. The end results are very promising with significant improvement in aromatic yield. Further improvement of aromatization and catalyst lifetime was also found with ZnHZSM-5 wherein the Zn evidently modifies the acidity. These model compound results show that the optimized use of zeolites for production of alkyl aromatics from light oxygenates at mild conditions may be effective for bio-oil refining.

# CHAPTER 1

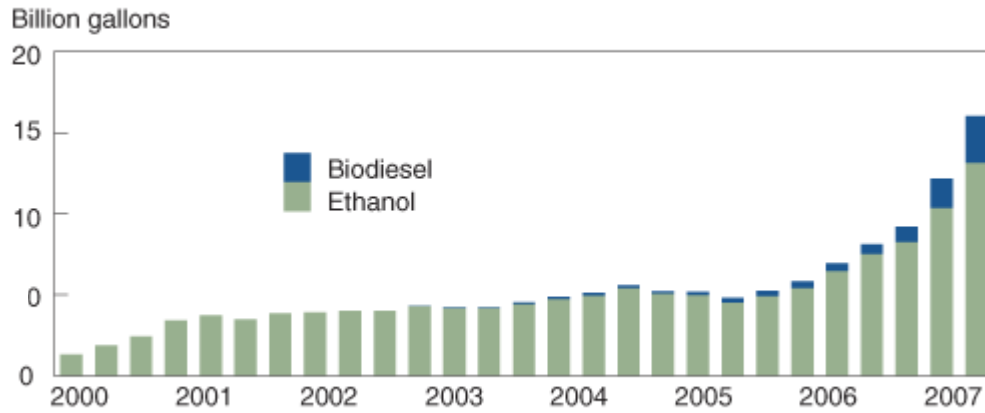
## INTRODUCTION

### 1.1. Overview

Biofuels is one of the key developments among other renewable energy initiatives to reduce fossil energy dependence, providing neutral CO<sub>2</sub> emissions, and contribute to the requirements of increasing energy consumption in the next several decades. In fact, it has been shown that in the next three decades, the projection for the U.S. transportation consumption will increase more than 50% and could reach 100% if the rate of consumption is the same for the 1980 – 2008 [1]. Rapid expansion of biofuel production has been seen in the last ten years. Indeed, as shown in Figure 1.1, the global production of mostly ethanol and some biodiesel has significantly increased from 3 to 15 billion gallons from 2000 to 2007 [2]. In addition, the “*Billion Ton Study*” has envisioned a feasible goal of 30% replacement of petroleum consumption by biofuels [3].

Conversion of biomass to fuels is mainly through two main strategies: (1) bio-conversion via fermentation to alcohol and (2) thermo-chemical with catalyst upgrading. The first strategy has been proven in ethanol production from sugar cane and corn, although there are several issues by using these feedstocks including little or no net reduction of CO<sub>2</sub> emissions, low energy efficiency, rising feedstock prices,

### Global biofuel production tripled between 2000 and 2007



Source: International Energy Agency; FO Licht.

Figure 1.1 – Global biofuel production from 2000 to 2007

### EU and Member States' Biodiesel Production (1000 tonnes)

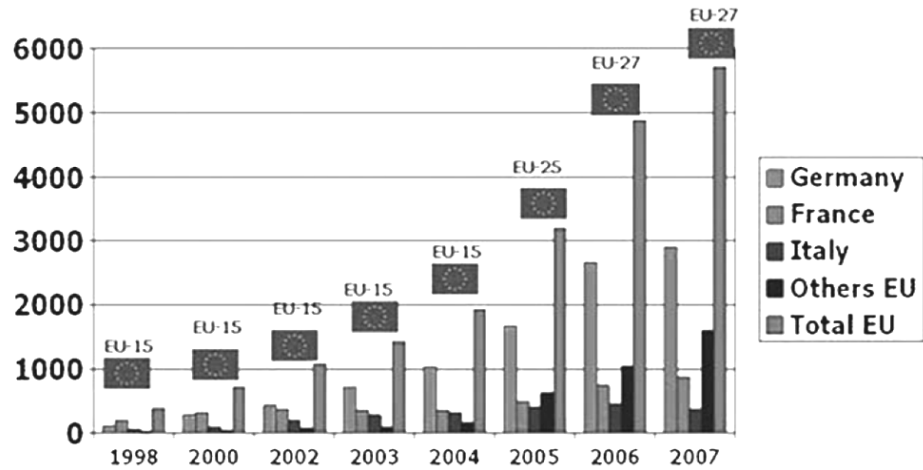


Figure 1.2 – European biodiesel production from 1998 to 2007

competition with food sources and high cost. Recent developments have focused on cellulosic ethanol from non-food source biomass that shows significant reduction of CO<sub>2</sub> emission by 85% and higher yield [4]. In the second strategy, biomass can be directly converted to synthesis gas CO, H<sub>2</sub>, CH<sub>4</sub>, C<sub>2</sub>H<sub>x</sub> by gasification processes with subsequent liquid fuel production or to liquid bio-oil by fast pyrolysis processes.

The bio-oil product from pyrolysis is a complex mixture of hundreds of compounds including aldehydes, ketones, acids, furans, phenols and other oxygenates as well as water, and thus has a low heating value [5-6]. The composition of bio-oil varies considerably depending on feedstock and reaction conditions (a range of composition might be: 54-58% C, 5.5-7% H, 35-40% O, and 0-0.2% N). Furthermore, they are thermally and chemically unstable and need to be converted to make them compatible with transportation fuels. For instance, acetaldehyde and propanal found in bio-oils can further oxidize to form corrosive acids or participate in polymerization reactions to form heavy products during storage and transportation. While small oxygenates are liquid, they tend to have high volatility and increase the vapor pressure of fuels. In contrast to hydrotreating [5-7] that converts the light oxygenates to gases, causes losses in liquid yield, and consumes valuable hydrogen, the conversion of light oxygenates via condensation and aromatization to larger, more stable molecules appears to be an attractive opportunity to enhance the liquid quality and yield.

Conversion of vegetable oil to biodiesel is another approach to utilize rich oil type of biomass resources such as canola, soy, corn, and others. In this process, fatty-

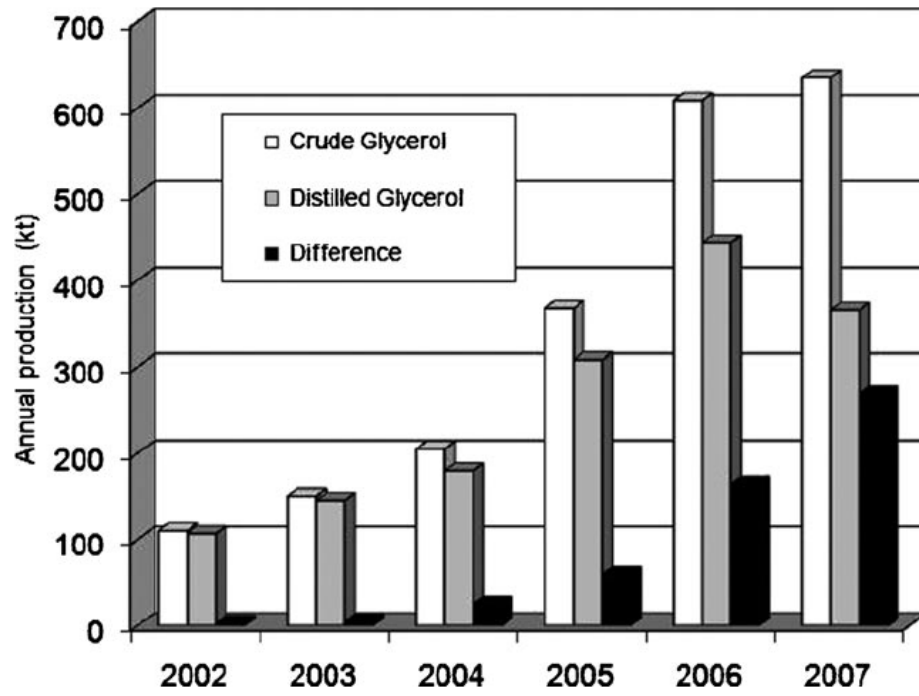


Figure 1.3 – Annual global production of glycerol from 2002 to 2007[8]

acid-methyl-esters (FAMES) are produced via a transesterification reaction of the original triglycerides with methanol. Although fuel from this type of biomass has been criticized because of using raw materials from food production, its production has progressively increased both in EU as shown in Figure 1.2 [9]. In the production of biodiesel, large amounts of glycerol are produced as a byproduct. Although glycerol and its derivatives are currently high value chemicals in the pharmaceutical and food industries among others, their volume from substantial increases of biodiesel production will greatly exceed the chemicals market. As shown in Figure 1.3, crude glycerol production reaches up to 600 kt in 2007[8]. In addition, the amount of unused impure crude glycerol, which is mostly burned, increased significantly from 0 in 2002 to 260 kt in 2007 as depicted in black column in the same figure. Glycerol can be reacted to produce chemical feedstocks, especially for production of acrolein (propenal) [8, 10-11]. However, there has been much less attention to the direct conversion of glycerol to fuel molecules that are compatible with existing fuels, such as gasoline.

## **1.2. Selecting a model compound and catalyst**

The complexity of bio-oil has created a great challenge in understanding reaction pathways and tailoring catalysts toward desirable fuel components. Thus, model compounds have been studied over different types of catalysts. e.g., metals[12], metal oxides[13-14] and zeolites[15-17]. Propanal is among the small aldehydes that can be

found in bio-oil light oxygenate components. Thus, it has been used as the model compound in this research.

Zeolites are crystalline microporous materials made of aluminosilicates with a well defined pore structure. More than 175 unique zeolite frameworks have been found[18]. They are commonly used as adsorbents, such as zeolite 3A for purifying ethanol from water or used as catalysts such as HY for FCC processes (fluidized-catalytic-cracking) or HZSM-5 for the MTG process (methanol-to-gasoline). Some examples of zeolite frameworks are shown in Figure 1.4 and the aromatization reaction of n-alkanes in a zeolite is illustrated in Figure 1.5. In fact, the reactions of aldehyde, ketone, acid, and furanic compounds on HZSM-5 have been extensively investigated [15-16] and in some of these studies substantial amounts of aromatics have been observed in the final products. Thus, in this research, HZSM-5 was chosen as the main zeolite catalyst for all the studies.

### **1.3 Objectives and methodology**

The objectives of this research are to understand the reaction pathways and the effects of different factors including catalyst properties and reaction conditions on the conversion of oxygenates to aromatics on acidic zeolites, particularly HZSM-5. From those results, one can find conditions and catalyst properties to maximize alkyl aromatics or selectively control product distribution for desirable applications. Alkyl

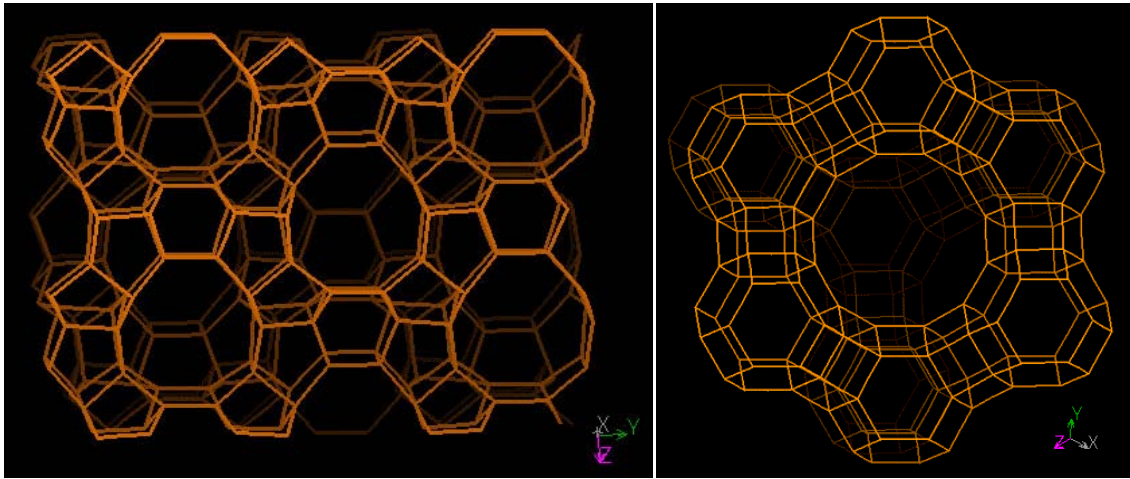


Figure 1.4 – Example zeolite framework of HZSM-5 (left) and HY (right)[18]

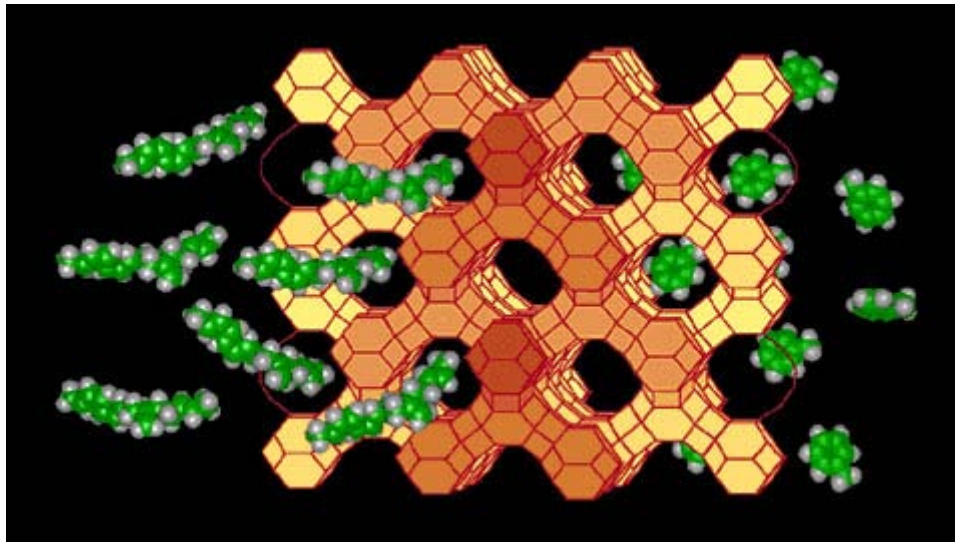


Figure 1.5 – Illustration of reaction in zeolite.[18]



aromatics make an excellent high octane, low vapor pressure blending component for gasoline. Benzene, however, is strictly regulated to very low levels and is undesirable. Aromatization from light hydrocarbons, typically produces significant benzene among the aromatics.

To achieve those objectives, a study of the reactions of propanal and propylene on HZSM-5 was conducted to study reaction pathways of aromatic formation from oxygenates and olefins. Chapter 2 is devoted to this subject, while in Chapter 3 the effect of catalyst properties on conversion of propanal was studied on different crystallite sizes of HZSM-5. Chapter 4 is the follow-up on the effect of pore structures by comparing the two zeolites HZSM-5 and HZSM-22. Finally, Chapter 5 gives an example of conversion of glycerol on different zeolites. From the understanding of reaction pathways, improvement of aromatic yield and catalyst performance can be achieved by combination of Pd/ZnO and HZSM-5 as well as by modified HZSM-5 incorporating Zn to alter the nature of the acid sites.

## **References**

- [1] EIA. 2010. Annual Energy Outlook 2010.
- [2] USDA. 2007. The Future of Biofuels: A Global Perspective.
- [3] DOE, and USDA. 2005. The Billion Ton Vision.
- [4] Wikipedia. Cellulosic Ethanol.

- [5] D. Mohan, C.U. Pittman, and P.H. Steele, *Energy & Fuels* 20 (2006) 848-889.
- [6] S. Czernik, and A.V. Bridgwater, *Energy & Fuels* 18 (2004) 590-598.
- [7] R. Maggi, and B. Delmon, *Hydrotreatment and Hydrocracking of Oil Fractions* 106 (1997) 99-113.
- [8] B. Katryniok, S. Paul, M. Capron, and F. Dumeignil, *Chemsuschem* 2 (2009) 719-730.
- [9] E.E. Commission. <http://epp.eurostat.ec.europa.eu/ion>.
- [10] K. Pathak, K.M. Reddy, N.N. Bakhshi, and A.K. Dalai, *Applied Catalysis A: General* 372 (2010) 224-238.
- [11] A. Corma, G.W. Huber, L. Sauvanauda, and P. O'Connor, *J Catal* 257 (2008) 163-171.
- [12] G.W. Huber, and J.A. Dumesic, *Catal Today* 111 (2006) 119-132.
- [13] E.L. Kunkes, E.I. Gürbüz, and J.A. Dumesic, *J Catal* 266 (2009) 236-249.
- [14] K.M. Dooley, A.K. Bhat, C.P. Plaisance, and A.D. Roy, *Appl Catal a-Gen* 320 (2007) 122-133.
- [15] A.G. Gayubo, A.T. Aguayo, A. Atutxa, R. Aguado, M. Olazar, and J. Bilbao, *Ind Eng Chem Res* 43 (2004) 2619-2626.
- [16] J.D. Adjaye, and N.N. Bakhshi, *Biomass Bioenerg* 8 (1995) 131-149.

- [17] J.L. Grandmaison, P.D. Chantal, and S.C. Kaliaguine, Fuel 69 (1990) 1058-1061.
- [18] IZA. International Zeolite Association, <http://www.iza-structure.org/databases/>.

## CHAPTER 2

### EXPERIMENTAL

#### 2.1. Catalyst preparation

A commercial HZSM-5 (Si/Al = 45) zeolite was supplied by Süd-Chemie, Inc. Other ZSM-5 samples were synthesized hydrothermally [1-2] using sodium aluminate (Aldrich) dissolved in deionized water as the Al source to which tetrapropylammonium hydroxide (Fluka, 20%) TPAOH) was first added under stirring as the structure directing agent, silica gel (Ludox, 40%) was then added dropwise while stirring, as the Si source. The resultant gel composition was 150 SiO<sub>2</sub>:1.0 Al<sub>2</sub>O<sub>3</sub>:8 TPAOH:1600 H<sub>2</sub>O (Si/Al=75). After stirring at 700 rpm for 10 h at room temperature, the gel was transferred to a Teflon-lined autoclave, where the zeolite crystallized at 180°C over 5 days with stirring at 60 rpm. The solid product was recovered by filtration, washed, dried at 110°C, and finally calcined in air at 550°C for 6 h to remove the template. The Si/Al ratio of the synthesized ZSM-5 sample was specified by modifying the amount of Al in the original recipe. The proton form of the zeolites was obtained from ion-exchange with NH<sub>4</sub>NO<sub>3</sub> at 80°C for 10 h. The process was repeated to completely replace the cations in the zeolite with NH<sub>4</sub><sup>+</sup>. The final synthesized HZSM-5 catalyst was obtained after drying at 100°C for 10 h and calcining at 600 °C for 3 h in dry air.

ZSM-22 was synthesized following the procedure described in [3]. Briefly,  $\text{Al}_2(\text{SO}_4)_3$  solution was mixed with KOH solution, to which hexamethyl enediamine solution was added. Then, silica gel solution was added. The incubation of the resultant gel was carried out at room temperature for 24 h at 500 rpm stirring. The crystallization was performed in an autoclave at 160 °C for 2 days with at 500 rpm stirring. The product was recovered by washing, filtering and calcination at 550 °C for 4 h in flowing air. The final HZSM-22 was obtained by the same method of ion-exchange described above.

## **2.2. Catalytic measurement**

The catalytic performance of the different catalyst samples was examined in a quartz reactor (1/4 inch o.d.) at atmospheric pressure, unless otherwise mentioned in each Chapter. The catalyst sample (40-60 mesh) was packed in the reactor between two layers of quartz wool. The thermocouple was affixed to the external wall of the reactor close to the catalyst bed. During pretreatment period, the temperature of the catalyst bed was increased to 400 °C using a rate of 10 °C/min and held constant at 400 °C for 1 h in flowing  $\text{H}_2$  (35 mL/min) before reaction. Liquid propanal or glycerol (from Aldrich) was fed using a syringe pump (kd scientific) equipped with a needle at a rate of 0.12 mL/min. The liquid was completely vaporized in the line before entering the reactor. All lines were kept at 300 °C to avoid condensation of reactant and products. The products were analyzed online using a gas chromatograph (GC 6890, Agilent) equipped with a flame ionization detector (FID). The effluent was trapped in

methanol using an ice-water bath, and analyzed using a QP2010s GC-MS (Shimadzu). Both GCs are equipped with an INNOWax capillary column. The reactor system was shown in Figure 2.1.

When operating at higher pressure, liquid products, including water, were collected in a cold trap after accumulating for each hour of time on stream. Non-condensed products passed through the back pressure regulator and went to vent and were not quantified, but some samples were sent to an online GC for product identification. After each run, the reactor was purged with dry carrier gas for 15 minutes to collect the residual products from the reactor. The collected liquid products were found to settle into two phases: a hydrocarbon phase containing aromatics and an aqueous phase containing the oxygenates with product water. Each phase was then individually analyzed using the same GCs described above.

Quantification of products was done by combination of GC-MS analysis and injection of known amounts of standard compounds. The space time (W/F) is defined as the ratio of catalyst mass (g) to organic mass flow rate (g/h). The different range of W/F was used in each, but in general was varied from 0.1 to 2 h. The propanal conversion and product yield were calculated based on mole of carbon.

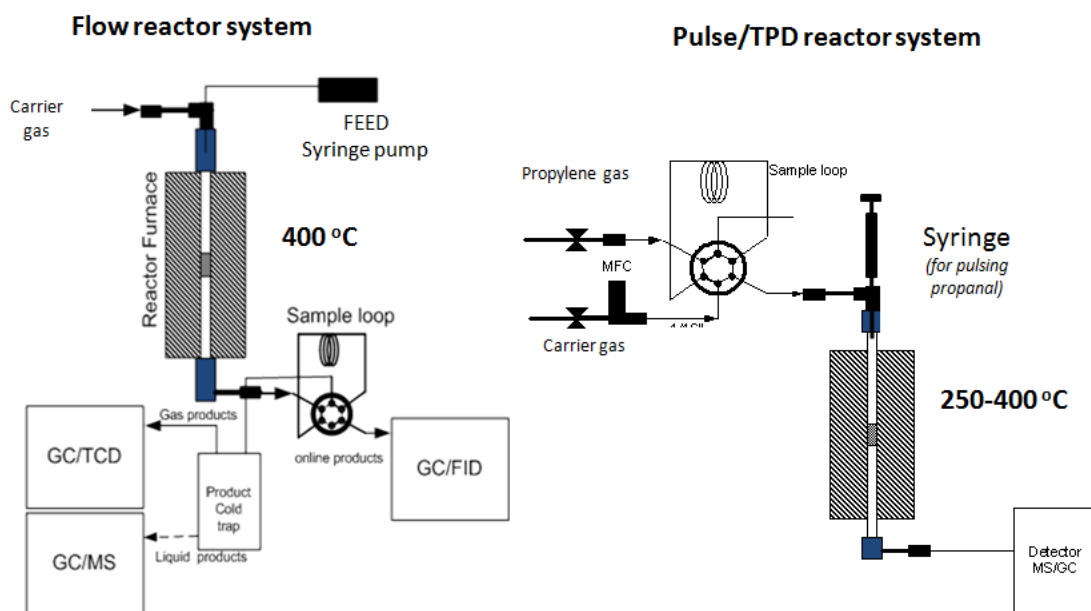


Figure 2.1 – Reactor system diagram and picture at atmospheric pressure and aromatic products shown in a vial.

### 2.3. Catalyst Characterization

Powder X-ray diffraction (XRD) patterns of the zeolite samples were recorded using a Bruker D8 Discover diffractometer. High resolution scanning electronic microscopy (SEM) observations were performed on gold-coated samples in a Jeol JSM-880 electron microscope equipped with X-ray elemental analyzer.

The acid properties of the various zeolites were characterized by temperature programmed desorption of isopropylamine (IPA-TPD), using a 1/4 in-diameter quartz reactor. Before each experiment, the zeolite sample (50 mg) was pretreated for 0.5 h in flowing He (30 mL/min) at 600°C to eliminate any adsorbed water. Then, the temperature was reduced to 100°C and the sample was exposed to IPA (5  $\mu$ L/pulse, 10 pulses, 3 min/pulse). After exposure to the adsorbate, He flowed for 0.5 h to remove weakly adsorbed IPA. To start the TPD, the temperature was increased to 650°C at a heating rate of 10°C/min. The evolution of desorbed species was continuously monitored by a Cirrus mass spectrometer (MKS) recording the following signals  $m/z=17$  and  $16$  ( $\text{NH}_3$ ),  $18$  ( $\text{H}_2\text{O}$ ),  $44$  (IPA), and  $41$  (propylene). The density of acid sites was quantified by calibrating the MS signals using the average of ten 100- $\mu$ L-pulses of propylene.

The amounts of coke deposits were quantified by temperature programmed oxidation (TPO) by passing a 2%  $\text{O}_2/\text{He}$  stream over a 20 mg spent catalyst sample, using a linear heating rate of 10°C/min. The signals of  $\text{H}_2\text{O}$  ( $m/z=18$ ),  $\text{CO}_2$  ( $m/z=44$ ), and  $\text{CO}$  ( $m/z=28$ ) were continuously monitored by MS. Quantification was calibrated on the basis of the signals from 100  $\mu$ L  $\text{CO}_2$  and  $\text{CO}$  pulses in flowing He.



## **Acknowledgements**

Author would like to thank Xinli, Grant, and Tanate for helps in preparing some of the catalysts using in this study.

## **References**

- (1) Argauer, R. J.; Landolt, G. R.; Mobil Oil Corporation; 1972; US Patent 3,702,886
- (2) Zhu, X.; Lobban, L.; Resasco, D.; Mallinson, R. J. Catal. 2010 (in press).
- (3) Robson, H. Verified syntheses of zeolitic materials; 2nd ed., 2001.

## CHAPTER 3

### A COMPARISON OF THE REACTIVITIES OF PROPANAL AND PROPYLENE ON HZSM-5

#### **Abstract**

The reactivities of propanal and propylene have been compared on HZSM-5 zeolites (Si/Al = 45 and 25). Propanal is found to be much more reactive than propylene and to form mostly 2-methyl-2-pentenal and C<sub>9</sub> aromatics as early products in the reaction network. Propylene, in contrast, requires more severe conditions to form C<sub>6</sub> and C<sub>7</sub> aromatics. It is proposed that propanal undergoes acid-catalyzed aldol condensation to form 2-methyl-2-pentenal. This dimer undergoes further condensation to form the aldol trimer, which subsequently dehydrates and cyclizes into C<sub>9</sub> aromatics. In contrast, it is well known that propylene, like other olefins, undergoes aromatization via oligomerization and formation of a hydrocarbon pool. While in the conversion of propanal, propylene is also produced, it appears that it does not play a major role in the formation of aromatics under conditions of shorter space times and lower temperatures, at which propanal produces aromatics in significant amounts.

*Keywords:* HZSM-5, aromatization, oxygenates conversion, aldehyde conversion, aldol condensation, deoxygenation, biofuels.

### 3.1. Introduction

Substantial production of oxygenates from biomass conversion and biodiesel production has generated growing interest in processes for upgrading these compounds to fuels and chemicals. Bio-oil production from fast pyrolysis of biomass has been estimated to have lower operating and capital costs compared to other biomass conversion processes [1-2]. Bio-oil contains large amounts of reactive oxygenated compounds with various functional groups including aldehydes, ketones, acids, and polyols. The composition of bio-oil varies considerably depending on feedstock and reaction conditions (a range of composition might be: 54-58% C, 5.5-7% H, 35-40% O, and 0-0.2% N) but contain large amounts of oxygenate species such as aldehydes, alcohols and acids., and thus has a low heating value [3,4]. Furthermore, these oxygenates are thermally and chemically unstable and need to be converted to make them compatible with transportation fuels [3-4]. For instance, acetaldehyde and propanal found in bio-oils can further oxidize to form corrosive acids or participate in polymerization reactions to form heavy products during storage and transportation. While small oxygenates are liquid, they tend to have high volatility and increase the vapor pressure of fuels. In contrast to hydrotreating [3-5] that converts the light oxygenates to gases, causes losses in liquid yield, and consumes valuable hydrogen, the conversion of light oxygenates via condensation and aromatization to larger, more stable molecules appears to be a an attractive opportunity to enhance the liquid quality and yield.

The complexity of bio-oil has created a great challenge in understanding reaction pathways and tailoring catalysts toward desirable fuel components. Thus, model compounds have been studied over different types of catalysts. e.g., metals, metal oxides, and zeolites. Reforming sugar/carbohydrate compounds from pretreated biomass, such as sorbitol, to produce synthesis gas and alkanes has been well demonstrated on metal catalysts by Dumesic et al. [6]. They have also proposed a strategy for making non-oxygenated diesel compounds, C<sub>9</sub>-C<sub>15</sub>, in sequential steps: dehydration, aldol condensation, and hydrodeoxygenation. At the same time, condensation of small aldehydes, acids, or ketones to form higher boiling point n- and iso- alkanes has been studied on metal oxide catalysts [7-8]. In contrast to noble metal and metal oxide catalysts, acidic zeolites [9-11] have the ability to directly convert oxygenates to primarily isoalkanes and aromatics in the gasoline boiling range.

HZSM-5 has been extensively studied for the conversion of methanol to hydrocarbons, in relation to the well-known MTG process (methanol-to-gasoline) [12], as well as other similar processes, such as the integrated gasoline synthesis process from Haldor Topsøe [13].

The reactions of aldehyde, ketone, acid, and furanic compounds on HZSM-5 also have been extensively investigated [9-11, 14]. In these studies substantial amounts of aromatics have been observed in the final products. In general, the most widely accepted aromatization pathway is that oxygenates are first converted to olefins and these are then oligomerized and dehydrocyclized to form aromatics [9]. Other

studies have found that greater aromatization activity is observed with propanal compared to other C<sub>3</sub> oxygenates such as ketone, alcohol, acid, or ester [14-16]. Similarly, researchers from our group have found that aromatics are produced to a much greater extent when starting from methyl-octanoate than when starting from n-octane [17-18]. They have proposed that aromatics are produced from the direct ring closure of an oxygenated intermediate keeping the original carbon chain, rather than via cracking / oligomerization / cyclization.

Therefore, it appears important to conduct a direct side-by-side comparison of the reactivity of a simple aldehyde and the corresponding olefin to determine whether they follow different reaction paths or they go through a common path. In this contribution, we report the results of the propanal conversion to aromatics in comparison with the conversion of propylene, obtained on two HZSM-5 catalysts under identical reaction conditions.

## **3.2. Experimental**

### *3.2.1. Catalyst Preparation.*

A commercial HZSM-5 (Si/Al = 45) zeolite was supplied by Süd-Chemie, Inc. Another ZSM-5 sample was synthesized in-house following a synthesis method described elsewhere [19]. The Si/Al ratio of the synthesized ZSM-5 sample was specified to be 25 by modifying the amount of Al in the original recipe. The proton form of the zeolites was obtained from ion-exchange with NH<sub>4</sub>NO<sub>3</sub> at 80°C for 10 h.

The process was repeated to completely replace the cations in the zeolite with  $\text{NH}_4^+$ . The final synthesized HZSM-5 catalyst was obtained after drying at  $100^\circ\text{C}$  for 10 h and calcining at  $600^\circ\text{C}$  for 3 h in dry air. The two zeolite samples used in this work are identified as HZSM-5(45) and HZSM-5(25), corresponding to the commercial HZSM-5 (Si/Al = 45) and the in-house synthesized HZSM-5 (Si/Al = 25), respectively.

### 3.2.2. Equipment and Procedures.

The continuous flow reactor used in the catalytic measurements was a 1/4" outside diameter, quartz tube fixed bed reactor. The reactor was heated in a split-tube furnace (Thermal Craft) with a digital feedback temperature controller (Omega). Before each run, the catalyst was treated *in situ* with  $\text{H}_2$  (35 sccm) for 1 h at  $400^\circ\text{C}$ . Propanal, obtained from Sigma-Aldrich, was fed into the reactor by using a syringe pump (KD Scientific) at a constant flow rate of 0.12 ml/h. Ultra high purity propylene was obtained from Airgas. The reactions were carried out at atmospheric pressure in flowing  $\text{H}_2$  at different space times (weight of catalyst to organic mass feed rate ratio: W/F).

In the pulse experiments, the same diameter quartz tube was used as in the continuous flow configuration. The catalyst was pretreated with the same procedure mentioned above. Liquid propanal was introduced into the reactor in 5  $\mu\text{l}$  (liquid) pulses using a GC syringe (Hamilton 10 $\mu\text{l}$ ). Propylene was introduced into the system using a 6-port valve with a 5 ml sample loop. For temperature programmed reaction-desorption experiments, propanal was pre-adsorbed by sending twenty 5  $\mu\text{l}$  pulses at

250 °C. After flushing with He, the reactor was heated up to 600 °C with a ramp rate 10 °C/min.

### *3.2.3. Product analysis.*

Every 30 min on stream, products were analyzed online by GC/FID (HP6890). The products were sampled using a 6-port valve with a 250 µl sample loop heated to 290 °C. After each run, the reactor was purged with pure He for 15 min to collect the residual products that desorb from the catalyst bed. The liquid products collected in solvent methanol were then identified by GC/MS (Shimadzu Q-2010). Both GCs are equipped with HP-INNOWax columns. In the pulse experiments, the products were analyzed by a mass spectrometer (MS) detector (MKS Cirrus 200).

### *3.2.4. Characterization.*

The commercial and in-house synthesized HZSM-5 samples were characterized by X-ray powder diffraction (Bruker D8 Discover) and scanning electron microscopy (SEM) to confirm the crystal structure and determine the morphology and crystallite size of the zeolites. The acidity of the HZSM-5 was determined by temperature programmed desorption (TPD) of iso-propyl amine (IPA) in a quarter inch quartz tube reactor with 50 mg of catalyst connected to an online MS detector (MKS Cirrus 200). Before each TPD run, the sample was pretreated in He at 400 °C for 1 h and then cooled down to 100 °C. The IPA adsorption was carried out by injecting four liquid pulses of IPA (4 µl each pulse) over the sample in He at 100 °C, at 2.5 min intervals. The catalyst was then flushed in He flow for 30 min at 100 °C and the TPD was started, using a temperature ramp of 10 °C/min up to 650 °C.

The MS signals of  $m/z$  44 (IPA), 41 (propylene), 17 (ammonia), 18 (water), 16 (fragment of ammonia) were monitored. The signals were calibrated with a 5 ml loop of 2 wt% ammonia in He.

### **3.3. Results**

#### *3.3.1. Characterization.*

The XRD pattern of the synthesized HZSM-5 sample is in agreement with those reported in the literature[12]. The SEM results show that the synthesized sample has a crystallite size of 1-2  $\mu\text{m}$ , significantly larger than the commercial HZSM-5 (100-150 nm).

The TPD profiles of the commercial HZSM-5(45) and synthesized HZSM-5(25) in Figure 3.1 show the evolution of propylene from adsorbed IPA with a maximum at about 350  $^{\circ}\text{C}$ . It has been suggested that the decomposition of adsorbed IPA is catalyzed by strong Brønsted sites and therefore the amount of propylene desorbed can be directly related to the density of Brønsted acid sites [20-21].

The calculated Si/Al ratios of the samples were obtained from elemental analysis in SEM by EDX. The summary of the physical properties of the HZSM-5(45) and HZSM-5(25) samples are shown in Table 3.1.



Table 3.1. Total acid density and Si/Al of zeolites

Zeolite	Si/Al <sup>a</sup>	Acidity <sup>b</sup> (mmol/g)
HZSM-5 (25)	25	0.421
HZSM-5 (45)	53	0.330

<sup>a</sup>Si/Al ratio calculated from elemental analysis in SEM by EDX

<sup>b</sup>Brønsted acid density derived from IPA-TPD

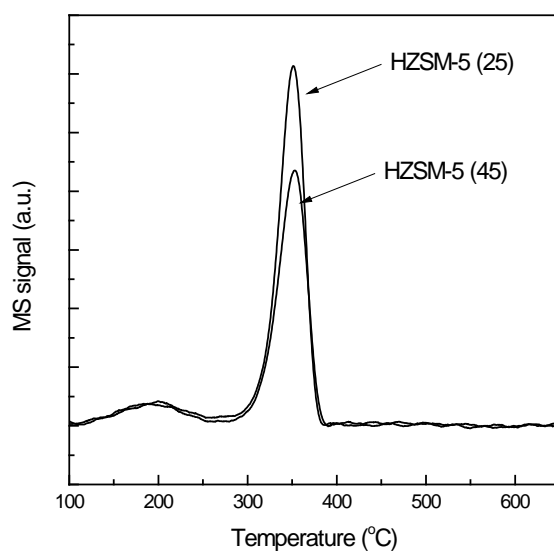


Figure 3.1. IPA-TPD profiles propylene evolution of HZSM-5 (45) and HZSM-5 (25)

### 3.3.2. Conversion of Propanal and Propylene in a Steady Flow Reactor

Propanal was converted to aromatics (C<sub>6</sub>-C<sub>9</sub>), gas (C<sub>1</sub>-C<sub>3</sub>), and isoalkenes (C<sub>4</sub>-C<sub>9</sub>) on HZSM-5 (45) at 400°C. The variation of product yields with space time (W/F) are shown in Figure 3.2 over the range of 0.07-0.25 h for data taken after 1 h on stream. In this range, the propanal conversion ranged from 59.5% to 99.8%. Aromatics and gas (C<sub>1</sub>-C<sub>3</sub>) yields increased more rapidly compared to the isoalkenes (C<sub>4</sub>-C<sub>9</sub>) yield as W/F increased. In fact, aromatics were always observed as major products even at the shortest W/F studied. In this range of W/F, the highest yield of aromatics was 51.9% obtained at 0.25 h W/F. The second major products were gases (C<sub>1</sub>-C<sub>3</sub>) of which the majority was propylene. The isoalkenes (C<sub>4</sub>-C<sub>9</sub>) were always relatively minor products.

A separate experiment under the same conditions as those used for propanal conversion, was conducted feeding 2-methyl-2-pentene to determine its propensity for further reaction and aromatics formation. The results showed that this isoalkene is reactive, forming only propylene and other isoalkenes, but did not form aromatics. These results are summarized in Table 3.2.

Conversion of propylene was performed at the same temperature, 400 °C, as the propanal experiments but to longer space times, up to W/F=4 h. However, the level of conversion with this feed was much lower and only traces of aromatics were obtained (<1%), as shown in Table 3.3. This result indicates that these reaction conditions are insufficient for the reaction to proceed through the intermediate steps typically observed at higher temperature, in which aromatization occurs via

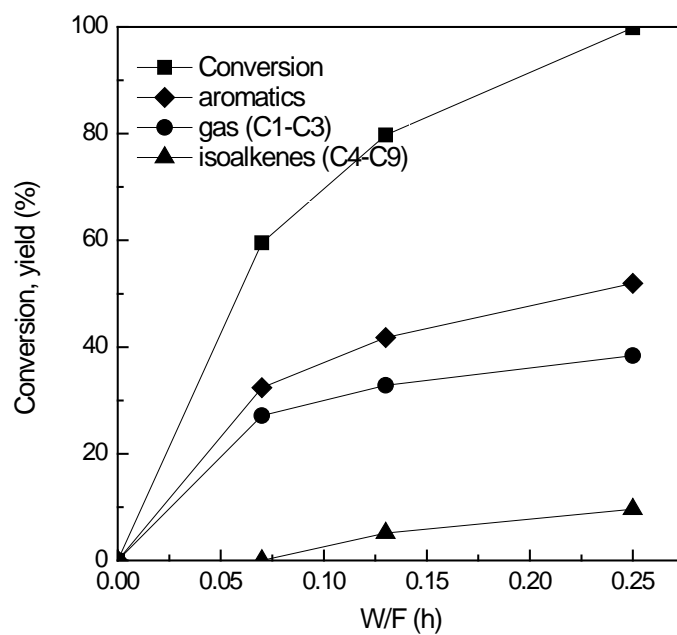


Figure 3.2. W/F series of propanal conversion on HZSM-5 (45) at 400 °C

Table 3.2. Product distribution of propanal and 2-methyl-2-pentene

Feed	Propanal	2-methyl-2-pentene
Conditions	W/F=0.2 h HZSM-5 (45) 400 °C	W/F =0.2 h HZSM-5 (45) 400°C
TOS (min)	60	60
Conversion	94.4	96.0
Gas (C <sub>1</sub> -C <sub>3</sub> )	37.8	44.6
isoalkenes (C <sub>4</sub> -C <sub>9</sub> )	5.5	51.4
Aromatics	51.1	-
C6 (Benzene)	0.1	-
C7 (Toluene)	10.3	-
C8 (Xylene)	13.1	-
C9 (MEB&TMB)	20.2	-
C10+	7.3	-

Table 3.3. Product distribution of propanal and propylene

Feed	Propanal				Propylene			
	W/F=0.07 h HZSM-5 (45) 400 °C		W/F =0.13 h HZSM-5 (45) 400 °C		W/F =4 h HZSM-5 (45) 400°C		W/F =4h HZSM-5 (25) 500°C	
TOS (min)	60	150	60	150	60	150	60	150
Conversion	52.5	39.4	76.3	56.8	42.4	41.0	65.6	64.4
Gas (C <sub>1</sub> -C <sub>3</sub> ) isoalkenes (C <sub>4</sub> -C <sub>9</sub> )	27.0	22.5	32.2	29.9	-	-	38.4	36.6
Aromatics	25.9	16.8	40.7	25.8	0.7	0.5	17.5	17.2
C6 (Benzene)	0.0	0.0	1.0	0.0	0.3	0.3	3.5	3.5
C7 (Toluene)	4.2	2.4	6.9	4.2	0.2	0.1	9.0	9.0
C8 (Ethyl- benzene)	0.8	0.5	1.3	0.9	-	-	0.2	0.2
C8 (p-Xylene)	2.7	1.5	3.8	2.4	0.2	0.1	1.3	1.3
C8 (m-Xylene)	2.3	1.4	3.9	2.5	-	-	2.6	2.5
C8 (o-Xylene)	2.1	2.2	1.5	2.3	-	-	1.0	0.9
C9	11.2	7.1	15.5	10.6	-	-	-	-
C10+	2.5	1.7	6.3	2.9	-	-	-	-
C9/others	0.93	0.89	0.84	0.86	-	-	-	-

oligomerization of olefins. In order to obtain significant yields of aromatics from propylene, a synthesized HZSM-5 with a higher acid density (Si/Al=25) was used and operated at a higher temperature of 500 °C and longer W/F. Table 3.3 shows that the propylene conversion under these severe conditions and with a much more active catalyst can reach a similar range to that obtained with propanal conversion. Only in this case, the aromatics yield from propylene becomes significant. These results are summarized in Figure 3.3. At short W/F, in contrast to the behavior observed with propanal, the major products are alkenes and light gases C<sub>1</sub>-C<sub>2</sub>. At longer W/F, yields of both aromatics and light gases continued to increase while the yield of alkenes reached a maximum and then declined. This trend suggests that the alkenes were consumed to produce more aromatics as well as cracking products. This behavior has been extensively reported in the literature for the aromatization of alkanes [22-23]. An interesting point is that aromatics formation with propanal was much higher than that from propylene. For example, at a similar conversion level (~60%), only 10% aromatic yield was obtained in comparison to 30% obtained with propanal. Understandably, at the severe conditions used in the propylene experiments, the extent of cracking is much greater.

The aromatic product distribution at 60 min and 150 min time on stream (TOS) for both the propanal and propylene experiments are summarized in Table 3.3. The conditions were adjusted so that in both cases the conversions were in about the same range. It is clearly seen that propanal yields larger amounts of heavier aromatics and much lower amounts of C<sub>6</sub> (benzene) and C<sub>7</sub> (toluene) compared to those from

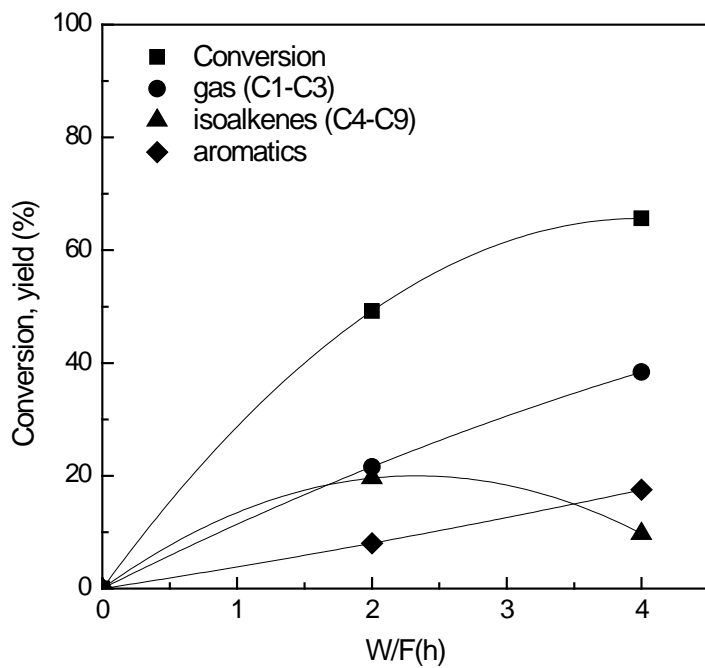


Figure 3.3. W/F series of propylene conversion on HZSM-5 (25) at 500 °C

propylene. That is, C<sub>8</sub> (xylene), C<sub>9</sub> (trimethylbenzene (TMB) and methylethylbenzene (MEB)), and C<sub>10+</sub> aromatics were observed as products from propanal but not from propylene at this conversion level. Because the distribution of aromatics produced from propanal appears to be different than those produced from propylene, transient pulse reaction experiments were performed for both propylene and propanal at the reaction conditions used in their respective steady flow experiments in order to better see the evolution of the product distributions through to the formation of the aromatics.

One difference in reaction conditions between experiments feeding propanal or propylene is the presence of water. The conversion of propanal, either via dehydration or aldol pathways, results in the formation of an equimolar amount water. In pyrolysis, it is also known that substantial amounts of water are produced and may be expected to be present in catalytic conversion of bio-oil and its oxygenate fractions. Therefore the effect of water on the catalysis may be an important consideration. An experiment was conducted with propanal as the feed in which water was injected part way through the run, injected for a period of time, and then stopped while the experiment was continued. The result showed that during the period when water was being injected, activity was reduced. After the water addition was stopped, the activity returned to a comparable level as if the water had never been injected.



### 3.3.3. Transient Conversion of Propanal.

The pulse reactor was loaded with 10 mg of HZSM-5 (45) and pretreated at 400 °C in He at a flow rate of 30 sccm. Propanal was introduced into the reactor, at 400 °C by injecting consecutive 5 $\mu$ l pulses until the catalyst was deactivated. This point was determined by observing the increase in the unreacted propanal peak size until it remained constant. The online MS detector was set to monitor the following signals: m/z 18 (Water), m/z 28 (C<sub>2</sub>H<sub>4</sub> and CO), m/z 41 (Propylene and fragment from the Dimer), m/z 58 (Propanal), m/z 78 (C<sub>6</sub>-B), m/z 92 (C<sub>7</sub>-T), m/z 98 (C<sub>6</sub> Dimer: 2-methyl-pentenal), m/z 105 (C<sub>9</sub>: TMB and MEB), m/z 106 (C<sub>8</sub>: xylene), m/z 138 (C<sub>9</sub> Trimer: dimethyl-heptenal). A reference sample containing all the aromatics in equal volumes, showed that the MS responses for C<sub>8</sub> and C<sub>7</sub> were somewhat higher than C<sub>9</sub>, but no attempt at calibration was made. The products obtained were consistent with the flow reactor results mentioned above. As shown in Figure 3.4a, the largest signals were primarily C<sub>9</sub> (TMB and MEB) and C<sub>8</sub> (X), less C<sub>7</sub> (T), and traces of C<sub>6</sub> (B). As the number of propanal pulses increased, catalyst deactivation was evidenced by a decrease in the size of the product peaks and an increase in the propanal peak. The water signal was reduced but did not completely disappear. In addition, the dimer (D) product was detected only in the last few pulses as deactivation proceeded, although the signal was small. The products from the first pulse showed a mixture of aromatics from C<sub>6</sub>-C<sub>9</sub> with the C<sub>8</sub> (X) and C<sub>9</sub> aromatics more pronounced compared to C<sub>6</sub> (B) and C<sub>7</sub> (T). As deactivation proceeded, it appears that C<sub>9</sub> and the dimer, were the only significant products observed at lower conversion. It also was observed that the ratio

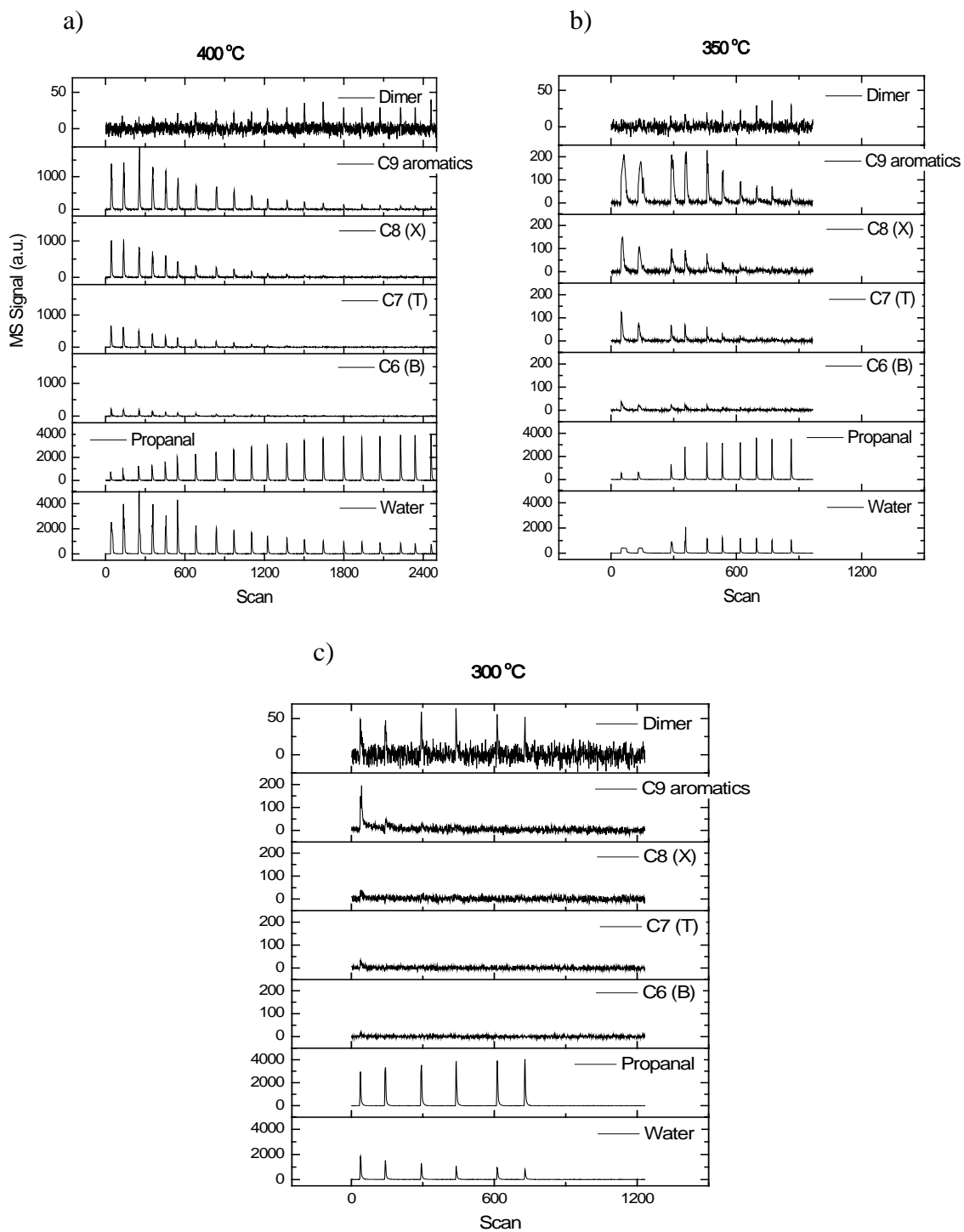


Figure 3.4. Pulse series of propanal on HZSM-5 (45) at different temperatures:  
a) 400 °C; b) 350 °C; c) 300 °C

of C<sub>9</sub> to C<sub>8</sub> aromatics increased as the catalyst deactivated, as shown in Figure 3.5. This trend suggests that aldol dimerization and then aromatization of an aldol trimer may be the initial pathway for aromatics formation under these mild conditions, as has been shown on other acidic systems [24-25]. When C<sub>9</sub> (TMB) was pulsed into the system at this temperature, a mixture of aromatics: C<sub>7</sub> (T), C<sub>8</sub> (X), C<sub>9</sub> (TMB), but no C<sub>6</sub>, was observed. With increasing number of pulses of TMB, deactivation occurred accompanied by a decrease in the amount of lighter aromatics. This experiment also showed that at 400 °C in this system, there are certainly cracking reactions taking place.

The same experiments were performed at lower temperatures, 350 °C and 300 °C with the results shown in Figures 3.4b and 3.4c. Much lower signals for products and much higher propanal signals show the decreased conversion obtained at the lower temperatures. A significantly higher C<sub>9</sub> aromatics signal was observed compared to those for C<sub>8</sub> (X), C<sub>7</sub> (T), C<sub>6</sub> (B), with a much higher ratio than at 400 °C. As the catalyst deactivates, the C<sub>9</sub> aromatics again become the dominant aromatic product. At even lower temperatures, i.e. 300 °C, C<sub>9</sub> aromatics appeared as the only major aromatic product but rapid deactivation occurred. In contrast to the results obtained at higher temperature, the dimer product was observed with the first pulses but not in the subsequent ones. The results at lower temperatures also suggest that as the conversion is lowered and the contribution from cracking decreases, the observed products are those expected as initial products from the aldol pathway, while the

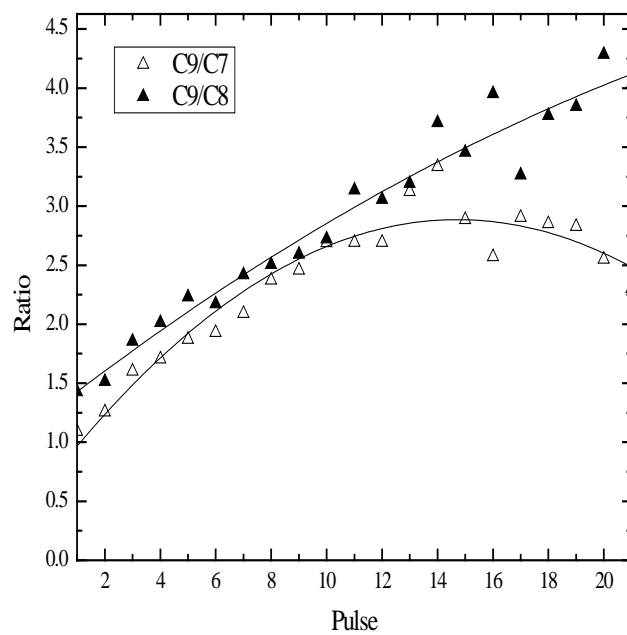


Figure 3.5. Pulse series of propanal on HZSM-5 (45) at 400 °C

lighter aromatics may result mostly from secondary cracking reactions of heavier aromatics.

A temperature programmed reaction-desorption experiment was conducted under the pulse reactor conditions. First, 20 pulses of propanal (5  $\mu$ l) were injected over the catalyst while keeping the temperature at 250 °C; then, the temperature was increased with a linear heating ramp of 10 °C per min. During the isothermal period at 250 °C shown in Figure 3.6a, the dimer and C<sub>9</sub> aromatics were the only products observed until the catalyst deactivated. With later pulses, while the dimer continued to appear, production of aromatics rapidly decreased, as shown by the disappearance of the C<sub>9</sub> aromatic peak. This trend suggests that while the weaker acid sites and even the Lewis acids may catalyze the aldol condensation of propanal to form the dimer (2-methyl-pentenal), stronger Brønsted acid sites, which are the first to deactivate, are required for the cyclization and dehydration steps required to produce C<sub>9</sub> aromatics.

After the isothermal pulse injections, He was allowed to flow for 10 min before the temperature ramp was started. As shown in Figure 3.6b, water along with significant amounts of C<sub>9</sub> aromatic appeared concurrently during the 316-330 °C range. Smaller peaks of C<sub>8</sub> (X) and C<sub>7</sub> (T) were also observed. This evolution of products suggests that some adsorbed intermediates are converted to the C<sub>9</sub> aromatics at higher temperature. The fact that water was produced along with formation of the C<sub>9</sub> aromatics points at the participation of a step involving the dehydration of an oxygenated intermediate. This is consistent with an aldol pathway forming a cyclic trimer oxygenate, which could be a precursor to aromatics.

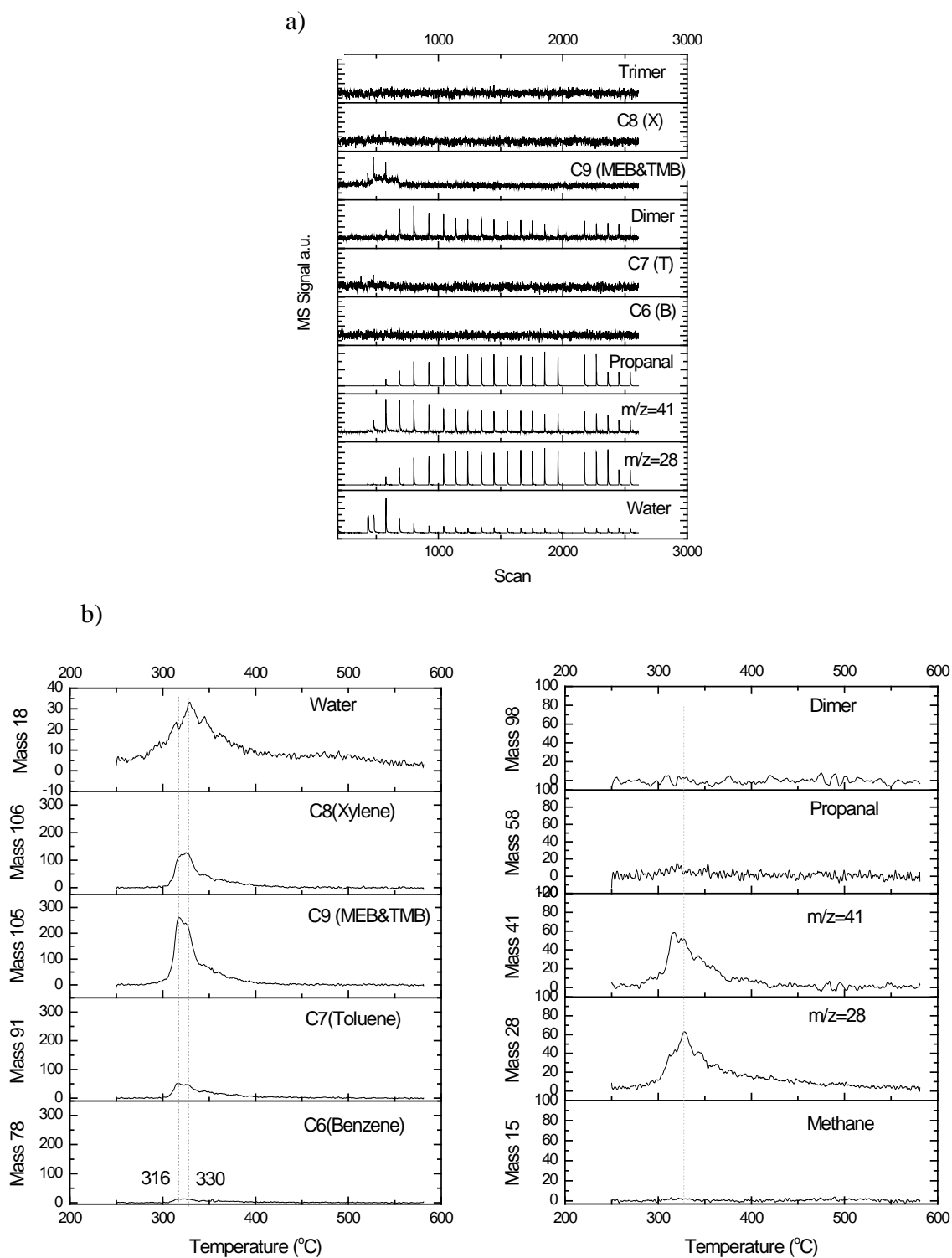


Figure 3.6. TPD of propanal on HZSM-5 (45) a) Pulse propanal at isothermal phase 250 °C; b) TPD phase from 250 °C – 600 °C at 10 °C/min ramp rate

### *3.3.4. Transient Conversion of Propylene.*

For the propylene pulse experiments, the same reactor system described above was used. The first experiment was conducted with 200 mg of the commercial HZSM-5 (45) at a temperature of 500 °C. No conversion to aromatics was observed under these conditions. In the second experiment, 200 mg of the synthesized HZSM-5 (25) and a temperature of 500 °C were employed. As shown in Figure 3.7, propylene was converted to C<sub>6</sub> (B) and C<sub>7</sub> (T) aromatics as the major products and only a small amount of C<sub>8</sub> (X) and C<sub>9</sub> aromatics were observed. This result is consistent with those observed in the flow reactor described above. This result further confirms that the initial aromatic formed from propylene conversion is C<sub>6</sub> (B), but that propylene does not convert to aromatics at 400 °C on HZSM-5 with a Si/Al of 45, in marked contrast with propanal.

## **3.4. Discussion**

It is well established that aromatization of propane proceeds via alkene intermediates yielding benzene as a primary aromatic product [22-23]. Other aromatics and light alkanes are the products of subsequent alkylation, diproportionation, and cracking reactions from a surface hydrocarbon pool [26-27]. The results observed in this contribution for the propylene conversion are in good agreement with these concepts. However, the results from the propanal conversion studies show much higher aromatization activity at milder reaction conditions and a significant difference in the initial aromatic product distribution compared to the

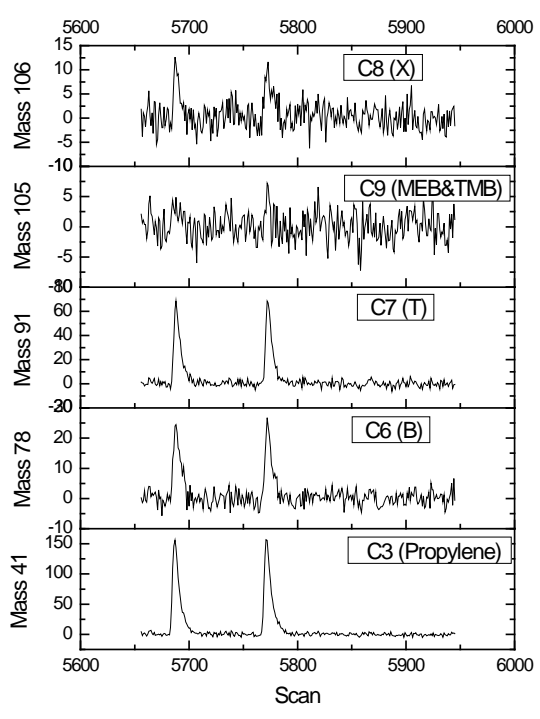
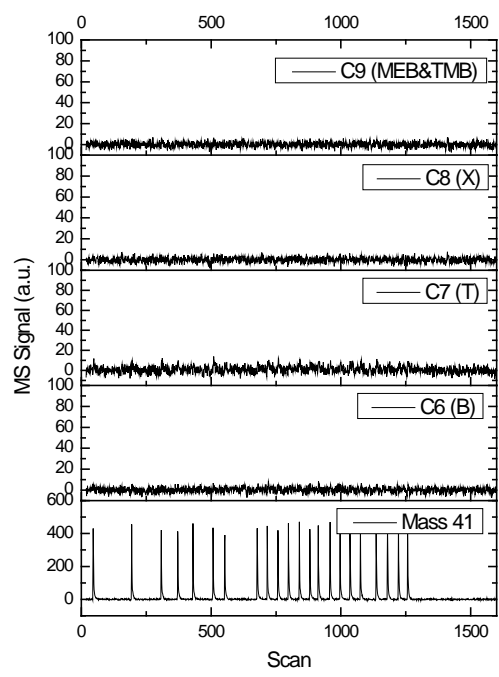


Figure 3.7. Pulse series of propylene on HZSM-5 (25)  
 a) At 400 °C; b) At 500 °C



results observed with propylene under the conditions at which aromatization occurs. This is an important difference that has not been previously pointed out. 2-methyl-2-pentene has a structure similar to those isoalkenes that might be derived from the hydrolysis of the aldol dimer (2-methyl-2-pentenal) of propanal. As shown in Table 3.2 above, no aromatics were produced from this isoalkene when it was fed by itself. This evidence suggests that aromatics are not predominantly produced from isoalkenes C<sub>4</sub>-C<sub>9</sub> but instead from a surface oxygenate pool.

The C<sub>9</sub> aromatic, TMB, is an interesting aromatic product to consider because it could, in principle, be produced from either alkylation of benzene or direct cyclization of a propanal trimer formed via an aldol condensation pathway. The fact that no C<sub>9</sub> aromatic was observed as a major product from a propylene feed at the conditions studied indicates that this alkylation pathway is not significant. By contrast, TMB along with EMB were observed as the major initial aromatic products from propanal, especially at low conversion of propanal either at low W/F, after some deactivation, or at lower temperatures. This result holds even in the presence of significant amounts of propylene formed from the propanal feed.

The reaction pathway involving condensation followed by cyclization of the aldol trimer is proposed in the scheme shown in Figure 3.8. It can be suggested that the ring closure involves the highly active hydrogen in position alpha to the carbonyl. After the ring closure, the carbonyl group can tautomerize to the enol form and further dehydrate to TMB and EMB on an acid site in the zeolite. These first aromatic products can then undergo the typical secondary reactions on acid sites, such as

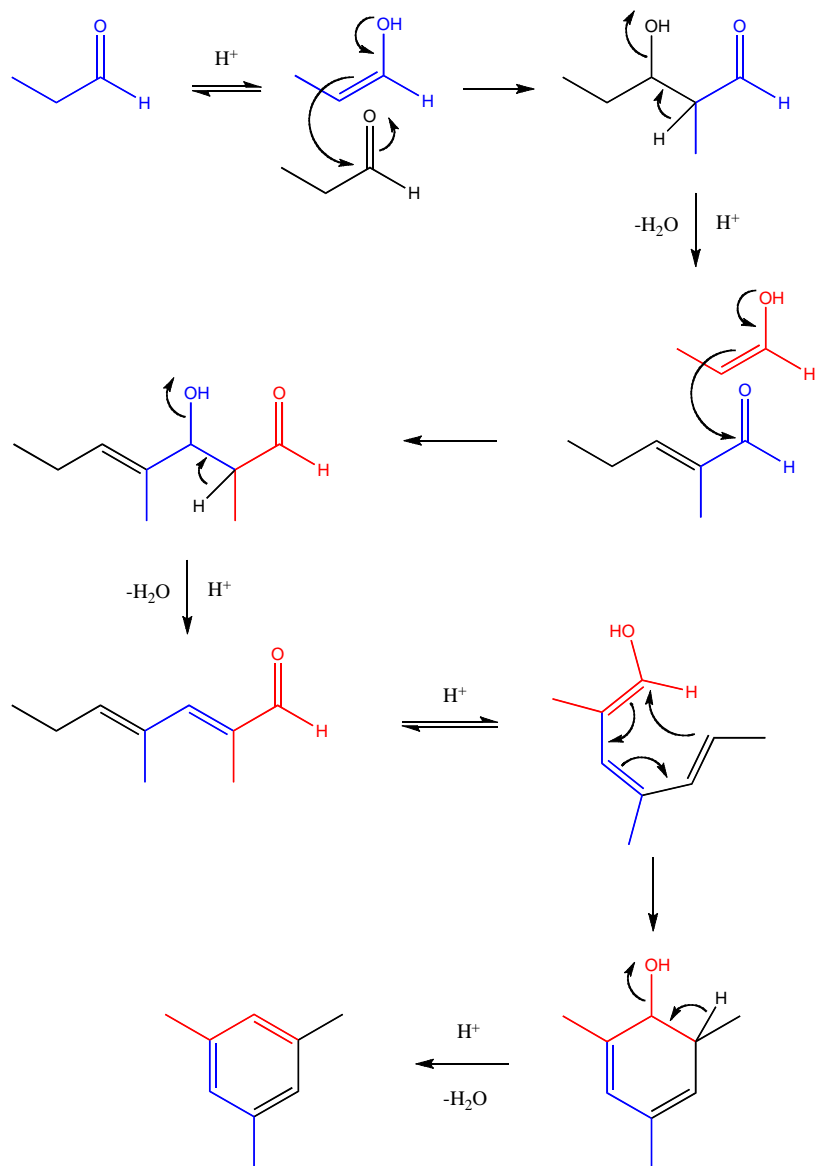


Figure 3.8. Proposed mechanism of TMB formation from propanal aldol trimer

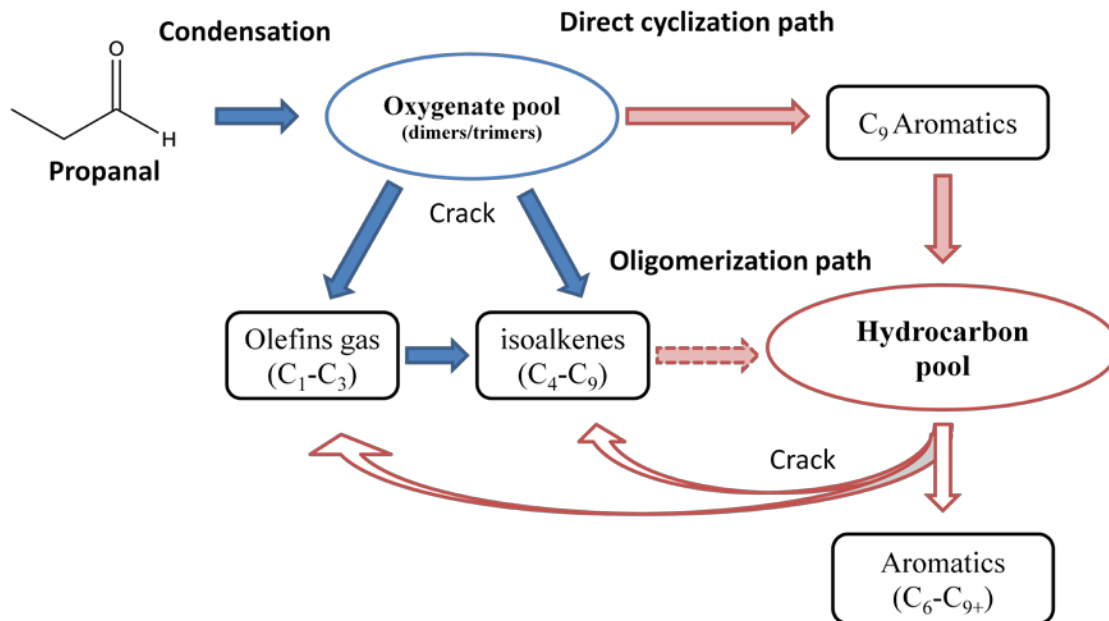


Figure 3.9. Proposed pathway of propanal conversion

dealkylation and disproportionation, producing light products and other aromatics.

The overall proposed pathway for propanal conversion is shown in Figure 3.9.

### **3.5. Conclusions**

The conversion of propanal at 400 °C has been investigated on an HZSM-5 zeolite and compared to the well-known behavior of propylene, which was also studied on a second, higher acidity, HZSM-5. While C<sub>9</sub> aromatics are the major products formed initially from propanal, propylene does not produce significant aromatics and is much less reactive under these conditions. It is suggested that the ring closure of propanal-derived products involves tautomerization of a polyunsaturated aldehyde (Trimer) to an enol form, followed by 1,6-cyclization and subsequent dehydration to TMB and EMB on acid sites. These aromatics can then undergo secondary reactions such as dealkylation, disproportionation and cracking. This pathway for aromatics formation is much more effective than the conventional acid-catalyzed alkane/alkene conversion on zeolites. In addition, it takes place at milder conditions than those required from alkane/alkenes, with consequently lower rates of deactivation and less undesirable cracking.

### **Acknowledgements**

Support from the National Science Foundation (EPSCoR 0814361), US Department of Energy (DE-FG36GO88064), Oklahoma Secretary of Energy and the Oklahoma Bioenergy Center are greatly appreciated.

## References

- [1] D.A. Simonetti, and J.A. Dumesic, *Chemsuschem* 1 (2008) 725-733.
- [2] J.N. Chheda, G.W. Huber, and J.A. Dumesic, *Angew Chem Int Edit* 46 (2007) 7164-7183.
- [3] D. Mohan, C.U. Pittman, and P.H. Steele, *Energy & Fuels* 20 (2006) 848-889.
- [4] S. Czernik, and A.V. Bridgwater, *Energy & Fuels* 18 (2004) 590-598.
- [5] R. Maggi, and B. Delmon, *Hydrotreatment and Hydrocracking of Oil Fractions* 106 (1997) 99-113.
- [6] G.W. Huber, and J.A. Dumesic, *Catal Today* 111 (2006) 119-132.
- [7] E.L. Kunkes, E.I. Gürbüz, and J.A. Dumesic, *J Catal* 266 (2009) 236-249.
- [8] K.M. Dooley, A.K. Bhat, C.P. Plaisance, and A.D. Roy, *Appl Catal A-Gen* 320 (2007) 122-133.
- [9] A.G. Gayubo, A.T. Aguayo, A. Atutxa, R. Aguado, M. Olazar, and J. Bilbao, *Ind Eng Chem Res* 43 (2004) 2619-2626.
- [10] J.D. Adjaye, and N.N. Bakhshi, *Biomass Bioenerg* 8 (1995) 131-149.
- [11] J.L. Grandmaison, P.D. Chantal, and S.C. Kaliaguine, *Fuel* 69 (1990) 1058-1061.

- [12] S.L. Meisel, in: C.D.C.R.F.H. D.M. Bibby, and S. Yurchak, (Eds.), *Studies in Surface Science and Catalysis*, Elsevier. 17-37.
- [13] J. Topp-Jørgensen, in: C.D.C.R.F.H. D.M. Bibby, and S. Yurchak, (Eds.), *Studies in Surface Science and Catalysis*, Elsevier. 293-305.
- [14] G.J. Hutchings, P. Johnston, D.F. Lee, A. Warwick, C.D. Williams, and M. Wilkinson, *J Catal* 147 (1994) 177-185.
- [15] F. Bandermann, and J. Fuhse, *Chemie Ingenieur Technik* 59 (1987) 607-608.
- [16] C.D. Chang, and A.J. Silvestri, *J Catal* 47 (1977) 249-259.
- [17] T. Sooknoi, T. Danuthai, L.L. Lobban, R.G. Mallinson, and D.E. Resasco, *J Catal* 258 (2008) 199-209.
- [18] T. Danuthai, S. Jongpatiwut, T. Rirksomboon, S. Osuwan, and D.E. Resasco, *Appl Catal A-Gen* 361 (2009) 99-105.
- [19] X. Zhu, L. Lobban, D. Resasco, and R. Mallinson, *J Catal* (2010) (in press).
- [20] W.E. Farneth, and R.J. Gorte, *Chem Rev* 95 (1995) 615-635.
- [21] T.J.G. Kofke, R.J. Gorte, G.T. Kokotailo, and W.E. Farneth, *J Catal* 115 (1989) 265-272.
- [22] J.A. Biscardi, and E. Iglesia, *J Catal* 182 (1999) 117-128.
- [23] T. Mole, J.R. Anderson, and G. Creer, *Appl Catal* 17 (1985) 141-154.

- [24] P. Dejaifve, J.C. Vedrine, V. Bolis, and E.G. Derouane, *J Catal* 63 (1980) 331-345.
- [25] G.S. Salvapati, K.V. Ramanamurty, and M. Janardanao, *J Mol Catal* 54 (1989) 9-30.
- [26] S. Kolboe, *Acta Chemica Scandinavica Series a-Physical and Inorganic Chemistry* 40 (1986) 711-713.
- [27] I.M. Dahl, and S. Kolboe, *J Catal* 149 (1994) 458-464.

## CHAPTER 4

### EFFECTS OF HZSM-5 CRYSTALLITE SIZE ON STABILITY AND AROMATICS DISTRIBUTION FROM CONVERSION OF PROPANAL

#### **Abstract**

The conversion of propanal on large (2-5  $\mu\text{m}$ ) and small (0.2-0.5  $\mu\text{m}$ ) crystallite HZSM-5 at 400 °C and atmospheric pressure showed significant effects on catalyst stability and product distribution. Improved catalyst stability was observed on small crystallites due to faster removal of products from the shorter diffusion path length of the small crystallites, reducing the formation of coke precursors. The main isomer of the C<sub>8</sub> aromatic products observed on small crystallites was the thermodynamically preferred meta-xylene, while the shape-selective preferred para-xylene was the predominant product on large crystallites. The higher internal diffusion rate of the para isomer results in higher shape-selectivity with the longer path of the large-crystallite zeolite. At the same time, higher ratio of C<sub>9</sub>/(C<sub>8</sub>+C<sub>7</sub>) aromatics was observed on the small crystallites. As previously shown, the C<sub>9</sub> aromatics are the initial aromatics produced from propanal via aldol condensation followed by cyclization. These C<sub>9</sub> aromatics have less opportunity to crack to lighter aromatics on the small crystallites. It is concluded that the use of smaller crystallite HZSM-5



improves results for production of alkyl aromatics from light oxygenates at mild conditions that may prove useful for bio-oil upgrading.

*Keywords:* Propanal; HZSM-5; Zeolites; Crystallite size; Aromatization; Shape selectivity; Bio-oil upgrading; Biofuels

#### **4.1. Introduction**

Bio-oil contains a large fraction of oxygenated compounds that are thermally and chemically unstable and need to be deoxygenated to form fuel compatible molecules [1-2]. Conversion of methanol to hydrocarbons has been extensively studied on HZSM-5[3-4]. There have also been many studies of the conversion of small oxygenates such as molecules with aldehyde, ketone, alcohol, and acid functionalities [5-7] as well as large oxygenates such as methyl-esters [8-9] on HZSM-5.

The effect of crystallite size has been recognized as an important factor in MTG, MTO, and alkylation of aromatics. This has been examined with HZSM-5[10] and SAPO-34[11-12]. The results from those studies show that light olefins are selectively produced on smaller crystallite sizes of less than 2  $\mu\text{m}$ . Those authors also found that in larger crystallites, intermediates can be converted in consecutive steps before they desorb from the crystallite and thus, more secondary products and faster deactivation were observed due to longer intra-crystalline diffusion path lengths. In smaller crystallites, they observed faster equilibration of methanol and DME at low

conversion and excellent catalyst lifetime. However, it was also found that catalyst active sites on the external surface, responsible for non-shape-selective products, are more significant on small crystallite size zeolites[13].

Significant yields of alkyl aromatic products were found from conversion of propanal on HZSM-5 at mild conditions in previous work[14]. Those results showed that the initial aromatics had significant alkylation and were predominantly produced via an aldol condensation pathway instead of a hydrocarbon pool.

Although the effect of crystallite size has been studied for some applications, there has been little research done with bio-oil derived oxygenate compounds. In this contribution a comparative study of catalyst activity and product distribution from propanal conversion are examined on small and large crystallite HZSM-5.

## **4.2. Experimental**

### *4.2.1. Catalyst Preparation.*

Small crystallite HZSM-5 with a Si/Al ratio of 45 was obtained from Süd-Chemie, Inc. The large crystallite HZSM-5 was synthesized following synthesis methods described elsewhere [15]. The Si/Al ratio of the synthesized large crystallite ZSM-5 was specified to be 45 by modifying the amount of Al in the original recipe. The proton form of this zeolite was obtained by ion-exchange with  $\text{NH}_4\text{NO}_3$  at 80 °C for 10 hrs. The process was repeated to completely replace the cations in the zeolite with

$\text{NH}_4^+$ . The final large crystallite HZSM-5 was obtained after drying at 100 °C for 10 hr and calcining at 600 °C for 3 hr in dry air.

#### 4.2.2. *Equipment and Procedures.*

The reactor was a 6 mm OD quartz tube fixed bed continuous flow reactor. The reactor was heated by a split-tube furnace (Thermal Craft) with a digital feedback temperature controller (Omega). The catalyst was treated *in situ* with  $\text{H}_2$  for 1 hr at 400 °C before each run and hydrogen continued to flow during the reaction experiments. Propanal, obtained from Sigma-Aldrich, was fed into the reactor by a syringe pump (kd Scientific). The reaction was carried out at atmospheric pressure at different space times (weight of catalyst to organic mass feed rate ratio, W/F, from 0.1 h to 1 h, with a carrier gas flow of 35 cc/min .

#### 4.2.3. *Product analysis.*

For each half hour time-on-stream (TOS), products were analyzed online by GC/FID (HP6890). The products were sampled using a 6-port valve with a 250  $\mu\text{l}$  sample loop heated at 290 °C. After passing through the valve, the stream passed through a condenser. After each run, the reactor was purged with dry carrier gas for 15 minutes to collect the residual products from the reactor in the condenser. The condensable liquid products were collected in methanol and were then identified by GC/MS (Shimadzu Q-2010). Both GCs were equipped with HP-INNOWax columns.

### **4.3. Characterization**

The synthesized HZSM-5 was characterized by X-ray powder diffraction (Bruker D8 Discover diffractometer). Scanning electron microscopy (Jeol JSM-880 electron microscope) was used to observe the morphology and crystallite size of both zeolites.

The acidity of the catalysts was determined by temperature programmed desorption (TPD) of iso-propylene amine (IPA) with an online mass spectrometer (MS) detector (MKS Cirrus.) The TPD was performed in a 6 mm quartz tube reactor with 50 mg of catalyst. The catalyst sample was first pretreated in He at 400 °C for 1 hr and cooled down to 100 °C.

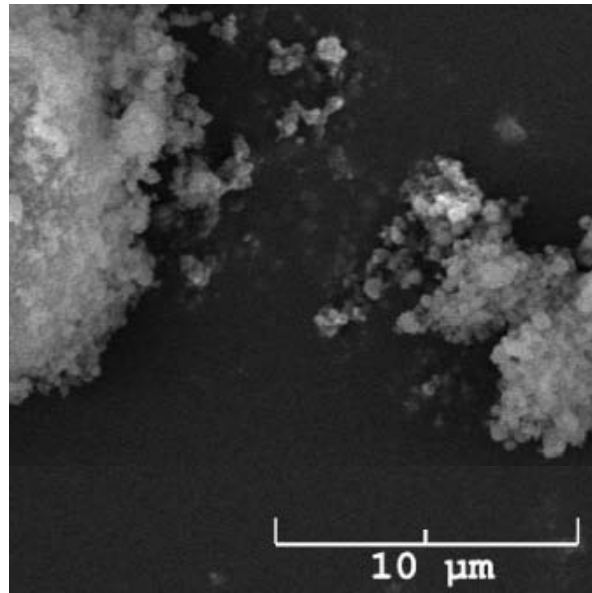
The adsorption of IPA was carried out in flowing He at 100 °C with 10 liquid pulses of IPA, 5 µl for each pulse and 3 min between pulses. The temperature program was from ambient to 650 °C with a rate of 10 °C/min in flowing He. The MS signals of m/z 44 (IPA), 41 (propylene), 17 (ammonia), 18 (water), 16 (fragment of ammonia) were monitored. The results were calibrated with a pulse of propylene using a 100 µl loop.

### **4.4. Results**

#### *4.4.1. Characterization*

The HZSM-5 XRD pattern of the synthesized large crystallites was confirmed by comparing with the literature[16]. As depicted in Figure 4.1, the SEM images

a) Small crystallite HZSM-5



b) Large crystallite HZSM-5

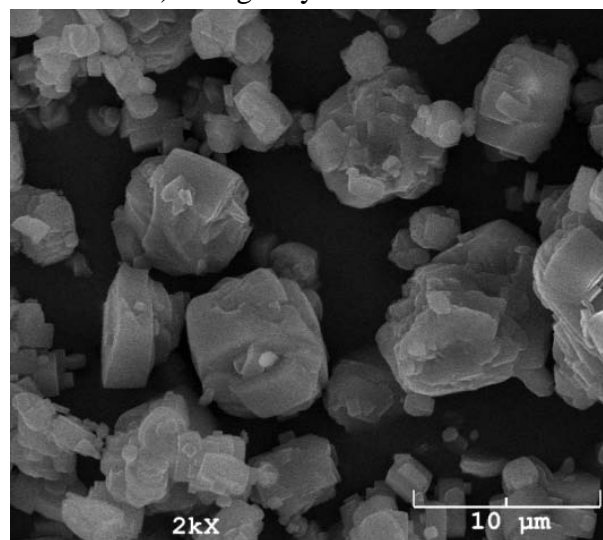


Figure 4.1. SEM of small (a) and large (b) crystallite HZSM-5 (Si/Al= 45)

show that the large crystallite HZSM-5 has an average crystallite size around 2-5  $\mu\text{m}$ , while the small crystallite HZSM-5 has a much smaller crystallite size averaging around 0.2-0.5  $\mu\text{m}$ .

Figure 4.2 shows the acidity profile of the large and small crystallite HZSM-5. The decomposition of IPA to propylene is due to Bronsted acid sites activated at high temperature [17]. The peak maximum in propylene evolution is observed at 350  $^{\circ}\text{C}$ . The large crystallite HZSM-5 has an acidity of 321  $\mu\text{mol/g}$ . The small crystallite HZSM-5 has a similar propylene peak and acidity of 337  $\mu\text{mol/g}$ . The calculated acidity, based upon the Al/Si ratio is 370  $\mu\text{mol/g}$ .

#### 4.4.2. Catalyst activity

Propanal conversion was performed on the small and large crystallite HZSM-5 at 400  $^{\circ}\text{C}$  and atmospheric pressure. The products are grouped into 3 categories: gas ( $\text{C}_1\text{-C}_3$ , mostly propylene), isoalkenes ( $\text{C}_4\text{-C}_9$ , mostly 2-pentene and iso-pentene), and aromatics ( $\text{C}_7\text{-C}_{9+}$ ).

Figure 4.3 shows the conversion as a function of W/F with curves for different TOS for both crystallite sizes. The results for the small crystallites are represented by solid lines, and the large crystallites by dashed lines. The TOS increases for each curve from the left to the right. It is clear that these curves are very close together at different W/F for the small crystallites. This indicates that for increasing TOS, there was no significant reduction in conversion, i.e. deactivation. In contrast, the results for the large crystallites show gaps between the individual TOS curves. At the same

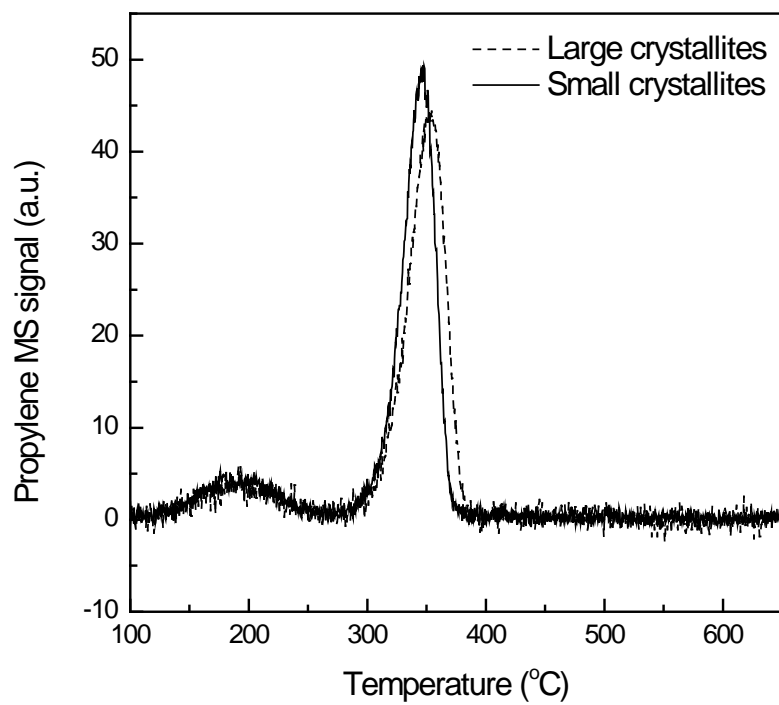


Figure 4.2. Acidity profile of small and large crystallite HZSM-5 (Si/Al=45)

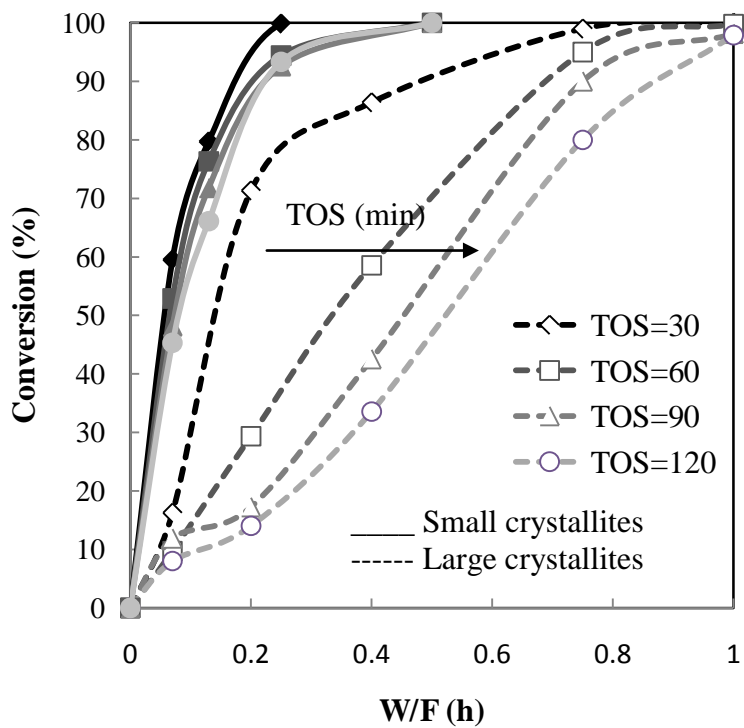


Figure 4.3. Effect of crystallite size on catalyst activity at different W/F and TOS at 400 °C, opened symbol (large crystallite), solid symbol (small crystallite)



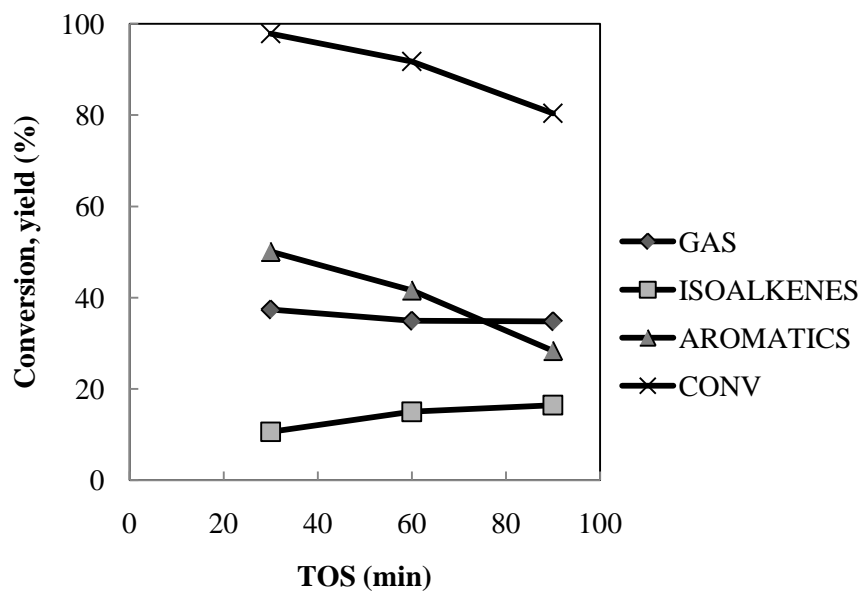
W/F, conversion decreased significantly with increasing TOS, indicating significant deactivation.

In Figure 4.4, conversion and product yields are shown as a function of TOS at 400 °C and W/F= 0.2 h. The left figure shows the results from the small crystallites and the right figure shows the results for the large crystallites. Only modest deactivation was observed with small crystallites under these conditions. However, the large crystallites showed a large decrease in conversion as well as aromatics and gas with TOS. The isoalkenes yield declined more slowly, indicating an increasing selectivity as deactivation proceeded while aromatization and cracking decreased.

Figure 4.5 combines results for both W/F and TOS and shows that similar trends for product yields were observed as a function of conversion for both sized crystallites. This indicates that the catalytic function is not significantly changed with the crystallite size. However, some effect can be seen with a somewhat higher yield of isoalkenes for the large crystallites.

The effect of crystallite size is significant when comparing the ratio of para-xylene with the sum of the ortho- and meta- xylene [ $p/(o+m)$ ] as depicted in Figure 4.6. At all conversion levels, the  $p/(o+m)$  ratio of the larger crystallites is much higher compared to that of the small crystallites. This behavior has also been observed in the literature for the conversion of hydrocarbons or methanol to aromatics on HZSM-5[10]. When comparing the ratio of  $C_9/(C_8+C_7)$  aromatics, the results show, in

**Small crystallite HZSM-5 (Si/Al=45) W/F= 0.2 h**



**Large crystallite HZSM-5 (Si/Al=45) W/F=0.2 h**

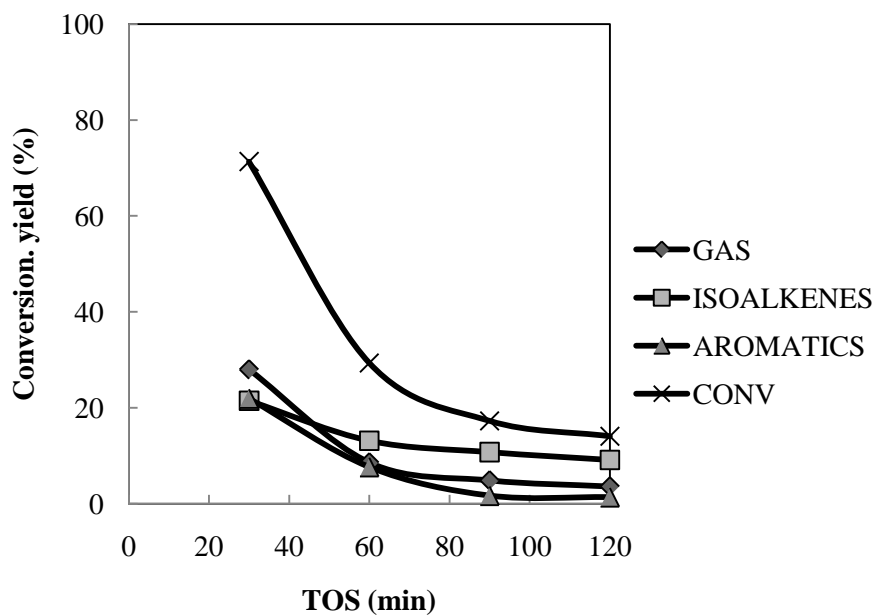


Figure 4.4. Effect of crystallite size on product distribution and conversion with TOS at 400 °C

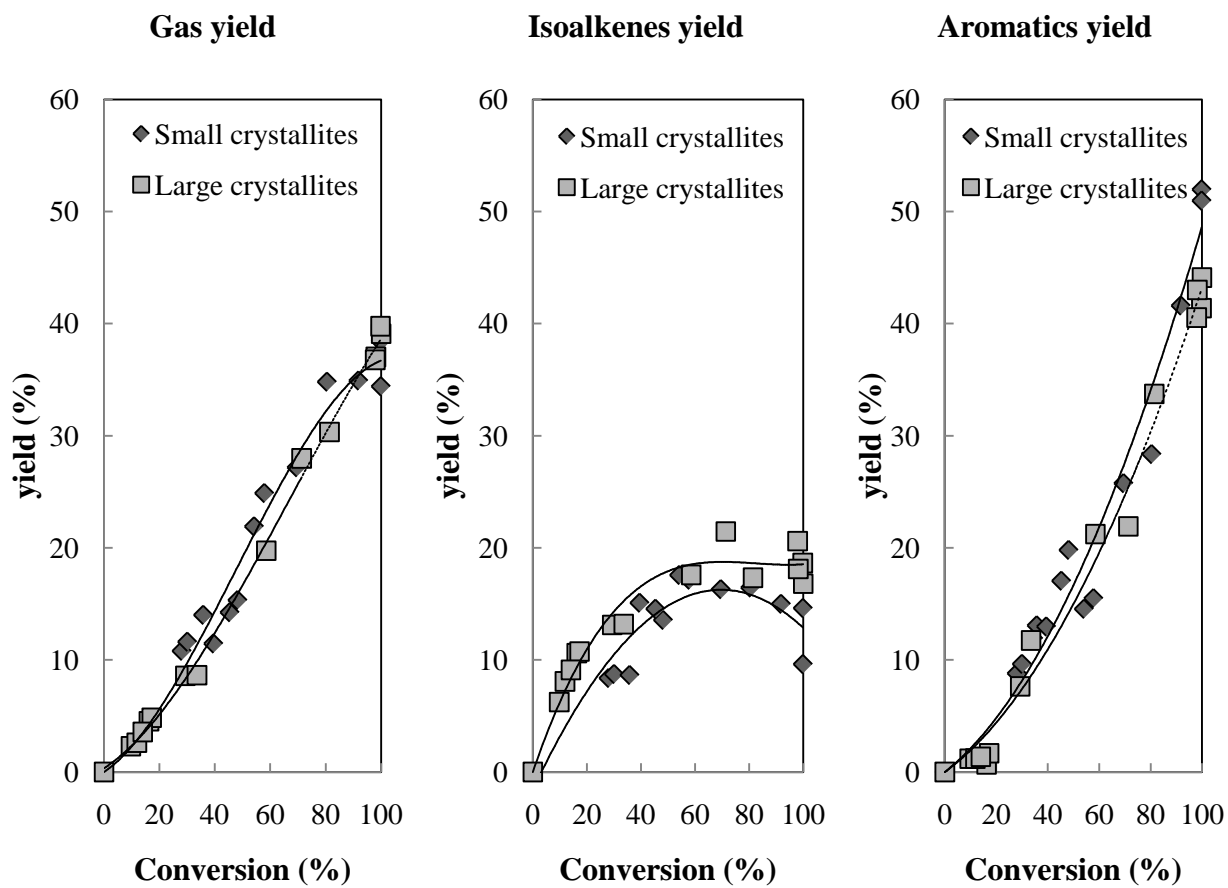


Figure 4.5. Product yields versus conversion at 400 °C (combined TOS and W/F data), solid line (small crystallite), dash line (large crystallite)

Figure 4.7, a much higher ratio of  $C_9/(C_8+C_7)$  on the small crystallites. This ratio decreases at longer W/F, where conversion is 100 %, with increasing amounts of excess catalyst and reaches a value similar to the large crystallites at W/F= 1 h on both crystallite sizes.

#### 4.5. Discussion

It is known in the literature [11, 18] that the different diffusivities of different sized and shaped products in the intracrystalline channels is the predominant mechanism for shape selectivity in HZSM-5 for the molecules of interest in this study. The HZSM-5 pore structure is a 10 member ring with a 3-dimensional channel system with two types of intersections with window openings of 0.54 x 0.56 nm and 0.51 x 0.55 nm and a maximum diameter of the intersections of about 0.9 nm. For this reason, aromatic molecules such as benzene, having a critical diameter of 0.68nm, and alkyl aromatics can easily form within the intersections of the HZSM-5 channels [19] and diffuse out. However, in a large crystallite, the diffusion path-length is longer, and differences in diffusion rates help control the selectivity.

Even at the shortest TOS, the large crystallites showed significant deactivation with lower conversion at the same W/F as the small crystallites. As previously mentioned, and shown in Figure 4.3, it may be seen that the larger crystallite curve approaches the small crystallite curve as TOS decreases, e.g. from right to left. In the limit of zero TOS, the curves should be co-incident, with no-deactivation of the large

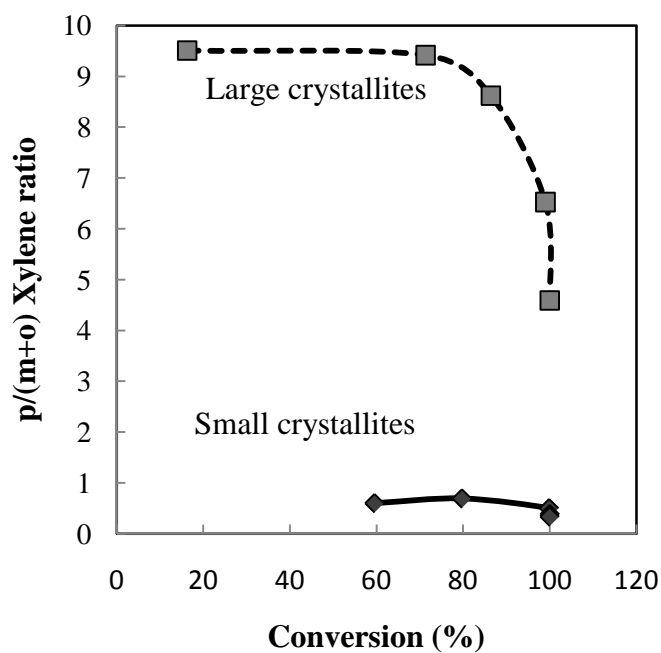


Figure 4.6. Effect of crystallite size on p-xylene ratio as function of conversion for different W/F at TOS= 30 min

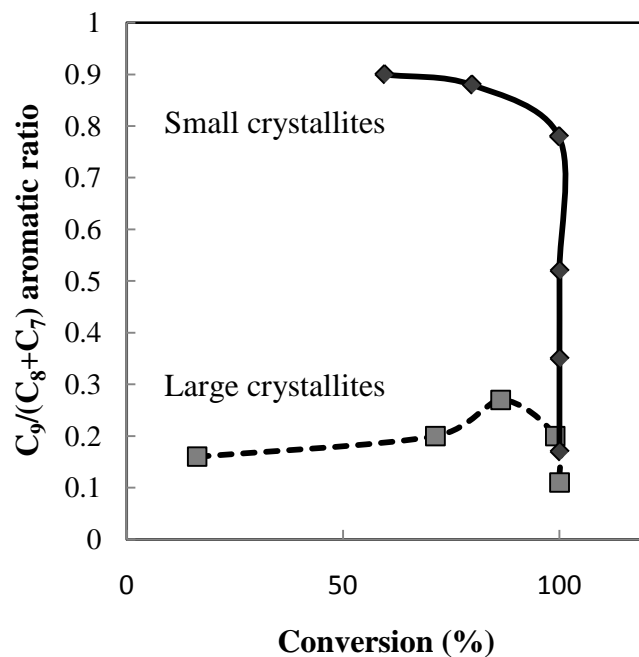


Figure 4.7. Effect of crystal size on  $C_9/(C_8+C_7)$  ratio as function of conversion for different W/F at TOS= 30 min

crystallites. With the longer diffusion path-length of the larger crystallites, products take longer to diffuse out and have more time to form coke precursors and coke.

The effect of diffusion is also apparent in the evolution of the p/(m+o) ratio, shown in Fig. 6. A much higher p/(m+o) ratio was obtained with the large-crystallite HZSM-5 since the higher diffusion coefficient of para-xylene helps this molecule diffuse out of the large crystallites more rapidly than the ortho and meta isomers, which are retained longer with a greater probability of isomerizing to the para, the preferred shape-selective product. In contrast, on small crystallites, with a shorter diffusion path length, all of the products are able to exit rapidly and the p/(m+o) ratio is much lower, being meta-xylene the favored product.

Aromatization of hydrocarbons and alcohols in HZSM-5 is generally accepted as occurring by oligomerization of intermediate olefins by the hydrocarbon pool pathway [20]. According to this consecutive oligomerization pathway, one would expect more isoalkenes and less aromatics on small crystallites because they have less chance (shorter time in the channels) to complete formation of the aromatics. However, the fact that aromatics were always present even at the lowest conversion, on the small crystallites, suggests that aromatics are produced from a pathway other than the hydrocarbon pool mechanism. In fact, it has been found that a predominant pathway for aromatics formation under these mild conditions is by aldol condensation with cyclization and dehydration of the aldol trimer of propanal[14] to give C<sub>9</sub> aromatics under these mild conditions. Due to the shorter diffusion path length of the

small crystallites, the C<sub>9</sub> aromatics leave the channels of a small crystallite with less chance of cracking to smaller secondary aromatic products, or coking. The effect is less pronounced, or not observed, at high levels of conversion where excess acid sites are available to react with the larger products, increasing the cracking. As a result, lighter aromatics, and a decrease in the ratio shown in Fig. 7 were observed at high conversion on the small crystallites.

#### **4.6. Conclusions**

The effect of crystallite size of HZSM-5 has been investigated for conversion of propanal to aromatics at mild conditions, 400 °C and atmospheric pressure. Much slower deactivation was observed on the small crystallites, compared to the large crystallites, due to rapid removal of products from the shorter path length channels, reducing production of coke precursors and coke. The smaller crystallites, with a shorter diffusion path length, showed significantly less isomerization of the product xylenes to the shape-selective preferred para-xylene because of its greater diffusion coefficient. A higher fraction of C<sub>9</sub> aromatics, the initial aromatic products from the predominant aldol pathway, was observed on small crystallites due to a shorter time for cracking before diffusion out of the channels. These results suggest that the use of smaller crystallite HZSM-5 improves results for production of alkyl aromatics from light oxygenates at mild conditions that may prove useful for bio-oil upgrading.

## **Acknowledgements**

Support from the National Science Foundation (EPSCoR 0814361), US Department of Energy (DE-FG36GO88064), Oklahoma Secretary of Energy and the Oklahoma Bioenergy Center are greatly appreciated.

## **References**

- [1] D. Mohan, C.U. Pittman, and P.H. Steele, *Energy & Fuels* 20 (2006) 848-889.
- [2] S. Czernik, and A.V. Bridgwater, *Energy & Fuels* 18 (2004) 590-598.
- [3] M. Stöcker, *Micropor Mesopor Mat* 29 (1999) 3-48.
- [4] G. F. Froment, in *Catalysis*, RSC, 1992, vol. 9, p. 1.
- [5] F. Bandermann, and J. Fuhse, *Chemie Ingenieur Technik* 59 (1987) 607-608.
- [6] C.D. Chang, and A.J. Silvestri, *J Catal* 47 (1977) 249-259.
- [7] G.J. Hutchings, P. Johnston, D.F. Lee, A. Warwick, C.D. Williams, and M. Wilkinson, *J Catal* 147 (1994) 177-185.
- [8] T. Danuthai, S. Jongpatiwut, T. Rirksomboon, S. Osuwan, and D.E. Resasco, *Appl Catal A-Gen* 361 (2009) 99-105.



- [9] T. Sooknoi, T. Danuthai, L.L. Lobban, R.G. Mallinson, and D.E. Resasco, *J Catal* 258 (2008) 199-209.
- [10] K.P. Möller, W. Böhringer, A.E. Schnitzler, E. van Steen, and C.T. O'Connor, *Micropor Mesopor Mat* 29 (1999) 127-144.
- [11] D. Chen, K. Moljord, T. Fuglerud, and A. Holmen, *Micropor Mesopor Mat* 29 (1999) 191-203.
- [12] N. Nishiyama, M. Kawaguchi, Y. Hirota, D. Van Vu, Y. Egashira, and K. Ueyama, *Appl Catal a-Gen* 362 (2009) 193-199.
- [13] G. Paparatto, E. Moretti, G. Leofanti, and F. Gatti, *J Catal* 105 (1987) 227-232.
- [14] T. Hoang, X. Zhu, T. Sooknoi, D. Resasco, and R. Mallinson, *J Catal* (2010) (in press).
- [15] R.J. Argauer, and G.R. Landolt. 1972. Crystalline zeolite ZSM-5 and method of preparing the same. U.S. Patent, Mobil Oil Corporation, U.S.
- [16] S.L. Meisel, *Studies in Surface Science and Catalysis*, Elsevier. 17-37.
- [17] W.E. Farneth, and R.J. Gorte, *Chem Rev* 95 (1995) 615-635.
- [18] N.Y. Chen, T.F. Degnan, and C.M. Smith, *Molecular Transport and Reaction in Zeolites: Design and Application of Shape Selective Catalysts*. Wiley-VCH, New York, 1994.
- [19] D. Bhattacharya, and S. Sivasanker, *J Catal* 153 (1995) 353-355.

[20] I.M. Dahl, and S. Kolboe, *J Catal* 149 (1994) 458-464.

## CHAPTER 5

### A COMPARISON OF THE EFFECTS OF CHANNEL STRUCTURE OF ZEOLITES HZSM-5 AND 22 ON CONVERSION OF PROPANAL TO ISOALKENES AND ALKYL-AROMATICS

#### **Abstract**

A comparison of the conversion of propanal at 400 °C over zeolites with different channel structures using HZSM-22 and HZSM-5 shows significant effects on the product distribution. It is shown that the structure of the HZSM-22, with a one-dimensional and narrower channel system, restricts the formation of aromatics. Thus, considerably less aromatics and a higher yield of C<sub>4</sub>-C<sub>9</sub> isoalkenes is produced on HZSM-22. In contrast, a higher yield of aromatic products is observed over HZSM-5 with its three-dimensional channel system. By increasing channel dimension and connectivity of the channels, increasing catalyst activity was also observed, in agreement with literature. The influence of water, which is produced from the dehydration of the intermediates during condensation, is investigated by addition to the feed and is found to reduce activity but the effect is reversed when the water addition is stopped.

*Keywords:* Propanal; HZSM-5; HZSM-22; Zeolites; Crystal size; Bio-oil upgrading; Aromatization; Shape selectivity

## **5.1. Introduction**

Production of oxygenates from biomass conversion has created the need to upgrade these compounds to fuels and chemicals to maximize yield and value. Bio-oil produced from pyrolysis contains a large fraction of oxygenated compounds with reactive functional groups such as aldehydes, ketones, acids, and polyols that are thermally and chemically unstable and need to be deoxygenated to fuel compatible molecules [1-2]. Bio-oil also contains substantial water, perhaps up to 50 % by weight. In addition, converting light oxygenates to larger, more stable, molecules can retain liquid yield in contrast to hydrotreating [1-3], that consumes hydrogen while lowering liquid yields because of conversion to light hydrocarbon gases. The complexity of bio-oil has created a great challenge in understanding the effect of catalyst properties and tailoring them to achieve stable production of desirable fuel products. Thus, model compounds have been studied extensively on different types of catalysts: metals[4-5], metal oxides[6], and zeolites[7], for example.

Acidic zeolites can directly convert oxygenates to primarily isoalkenes and aromatics in the gasoline boiling range. HZSM-5 has been employed in conversion of methanol commercially by the well known and well studied MTG process (Methanol-to-Gasoline)[8]. It has been found that substantial amounts of aromatics are observed

in the final products. In general, the major aromatization pathway reported is that oxygenates first convert to olefins and these then oligomerize and dehydrocyclize to form aromatics. However, other studies have found that greater aromatization was observed with propanal compared to other C<sub>3</sub> oxygenates (ketone, alcohol, acid, ester)[9-11] as well as other oxygenates compared with alkanes [12-13]. Significant aromatics formation from propanal at mild conditions has been found to occur predominantly via an acid-catalyzed aldol pathway instead of via oligomerization and formation of a hydrocarbon pool [14].

The zeolite channel structure is one of the factors controlling product selectivity via shape selectivity. This relationship has been characterized by the “Constraint Index” in the paper of Frillette et al. [15]. It associates the activity and selectivity of a zeolite to the ratio of the cracking of n-hexane and 3-methylpentane. HZSM-5 has a unique three-dimensional channel system that reduces coke formation and enhances catalyst lifetime. This type of pore structure allows the production of gasoline boiling range molecules such as aromatics. Another 10-MR zeolite, but with a tubular pore one-dimensional channel structure, HZSM-22, is reported to be stable and selective for trimerization of propene [16]. Although there are extensive studies on these two zeolites, the effect of the zeolite channel structures on conversion of small oxygenates such as propanal has not been studied.

An important factor in the reaction of oxygenates is the water produced as a major byproduct of the deoxygenation reactions and its presence has significant effects on the zeolite catalysts’ performance. Its stoichiometric yield can be up to 31 %wt

(propanal), 56 %wt (methanol), and 59 %wt (glycerol). As mentioned above, water is also a substantial component of the bio-oil produced from pyrolysis. The effect of addition of water has been investigated for the MTO reaction [17-18]. Those authors found that water reduced catalyst activity but improved lower olefin selectivity. This was ascribed to preferential adsorption of water molecules on the acid sites, therefore facilitating desorption of lower olefins and inhibiting oligomerization. The presence of water also showed reduced deactivation that could be due to inhibition of the formation of larger oligomers that are coke precursors [19].

## **5.2. Experimental**

### *5.2.1. Catalyst Preparation.*

HZSM-5 and HZSM-22 samples with a Si/Al ratio of 45 were synthesized following synthesis methods described elsewhere [20-21]. The Si/Al ratio of the synthesized ZSM-5 sample was specified to be 45 by modifying the amount of Al in the original recipe. The proton form of the zeolites was obtained by ion-exchange with  $\text{NH}_4\text{NO}_3$  at 80 °C for 10 hrs. The process was repeated to completely replace the cations in the zeolite with  $\text{NH}_4^+$ . The final synthesized HZSM-5 and HZSM-22 catalysts were obtained after drying at 100 °C for 10 hr and calcining at 600 °C for 3 hr in dry air.

### 5.2.2. Equipment and Procedures.

The reactor was a 6mm ID quartz tube fixed bed continuous flow reactor. The reactor was heated by a split-tube furnace (Thermal Craft) with a digital feedback temperature controller (Omega). The catalyst was treated *in situ* with H<sub>2</sub> for 1 hr at 400 °C before each run. Propanal, obtained from Sigma-Aldrich, was fed into the reactor by a syringe pump (KD Scientific). The reaction was carried out at atmospheric pressure and at different space times (weight of catalyst to mass feed rate ratio, W/F) from 0.1 h to 2 h with a hydrogen carrier flowing at 35 sccm.

### 5.2.3. Product analysis.

At each half hour time on stream, products were analyzed online by GC/FID (HP6890). The products were sampled using a 6-port valve with a 250 µl sample loop heated at 290 °C. After each run, the reactor was purged with dry carrier gas for 15 minutes to collect the residual products from the reactor. The condensable liquid products were collected in a solvent (Methanol) and were then identified by GC/MS (Shimadzu Q-2010). Both GCs are equipped with HP-INNOWAX columns.

## 5.3. Characterization

The synthesized HZSM-5 and HZSM-22 were characterized by X-ray powder diffraction (Bruker D8 Discover diffractometer). Scanning electron microscopy (Jeol JSM-880 electron microscope) was used to observe the morphology of the synthesized zeolites.

The acidity of HZSM-5 and HZSM-22 was determined by temperature programmed desorption (TPD) of iso-propylene amine (IPA) with an online mass spectrometer (MS) detector (MKS Cirrus.) The TPD was performed in a 6mm quartz tube reactor with 50 mg of catalyst. The catalyst sample was first pretreated in He at 400 °C for 1 hr and cooled down to 100 °C

The adsorption of IPA was carried out in flowing He at 100 °C with 10 liquid pulses of IPA with 5 µl for each pulse and 3 min between pulses. The temperature program was from ambient to 650 °C with a rate of 10 °C/min in flowing He. The MS signal of mass 44 (IPA), 41 (propylene), 17 (ammonia), 18 (water), 16 (fragment of ammonia) were monitored. The results were calibrated with a 100 µl loop of propylene.

The amounts of coke deposits were quantified by temperature programmed oxidation (TPO) by passing a 5% O<sub>2</sub>/He stream over a 50 mg spent catalyst sample, using a linear heating rate of 5 °C/min. The signals of H<sub>2</sub>O (m/z=18), CO<sub>2</sub> (m/z=44), and CO (m/z=28) were continuously monitored by MS. Quantification was calibrated on the basis of the signals from 100 µL CO<sub>2</sub> and CO pulses in flowing He.



## 5.4. Results

### 5.4.1 Characterization

The SEM images and XRD patterns of HZSM-5 and HZSM-22 samples are shown in Figure 5.1 and are similar to those in the literature [20-21]. No significant impurities or amorphous materials are seen in the XRD patterns as shown in Figure 5.1a. The SEM images show that all the samples have similar crystallite sizes averaging around 2-4  $\mu\text{m}$ . While the crystal shape of HZSM-5 is nearly cuboid, the crystal shape of the HZSM-22 is a single needle or conglomerates of needles as seen in Figure 5.1b. The SEM images also confirmed that there are no amorphous materials present in the samples.

Figure 5.2 shows the acidity profile of the HZSM-5 and HZSM-22. The decomposition of IPA to propylene is due to Bronsted acid sites activated at high temperature [22]. The peak maximum in propylene evolution is observed at 350  $^{\circ}\text{C}$ . HZSM-5 has higher amounts of Bronsted sites, 350  $\mu\text{mol/g}$ , compared to HZSM-22, 297  $\mu\text{mol/g}$ . The measured acidities of both catalysts are lower than the calculated acidity for a Si/Al=45 of 370  $\mu\text{mol/g}$  due to some inaccessible sites, but HZSM-5 is closer to the theoretical value due to its more extensive pore structure.

### 5.4.2. Catalyst activity

Propanal conversion was performed on HZSM-22 and HZSM-5 at 400  $^{\circ}\text{C}$  and atmospheric pressure. The products are grouped into 3 categories: gas ( $\text{C}_1\text{-C}_3$ , mostly

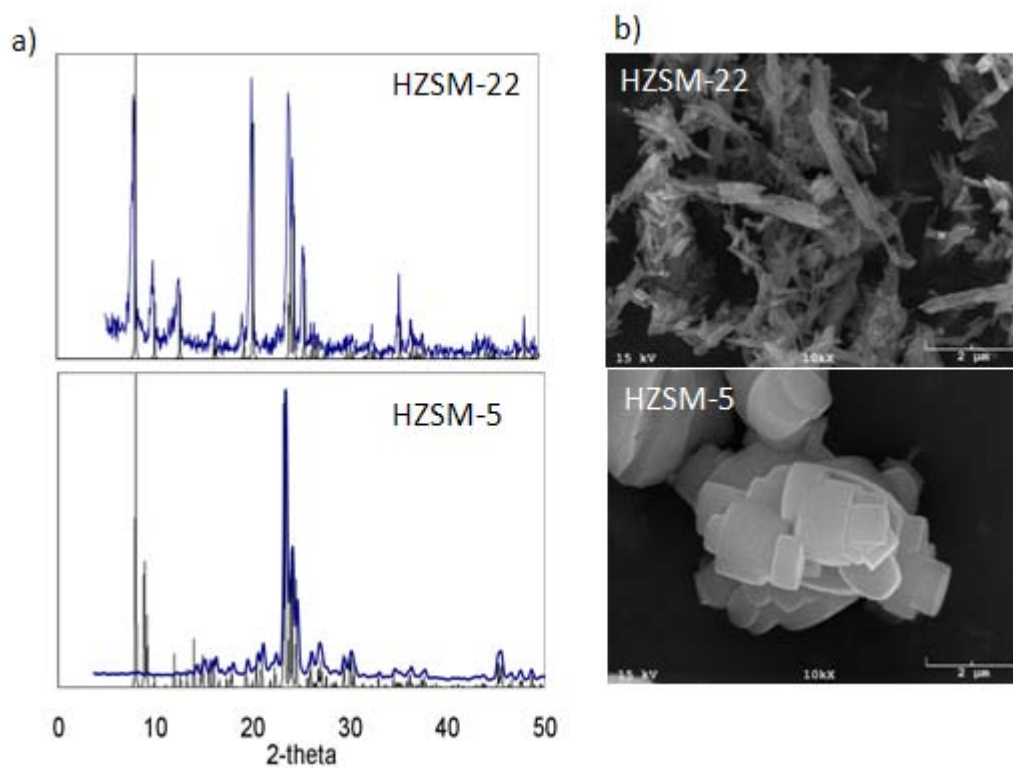


Figure 5.1. XRD (a) & SEM (b) of synthesized HZSM-22 and HZSM-5

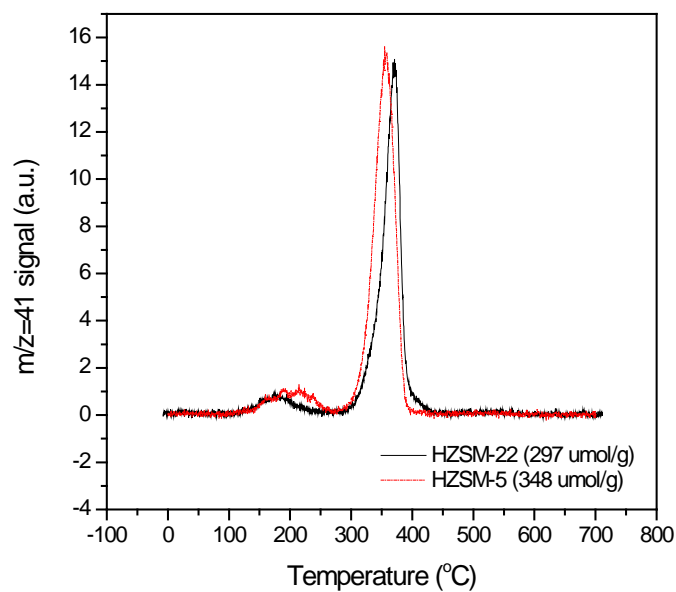


Figure 5.2. Acidity profile of HZSM-5 and HZSM-22 (both with Si/Al=45)

propylene), isoalkenes (C<sub>4</sub>-C<sub>9</sub>, mostly 2-pentene and iso-pentene), and aromatics (C<sub>7</sub>-C<sub>9+</sub>).

At the same W/F, HZSM-5 shows higher activity toward propanal conversion compared to HZSM-22, as shown in Figure 5.3. For W/F of 0.5h, the conversion is significantly higher for HZSM-5. The lower level of conversion for HZSM-22 at that W/F shows no deactivation, while HZSM-5 has significant deactivation, even from the earliest TOS measured. At W/F= 1h, the conversion on HZSM-5 was 100% for some time, reflecting excess catalyst, before sufficient deactivation begins affecting the observed conversion after two hours. For HZSM-22 at that W/F, the conversion at the shortest TOS was already at 63% and showing deactivation with a slope similar to that of HZSM-5, once its conversion is reduced below 100 %. If we compare at similar conversions, with HZSM-5 at a W/F of 0.5h and HZSM-22 at a W/F of 1.0h, we see that the slope, or deactivation rate, initially appears similar, but at longer TOS the HZSM-22 deactivation rate is reduced compared to that for HZSM-5.

In Figure 5.4, conversion and product yields are shown as a function of W/F. At short W/F in both zeolites, isoalkenes are the major product. However, at longer W/F, aromatics and gas become the dominant products on HZSM-5 in contrast to HZSM-22, where isoalkenes remain the major product.

Figure 5.5 shows the major product categories as a function of TOS for one W/F for each catalyst at similar conversion, W/F = 1h for HZSM-22 and 0.5h for HZSM-5. As the deactivation occurs, the aromatic and gas product yields decline

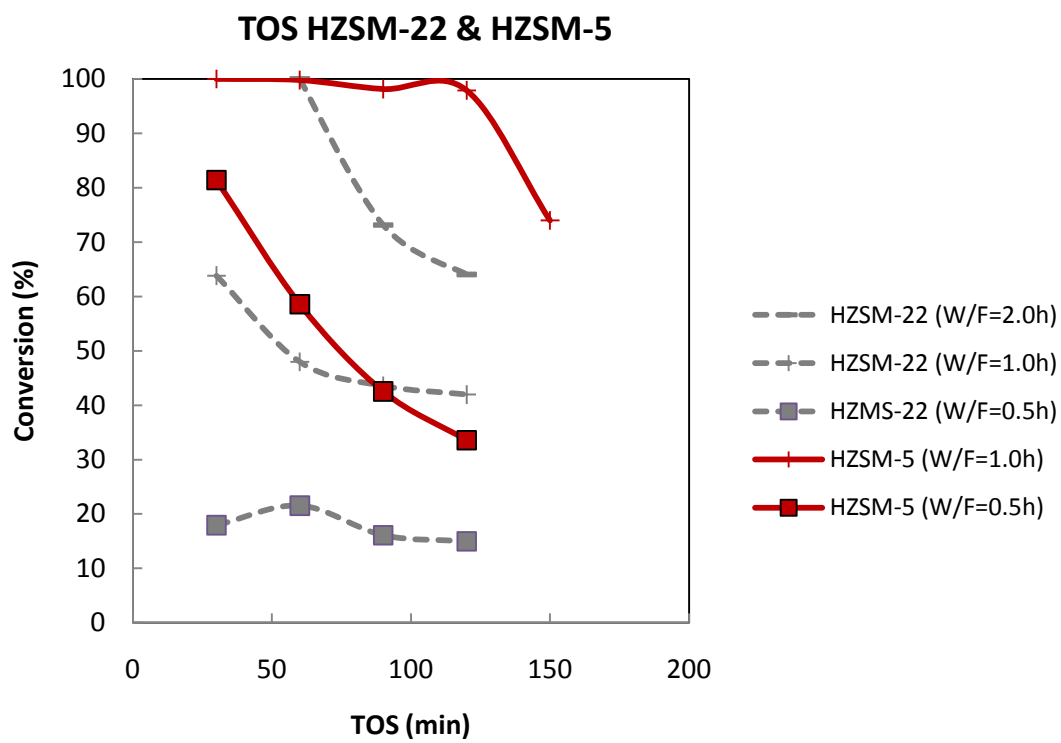


Figure 5.3. Conversion vs. TOS HZSM-22 & HZSM-5 at 400 °C, 0.12ml/h of propanal

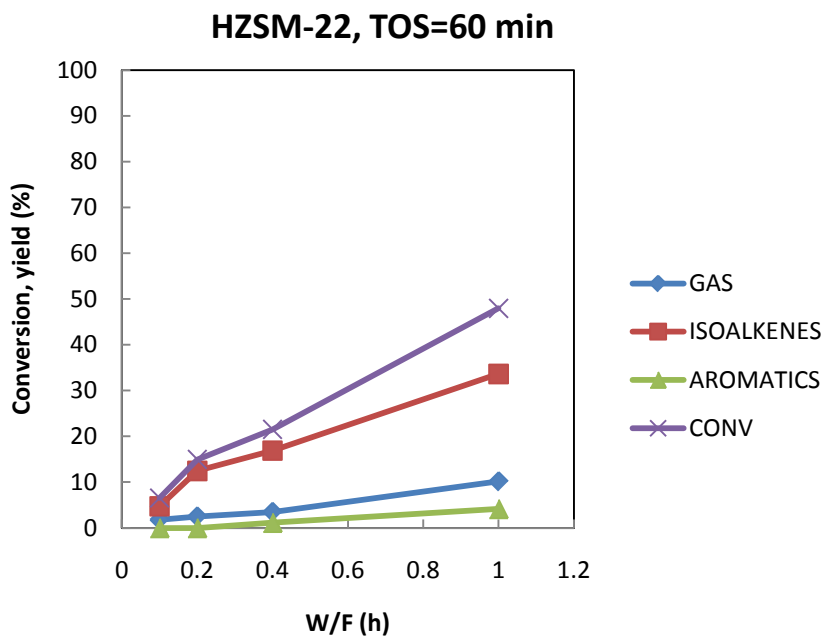
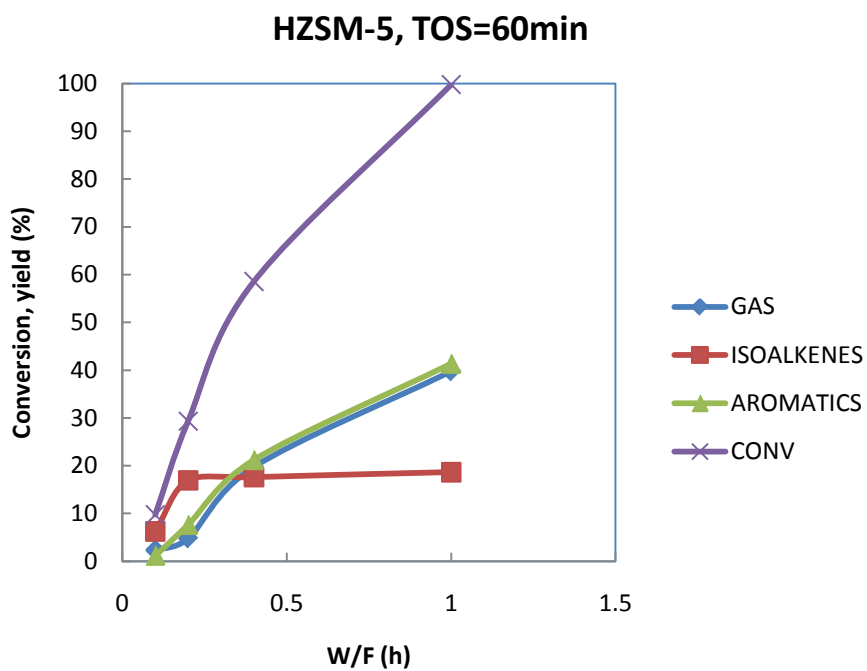


Figure 5.4. W/F series of HZSM-5 & HZSM-22 at 400 °C and TOS=60 min

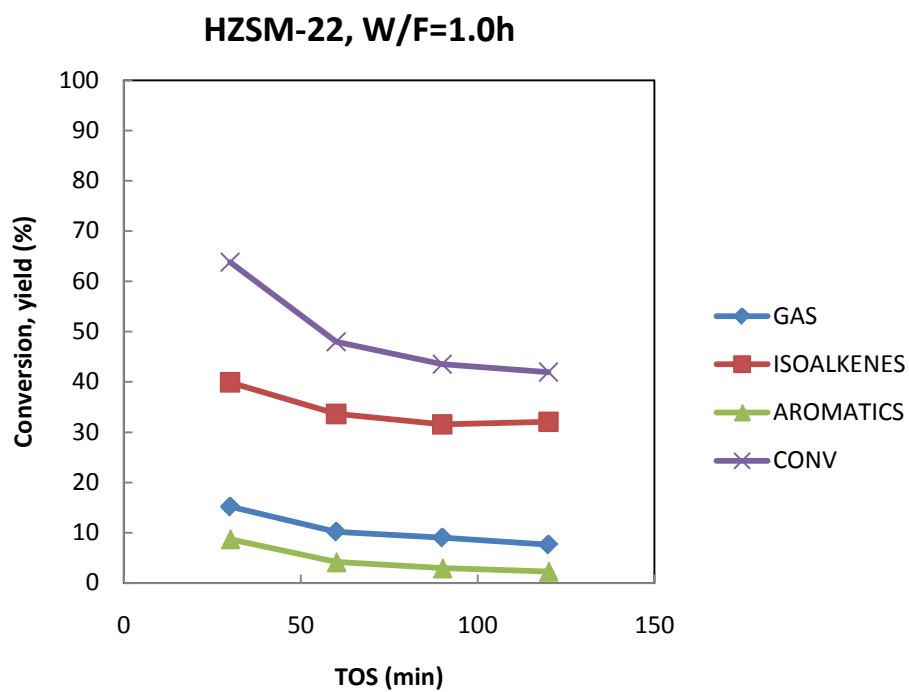
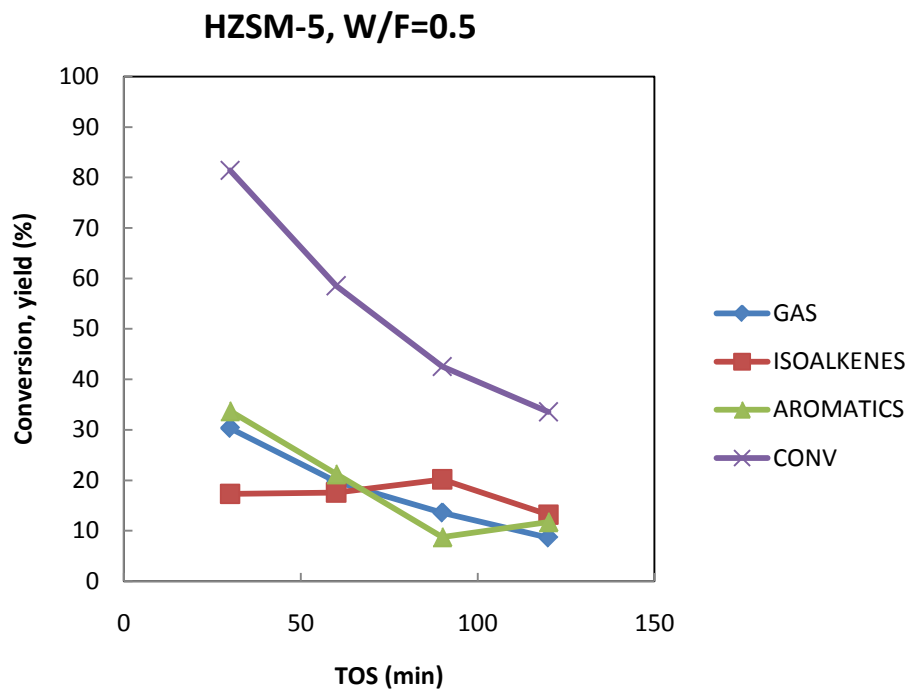


Figure 5.5. TOS of HZSM-5 & HZSM-22 at 400 °C

significantly with TOS on HZSM-5 while the isoalkene yield stays quite flat, indicating an increasing selectivity. For HZSM-22, all of the yields decline proportionally and the selectivities are essentially unchanged as deactivation proceeds.

Figure 5.6 combines results for both W/F and TOS and shows that similar trends for product yields are also observed as a function of conversion. This indicates that the catalytic function of HZSM-22 is not dramatically affected at lower conversions either at short W/F or from deactivation at longer TOS. HZSM-5 however, shows decreased aromatization at both low W/F and long TOS, in agreement with the literature indicating that the isoalkenes are intermediates for aromatization.

#### *5.4.3. Coke analysis of HZSM-22 and HZSM-5*

TPO was conducted on used catalyst samples from the experiments shown in Figure 5.5, after 120 minutes on stream and at W/F = 1h for HZSM-22 and at W/F = 0.5h for HZSM-5. The TPO profile for HZSM-22 was found to follow a bell-shape curve with a broad CO<sub>2</sub> peak from 400 °C to above 800 °C as shown in Figure 5.7a. While for HZSM-5, the peak of CO<sub>2</sub> is much larger and shows a maximum at 650 °C. Figure 5.7b shows the water peak which occurs over the temperature range of the CO<sub>2</sub> peaks up to 800 °C, but not above. There is little difference between the coke on the two catalysts below 800 °C other than the amount, with both having a similar H<sub>2</sub>O/CO<sub>2</sub> signal ratio that decreases with increasing temperature, shown in Figure 5.7c. The highest temperature peak that appears only for HZSM-22 may be an artifact that occurs because HZSM-22 has long needle shaped crystallites with pore openings

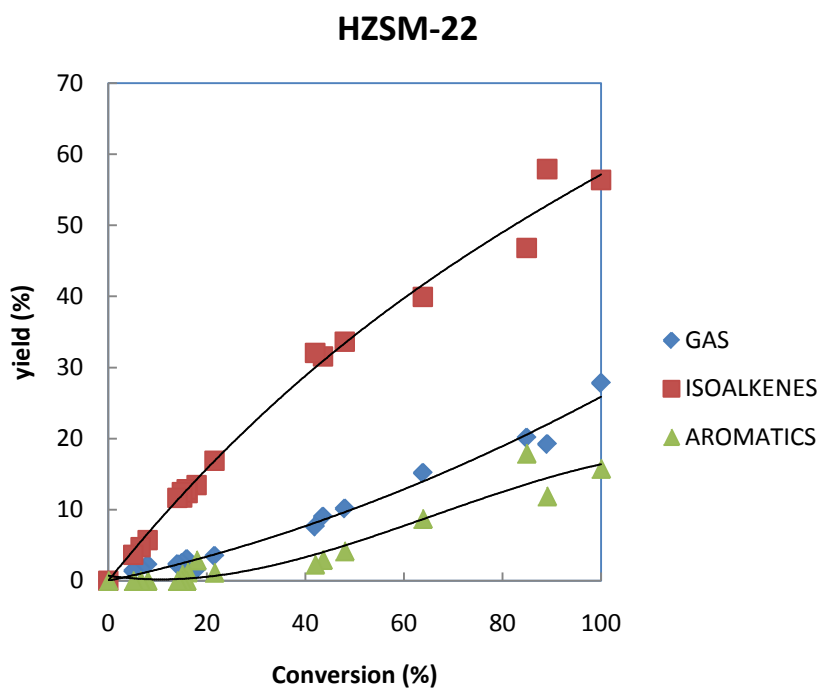
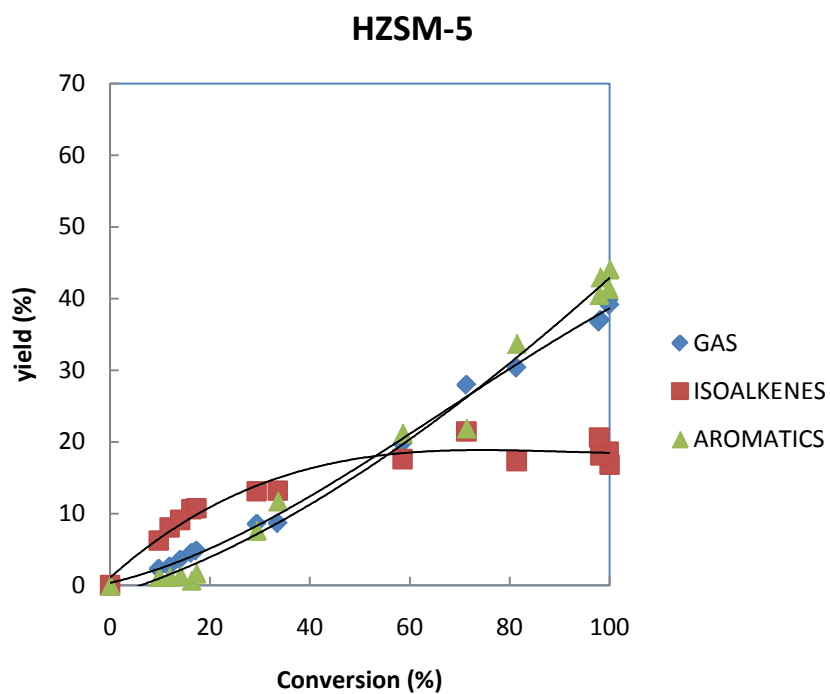


Figure 5.6. Product distribution as the function of conversion on HZSM-5 & HZSM-22, at 400 °C, with both data from TOS and W/F



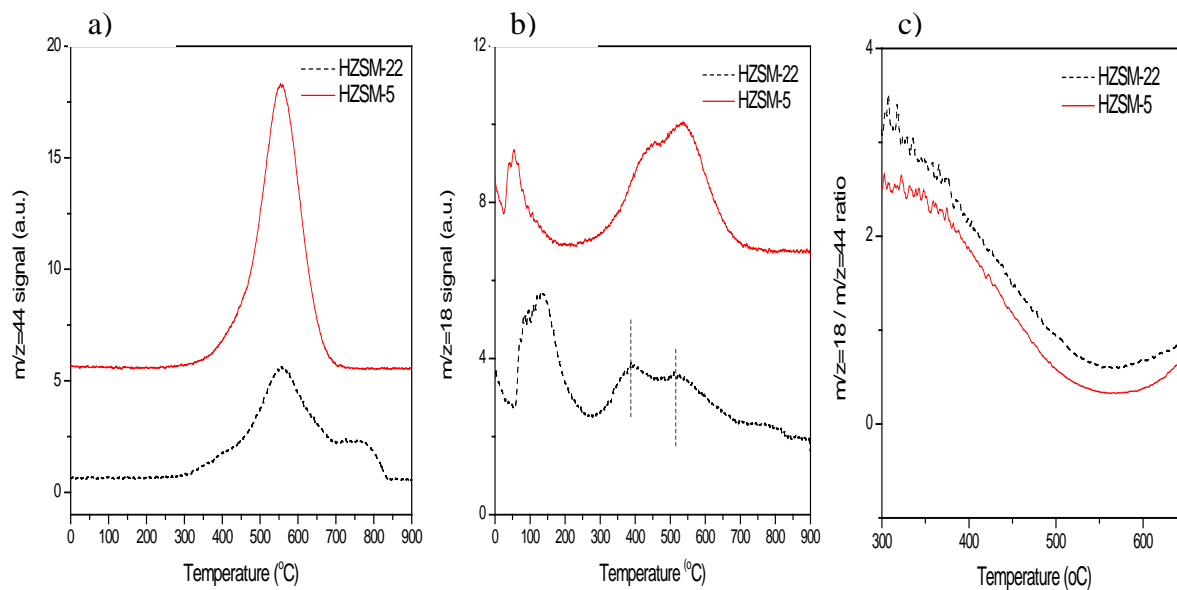


Figure 5.7. TPO of HZSM-22 at W/F=1h & HZSM-5 at W/F=0.5h, TOS=2h  
 %coke (HZSM-22) = 2.2%, %coke (HZSM-5) = 3.8%, Total coke (HZSM-22) = 1.10  
 mg/50mg CAT, Total coke (HZSM-5) = 1.98 mg/50mg CAT

on the ends that may cause a diffusion limitation for oxygen with coke present, causing a delay in the burning of the coke deep in the crystals.

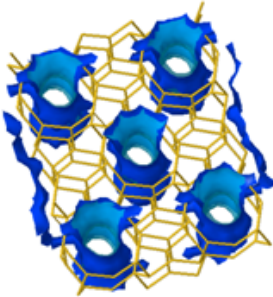
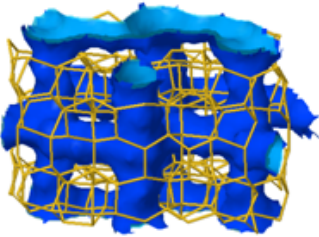
#### *5.4.4. Effect of water on catalyst activity*

To understand the effect of water on catalyst activity, water was added to the feed at a 2:1 water to propanal molar ratio after the first hour of TOS, continued for one hour and the water was stopped after that while the feed of propanal was continued, in an experiment with HZSM-22. The results show that the catalyst activity dropped as soon as water was fed. However, the catalyst activity was regained after the water was removed from the feed (Figure 5.8.) When the same experiment was conducted with HZSM-5, a similar effect was observed.

## **5.5. Discussion**

As described above, there are significant differences in the results for catalyst activity and product distribution between HZSM-5 and HZSM-22. Both zeolites have a medium pore 10 oxygen member ring structure, but, as shown in Table 5.1, the HZSM-5 pore structure is 3-dimensional with two types of intersections with window openings of 0.54 x 0.56 nm and 0.51 x 0.55 nm and a maximum diameter at the intersections of about 0.9 nm. HZSM-22 has unidimensional channels along the length of the crystallites that have pore openings of 0.55 x 0.45 nm giving more restricted accessibility. For this reason, there are more inaccessible sites on HZSM-22,

Table 5.1 – Structure properties of HZSM-22 and HZSM-5

	<b>HZSM-22</b>	<b>HZSM-5</b>
IZA code	TON	MFI
Channel dimensionality	1-D	3-D
Channel entrances	10	10-10-10
Channel diameter (nm)	0.46 x 0.57	0.53 x 0.56
View of channel system		

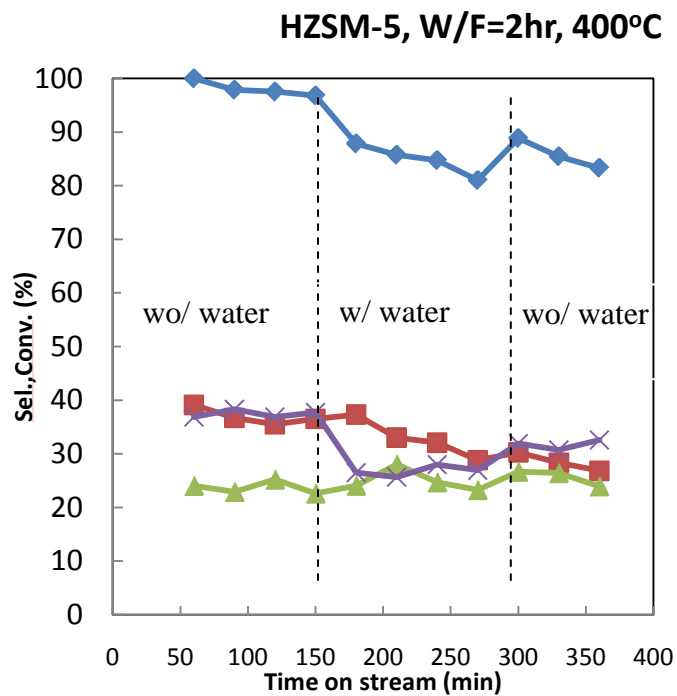
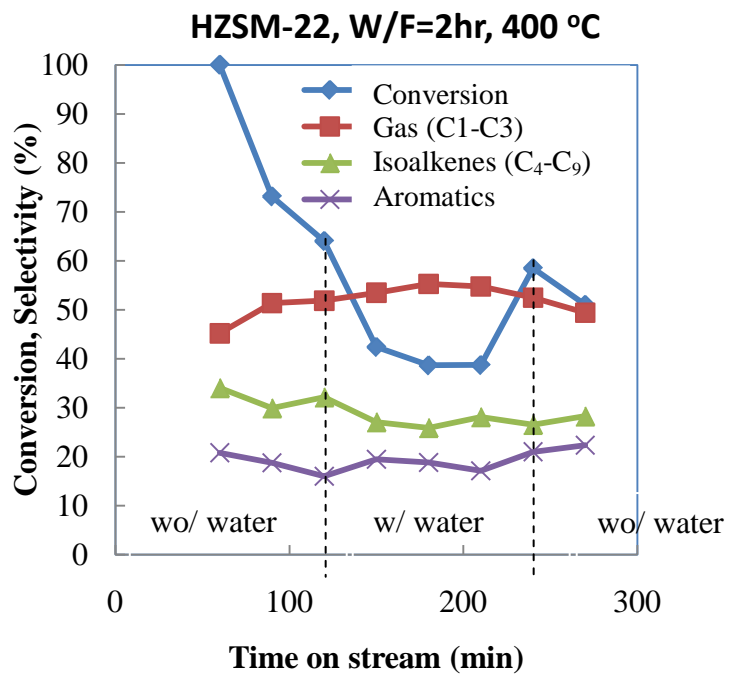


Figure 5.8. Effect of water with propanal conversion on HZSM-22 & 5

which is demonstrated by the IPA TPD results. With a higher measured acidity level, higher channel dimension, and more connectivity of channels, it is expected that the HZSM-5 has a higher activity. In addition, the pore restrictions of HZSM-22 [21] reduces access and may limit diffusion, which can further reduce activity. Moreover, aromatic molecules, having a critical diameter of 0.68nm and larger, bigger than the HZSM-22 channels, fit well within the intersection of the HZSM-5 channels. Thus, aromatics are easier to produce with HZSM-5 compared to HZSM-22, as is well known in the literature [23]. In addition, the cyclization of oligomers to form aromatics is more difficult in the smaller straight channels of HZSM-22. In fact, it has been shown using the “Refined Constraint Index” that the value for ZSM-22 is 14.5, higher than that of ZSM-5, which has a value of 10.2 [21]. This indicates HZSM-22 is more shape-selective. As found in previous work for propanal conversion on HZSM-5[14], significant aromatics were formed via cyclization of an aldol trimer. The channel structure of HZSM-22 may be expected to have significantly reduced formation and cyclization of the trimer to form aromatics via the aldol pathway.

The results from the W/F series are also consistent with previous work [14] where at short W/F, the aldol dimer oxygenate has been proposed as the major intermediate that decomposes to form isoalkenes on acid sites in HZSM-5. As W/F increases, an aldol trimer oxygenate is produced and converts to alkyl aromatics in HZSM-5, with a decrease in selectivity for isoalkenes. The increasing gas yield at higher W/F results from contributions of both dealkylation reactions of aromatics and cracking of isoalkenes. However, on HZSM-22, the channels prevent significant

formation of the trimer or aromatics, even with high conversion at long W/F. The isoalkenes that form are also less susceptible to cracking, thus the gas yield remains relatively low.

It is well recognized that intracrystalline coke formation is directly related to zeolite channel structure [24-25]. The TPO results clearly indicate that much more coke was observed on HZSM-5 even at smaller W/F. The similar deactivation rates at shorter TOS suggest that the coverage of acid sites by coke precursors occurs at similar rates. At longer TOS, as conversion is lowered, the availability of coke precursors is lower and the deactivation rate slows. The smaller decrease in deactivation rate for HZSM-5 reflects the fact that it already has almost double the amount of coke and is thus more severely impacted. In addition to coke, water also affected the performance of catalyst activity, but not the selectivity. The key reason is the reversible competitive absorption of water on the active acid sites. The fact that, in the case of bio-oil, water will be ubiquitously present, suggests that its effect can be overcome by additional catalyst.

## **5.6. Conclusions**

Direct conversion of propanal to gasoline components is demonstrated on two different structure types of medium pore zeolites. High yields of aromatics were found on HZSM-5 with its 3 dimensional pore structure. However, less aromatics and higher C<sub>4</sub>-C<sub>9</sub> isoalkenes yield were found on HZSM-22 with its 1 dimensional pore structure.

The restricted pore dimensions of HZSM-22 limited the formation of bulky aromatic molecules while allowing formation of isoalkenes from C<sub>4</sub>-C<sub>9</sub>, indicating a different shape-selective control. Propanal conversion increases on HZSM-5 with its increased micropore volume and connectivity of the channels. In contrast, a decrease in activity is associated with decreased micropore volume and no connectivity of the channels. Deactivation rates are similar at short times on stream, but HZSM-5 has a significantly higher capacity for coke. The presence of water as a byproduct reversibly deactivates sites due to competitive adsorption.

### **Acknowledgements**

Support from the National Science Foundation (EPSCoR) and US Department of Energy, Oklahoma Secretary of Energy and the Oklahoma Bioenergy Center are greatly appreciated.

### **References**

- [1] D. Mohan, C.U. Pittman, and P.H. Steele, *Energy & Fuels* 20 (2006) 848-889.
- [2] S. Czernik, and A.V. Bridgwater, *Energy & Fuels* 18 (2004) 590-598.
- [3] R. Maggi, and B. Delmon, *Hydrotreatment and Hydrocracking of Oil Fractions* 106 (1997) 99-113.
- [4] G.W. Huber, and J.A. Dumesic, *Catal Today* 111 (2006) 119-132.

- [5] E.L. Kunkes, E.I. Gürbüz, and J.A. Dumesic, *J Catal* 266 (2009) 236-249.
- [6] K.M. Dooley, A.K. Bhat, C.P. Plaisance, and A.D. Roy, *Appl Catal A-Gen* 320 (2007) 122-133.
- [7] J.D. Adjaye, and N.N. Bakhshi, *Biomass Bioenerg* 8 (1995) 131-149.
- [8] S.L. Meisel, *Studies in Surface Science and Catalysis*, Elsevier. 17-37.
- [9] F. Bandermann, and J. Fuhse, *Chemie Ingenieur Technik* 59 (1987) 607-608.
- [10] C.D. Chang, and A.J. Silvestri, *J Catal* 47 (1977) 249-259.
- [11] G.J. Hutchings, P. Johnston, D.F. Lee, A. Warwick, C.D. Williams, and M. Wilkinson, *J Catal* 147 (1994) 177-185.
- [12] T. Danuthai, S. Jongpatiwut, T. Rirksomboon, S. Osuwan, and D.E. Resasco, *Appl Catal A Gen* 361 (2009) 99-105.
- [13] T. Sooknoi, T. Danuthai, L.L. Lobban, R.G. Mallinson, and D.E. Resasco, *J Catal* 258 (2008) 199-209.
- [14] T. Hoang, X. Zhu, T. Sooknoi, D. Resasco, and R. Mallinson, *J Catal* (2010) (in press)
- [15] V.J. Frillette, W.O. Haag, and R.M. Lago, *J Catal* 67 (1981) 218-222.
- [16] Johan A. Martens, *Angewandte Chemie International Edition* 44 (2005) 5687-5690.



- [17] A.J. Marchi, and G.F. Froment, *Appl Catal* 71 (1991) 139-152.
- [18] W.J.H. Dehertog, and G.F. Froment, *Appl Catal* 71 (1991) 153-165.
- [19] A.A. Cichowlas, P.T. Wierzchowski, and L.W. Zatorski, *React Kinet Catal L* 32 (1986) 341-346.
- [20] X. Zhu, L. Lobban, D. Resasco, and R. Mallinson, *J Catal* (2010) (in press)
- [21] S. Ernst, J. Weitkamp, J.A. Martens, and P.A. Jacobs, *Appl Catal* 48 (1989) 137-148.
- [22] W.E. Farneth, and R.J. Gorte, *Chem Rev* 95 (1995) 615-635.
- [23] D. Bhattacharya, and S. Sivasanker, *J Catal* 153 (1995) 353-355.
- [24] L.D. Rollmann, *J Catal* 47 (1977) 113-121.
- [25] L.D. Rollmann, and D.E. Walsh, *J Catal* 56 (1979) 139-140.

## CHAPTER 6

### CATALYTIC AROMATIZATION OF GLYCEROL FOR BIOFUELS

#### Abstract

Substantial production of oxygenates from biomass conversion and biodiesel production create interest in upgrading these compounds to C<sub>6</sub>+ gasoline range hydrocarbon products as well as chemicals. Glycerol is the byproduct of biodiesel production and also is a model for polyol compounds in the products produced from cellulosic biomass conversion, pyrolysis in particular. This paper screens the oligomerization of glycerol on different zeolites from 300 to 400 °C and from atmospheric pressure to 300 psi in hydrogen. The main products in glycerol conversion using one dimensional zeolites MOR, OMEGA, and ZSM-22 are partially deoxygenated to carbonyl products, mainly propenal and acetol, with little evidence of oligomerization. However, it is found that glycerol can be converted to high yields of aromatics over HY and HZSM-5. Aromatics formation was observed at longer contact times, and at higher temperatures (i.e. W/F 1h and 400 °C). When the HZSM-5 catalyst bed was preceded by a bed containing a deoxygenation/hydrogenation catalyst, Pd/ZnO, the aromatics yield was further increased. The effect of Zn loading on HZSM-5 was also investigated. The presence of Zn enhances catalyst lifetime and shifts the product distribution to lighter hydrocarbon compounds. The observed

catalytic functions occur in the presence of substantial fractions of water, produced in the initial deoxygenation/dehydration of glycerol. The results shown are consistent with previous studies showing that the formation of aromatics is via an aldol condensation pathway at these relatively mild conditions.

*Keywords:* glycerol; zeolites; biodiesel; aromatization; biofuels; HZSM-22; HZSM-5; Zn-HZSM-5

## **6.1. Introduction**

Biodiesel is among the biofuels in development to reduce the dependency on fossil fuels. However, in the production of biodiesel using the transesterification reaction large amounts of glycerol are produced as a byproduct. Although glycerol and its derivatives are currently high value chemicals in the pharmaceutical and food industries among others, their volume from substantial increases of biodiesel production will greatly exceed the chemicals market. Additionally, glycerol is a model for polyols produced during pyrolysis of cellulosic feedstocks. Glycerol can be reacted to produce chemical feedstocks, especially for production of acrolein (propenal)[1-5]. However, there has been much less attention to the direct conversion of glycerol to fuel molecules that are compatible with existing fuels, such as gasoline. Therefore, the objective of this work is to study the conversion of glycerol to produce fungible hydrocarbon fuel molecules via catalytic conversion on zeolite catalysts.

Methanol to Gasoline (MTG) is a well known process for converting methanol to hydrocarbons developed by Mobil [6-8]. The products obtained by this reaction are hydrocarbons, principally aromatics, in the gasoline boiling range (C<sub>6</sub>-C<sub>10</sub>). Acidic zeolites such as HZSM-5 have been used as catalysts for MTG. The conventional reaction pathway includes three main sequential steps: (i) the dehydration of methanol to dimethyl ether; (ii) the dehydration of dimethyl ether to olefins; and (iii) the oligomerization of olefins to paraffins and aromatics. Costa and Gayubo et al. [9-11] reported the successful transformation of other alcohols and oxygenates, such as, propanol, butanol, acetone, and butanone to higher paraffins and olefins over HZSM-5. The proposed reaction scheme involves the dehydration of oxygenates to the corresponding olefins and paraffins as the first step, followed by oligomerization. Hoang et al [12] have shown that propanal is aromatized by oligomerization via an aldol pathway under mild conditions where olefins do not form significant aromatics.

In the methanol to gasoline process (MTG), the 10-MR (10-membered ring) zeolite, HZSM-5 was employed. This type of pore structure allows the production of larger molecules from C<sub>6</sub>-C<sub>10</sub> aromatics using its unique molecular traffic control of the three-dimensional channel system that also reduces the impact of coke formation, enhancing catalyst lifetime. A uniform 10-MR tubular one dimensional pore zeolite such as ZSM-22 is reported to be stable and selective for trimerization of propene[13], but did not produce substantial yields of aromatics. In the methanol to olefins process (MTO) [14], a small pore diameter zeolite was used, such as SAPO-34 with an 8-MR

opening. In that process, the main products are light olefins in the range of C<sub>2</sub>-C<sub>4</sub>, with insufficient space for formation of aromatics and larger oligomers.

Zinc has been found in the literature to be a promoter of aromatization on HZSM-5[15-17]. Introducing Zn into the zeolite framework redistributes acid-site strength and generates relatively strong Lewis acid sites that favor aromatization. It was observed that the total acidity of the zeolite was not reduced. Biscardi *et. al* [18] has suggested that the role of Zn is to facilitate the dehydrocyclodimerization reaction. Incorporation of Zn has also shown enhancement of aromatization and significant improvement of catalyst lifetime in conversion of alkyl-methyl-esters over HZSM-5[19].

The objective of this work is to investigate the conversion of glycerol using acidic zeolites with different pore geometries, specifically HZSM-5, HY, HZSM-22, HMOR, and H-OMEGA, to form aromatics. In order to achieve higher aromatics yields, a study of a dual bed system, Pd/ZnO followed by HZSM-5, and also of Zn/HZSM-5 were investigated.

## **6.2. Experimental**

### *6.2.1. Catalyst Preparation.*

HZSM-5 and HOMEAGA zeolites were supplied by SUD-CHEMIE. HY and Na-MOR zeolites were supplied by Zeolyst International. Na<sup>+</sup> ions in the Na-MOR zeolites were replaced with NH<sub>4</sub><sup>+</sup> ions by ion exchange with a NH<sub>4</sub>NO<sub>3</sub> solution at

80 °C for 10 h calculated to obtain 20% HNaMOR and 40% HNaMOR, respectively. The ZSM-22 zeolite was synthesized by following a procedure in the literature [20]. The XRD and SEM images, shown in previous work [21] confirmed that the structure was highly crystalline ZSM-22. HZSM-22 was obtained from a complete exchange with a 1M solution of  $\text{NH}_4\text{NO}_3$ . The properties of the zeolites used are shown in Table 6.1. Zn-HZSM-5 was prepared by ion exchange with a Zinc (II) nitrate solution to give a material with a Zn loading of 5 or 7 wt%. The ZnO-supported Pd catalyst (Pd/ZnO) were prepared by incipient wetness impregnation (IWI) with Palladium (II) nitrate solution (Aldrich) with an amount to obtain a metal loading of 1% Pd.

#### 6.2.2. Equipment and Procedures.

The reactor was a 10 mm inner diameter, 316 stainless steel, fixed bed continuous flow tubular reactor. The reactor was heated by a split-tube furnace (Thermal Craft) with a digital feedback temperature controller (Omega). The catalyst was treated *in situ* with He or  $\text{N}_2$  for 1hr at 400 °C before each run. Glycerol was fed using a syringe pump or high pressure piston pump, depending on reaction pressure. At elevated pressure, a back pressure regulator was used, but at atmospheric pressure, this was removed. The reaction was carried out over a range of temperatures from 300 °C to 400 °C and at W/F from 0.1h.to 1h (mass of catalyst/mass rate of organic). During reaction, the glycerol was fed together with a  $\text{H}_2$  carrier at a flow rate of 35 cc/min, giving a molar ratio of  $\text{H}_2$ : glycerol of 15:1.

When operating at higher pressure, liquid products, including water, were collected in a cold trap after accumulating for each hour of time on stream. Non-condensed products passed through the back pressure regulator and went to vent and were not quantified, but some samples were sent to an online GC for product identification. After each run, the reactor was purged with dry carrier gas for 15 minutes to collect the residual products from the reactor. The collected liquid products were found to settle into two phases: a hydrocarbon phase containing aromatics and an aqueous phase containing the oxygenates with product water. Each phase was then individually analyzed using an FID gas chromatograph (HP 6980) equipped with a capillary HP-INNOWax column and products were identified using a Shimadzu (Q2010) GC/MS. For some experiments at atmospheric pressure, where no back pressure regulator was required, all products were directly sent to the GC for online analysis. This provided a consistent basis for determining yields of all products without having to estimate separately based on the collected phase volumes.

## **6.3. Results**

### *6.3.1. Activity and stability of the zeolites.*

The reactivity of zeolites with varying pore size and channel geometry has been investigated (Table 6.1). Experiments for glycerol conversion were performed on HZSM-5, HY, HOMEGA, HNaMOR, and HZSM-22 at W/F= 0.5 hr, 300 °C and 400 °C and 300 psi pressure.

Table 6.1. – Pore structure of zeolite catalysts use

<b>Zeolite Catalyst</b>	<b>Topology code</b>	<b>Channel structure</b>	<b>Ring Members</b>	<b>Pore diameter, Å<sup>o</sup></b>
HMOR	(MOR)	1-D	12-MR	6.5 x 7 (large)
			8-MR	2.6 x 5.7 (small)
H-OMEGA	(MAZ)	1-D	12-MR	7.4 x 7.4 (large)
			8-MR	3.1 x 3.1 (small)
HZSM-22	(TON)	1-D	10-MR	4.6 x 5.7 (medium)
HY	(FAU)	3-D	12-MR	7.4 x 7.4 (large)
ZSM-5	(MFI)	3-D	10-MR	5.1 x 5.5 (medium)
				5.3 x 5.6 (medium)



Table 6.2. Products observed from glycerol conversion over HNaMOR, H-OMEGA, and HZSM-22 zeolite catalysts at 300 °C and 400 °C, W/F= 0.5h

<b>Catalysts</b>	<b>Pressure (psig)</b>	<b>Temperature (°C)</b>	<b>Products observed</b>
HNaMOR	0	300	Oxygenates
	0	400	Oxygenates
HOMEGA	0	400	Oxygenates
	300	400	Oxygenates
HZSM-22	0	400	Oxygenates

Table 6.3. Products observed from HZSM-5 and HY zeolite catalysts at 300 °C and 400 °C, W/F= 0.5h

<b>Catalysts</b>	<b>Pressure (psig)</b>	<b>Temperature (°C)</b>	<b>Products observed</b>
HZSM-5	0	400	Oxygenates and Aromatics
	300	300	Oxygenates
	300	400	Oxygenates and Aromatics
HY	300	300	Oxygenates
	300	400	Oxygenates and Aromatics

Condensed products obtained from the conversion of glycerol over HNaMOR, HOMEAGA, and HZSM-22 catalysts are all oxygenates, primarily propenal, acetol, acetaldehyde and small amounts of heavier oxygenates, in that order, and no hydrocarbons phase, including aromatics, were produced at W/F= 0.5 h (Table 6.2). The heavier oxygenates were identified by the GC/MS as a number of molecules such as: 3-methyl-2-Butanone, 2-Cyclopenten-1-one, 4-hydroxy-4-methyl-2-Pentanone, 3-Hepten-1-one, 5-ethyl-4-methyl-3-Heptanone. Results at atmospheric pressure were similar. At elevated pressure, 300 psi, the condensed products were also only oxygenates for the conversion of glycerol over HOMEAGA. Table 6.3 provides a summary of products from the conversion of glycerol over HZSM-5 and HY catalysts. It was found that at low temperature, 300 °C, oxygenate compounds were produced on HZSM-5 and HY catalysts, acetaldehyde, formaldehyde, propenal, acetol and small amounts of heavier oxygenates. At higher temperature, 400 °C, aromatics were identified. Aromatic compounds were also formed at elevated pressure (300 psi). Similar behavior was also observed on HY.

The detailed product distribution from the experiment at 400 °C, 300 psi and W/F= 0.5 h over the different zeolites is shown in Table 6.4. For 1-D zeolites, propenal is the major product and its yield is 80% on HZSM-22. While only a small amount of heavier oxygenates was observed on HZSM-22, they were more significant on HNaMOR and HOMEAGA. In contrast, on 3-D zeolites HZSM-5 and HY, aromatics, including C<sub>9</sub>, xylenes toluene and benzene, were observed. It should be pointed out

Table 6.4. Product distribution on different zeolites, T=400 °C, TOS=3 hrs,  
W/F= 0.5 hr, 300 psi

<b>CATALYST</b>	<b>HZSM-5</b>	<b>HY</b>	<b>HOMEGA</b>	<b>HNaMOR</b>	<b>HZSM-22</b>
<b>Conversion (%)</b>	<b>95.1</b>	<b>95.2</b>	<b>75.2</b>	<b>92.9</b>	<b>100</b>
<b>Oxygenates (% yield)</b>	<b>76.1</b>	<b>85.2</b>	<b>75.2</b>	<b>92.9</b>	<b>100</b>
Acetaldehyde	5.4	13.6	5.9	14.2	14.1
Propanal	4.7	13.7	0	8.9	1.1
Propenal	59.4	30.7	10.7	27.4	80.4
Acetol	1	8.2	14.7	7	2.5
Large oxygenates C <sub>4+</sub>	5.6	19	43.8	35.4	1.9
<b>Hydrocarbons (% yield)</b>	<b>20.9</b>	<b>10.1</b>			
Benzene	1.2	0.3			
Toluene	2.6	0.9			
C8 aromatics	3.6	1.9			
C9 aromatics	3.9	3.3			
C10 aromatics	4.5	3.1			
C11 aromatics	2	0.6			
C12 aromatics	3.1	0			

that fewer aromatics were produced on HY because deactivation has already occurred to a significant extent at TOS= 3h.

### 6.3.2. Glycerol conversion on HZSM-5 & HZSM-22 at different W/F.

Experiments on HZSM-5 over a range of W/F at 300 psi and 400 °C were performed. The results show that only the aqueous phase was obtained at low W/F < 0.3 h. The product mixture, mainly contained propenal, with smaller amounts of acetol, acetaldehyde, propanal, propandiol, propenol, acetone, and other heavier oxygenates, as shown in Figure 6.1a. As W/F was increased up to 1 h, the liquid products separated into two phases (aqueous and hydrocarbon). The hydrocarbon phase consisted of C<sub>9</sub>-C<sub>12</sub>, xylenes, toluene and benzene aromatics. The volume of aromatics increased with increasing W/F as shown in Figure 6.1b, up to a yield of about 35 % (carbon molar basis of liquid products) at these conditions.

At atmospheric pressure, with otherwise the same conditions as above (with online GC analysis), the results give similar product compositions with oxygenate products, mainly propenal and acetaldehyde, and aromatic products containing C<sub>6</sub>-C<sub>9</sub>, as shown in Figure 6.2a. The olefin gas yield shown, is comprised mainly of propene with a smaller amount of ethene. Experiments at much longer W/F, up to 8 h, were conducted to observe the change in product distribution even though glycerol conversion was 100% for all experiments. Propenal is a primary product and, similar to the results at high pressure, aromatics appeared beginning at W/F= 0.25 and

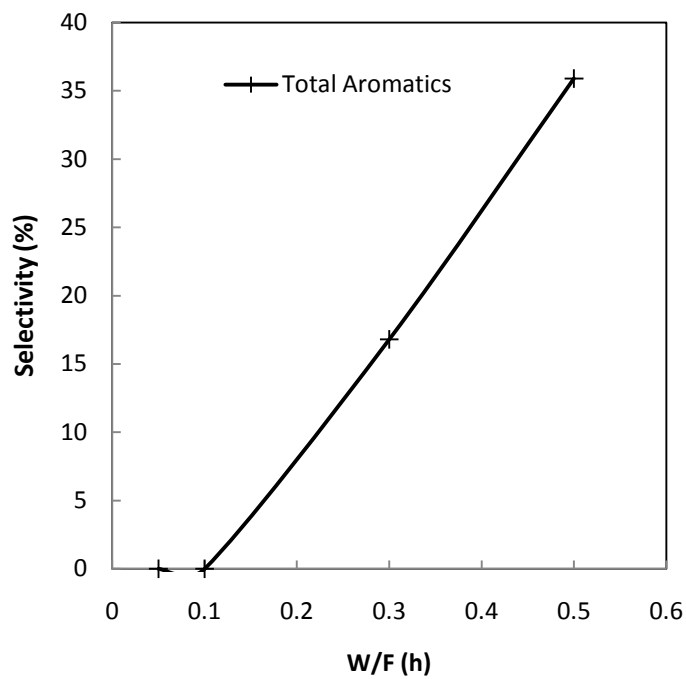
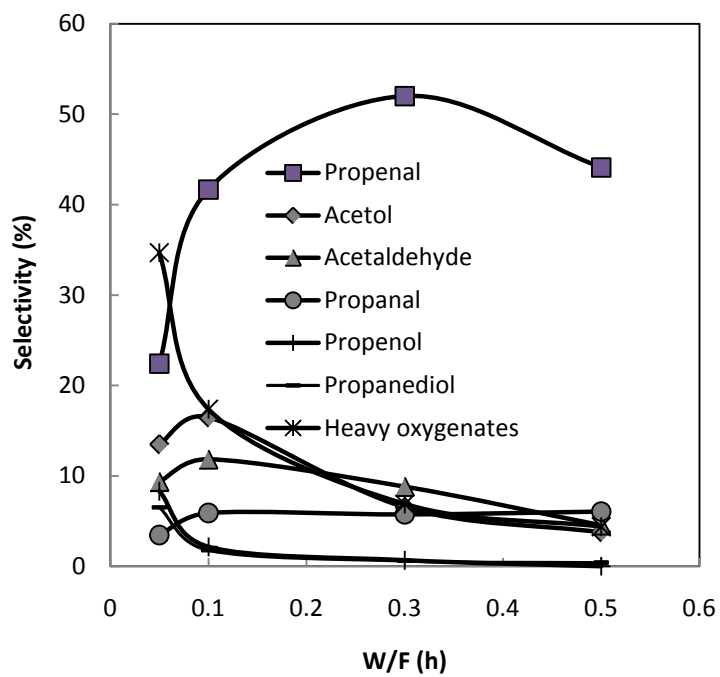


Figure 6.1. The product selectivities of glycerol conversion over HZSM-5 as a function of W/F: (a) Polar phase and (b) Non-polar phase. Reaction conditions: T = 400 °C, P = 300 psi, (data taken offline)

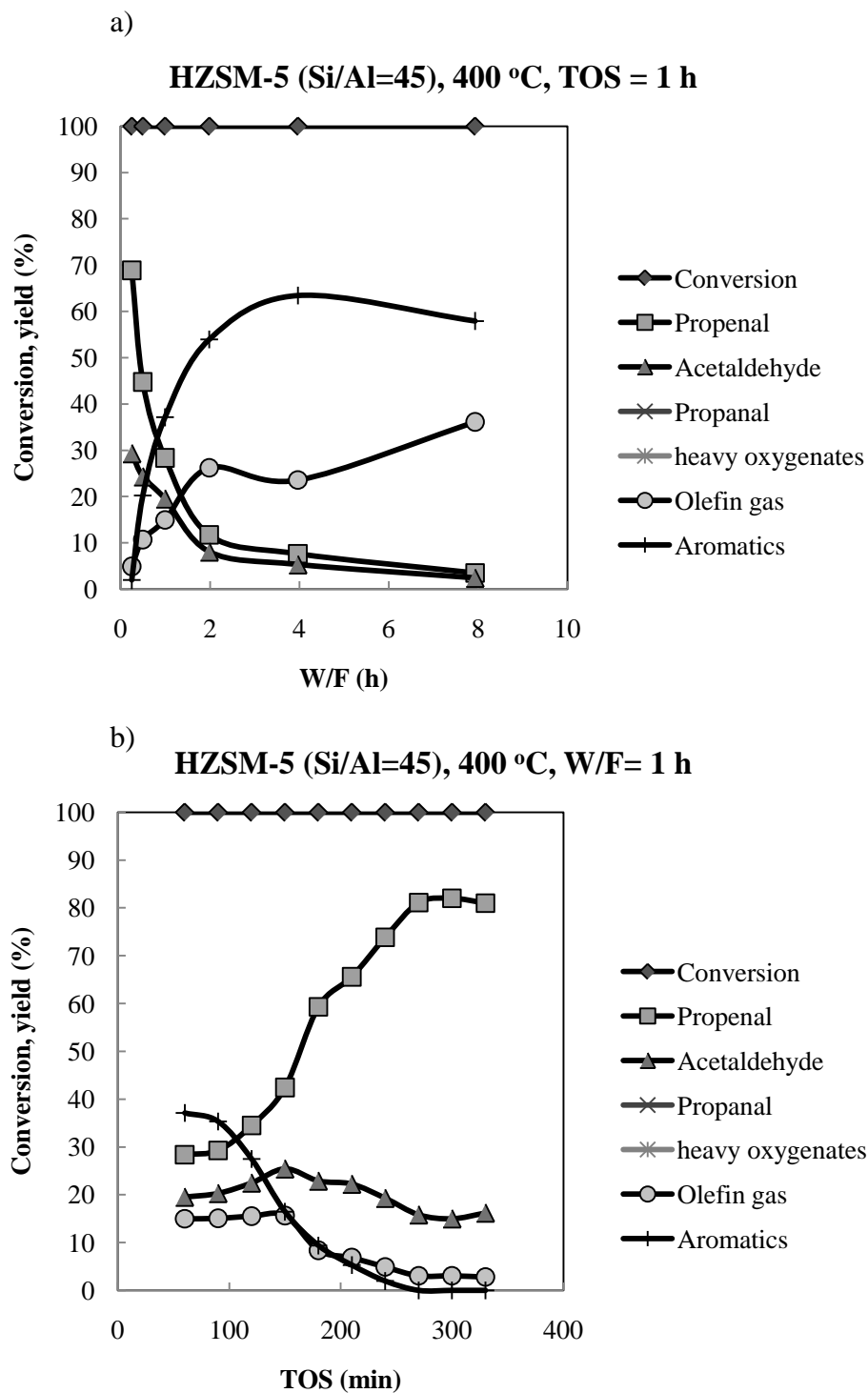


Figure 6.2. W/F series (a) and TOS (b) of glycerol conversion on HZSM-5, 400 °C, atmospheric pressure (data taken online)

increased with increasing W/F. It can be seen that aromatic yields up to 60 % are observed, with some decrease at the longest W/F due to cracking, with a concomitant increase in olefin gas yield. Figure 6.2b shows the results for W/F of 1 h as a function of time on stream (TOS). Although conversion continued at 100% with increasing TOS, significant reduction of aromatics yield is observed while propenal increases, becoming the major product. Aromatics require the internal pore configuration of the HZSM-5 to form and as deactivation and coking in the pores increases, this serial pathway is reduced [22], even with continued complete conversion of glycerol. It should be pointed out that operation at 100 % conversion of glycerol is not an indicator of lack of deactivation, but rather that an excess of catalyst has been used and that deactivation has not proceeded to an extent that shows conversion of less than 100 percent. In this case, the change in product yields is indicative of the occurrence of deactivation.

In order to investigate the activity for glycerol conversion on HZSM-22, a series of experiments was performed at different W/F at 400 °C. The results are shown in Figure 6.3. The major products are propenal and acetaldehyde. For increasing W/F from 0.12 hr to 4 hr, the propenal yield decreased from 84.4% to 68.2%, while the acetaldehyde yield increased from 11.5% to 19.6%. The olefin gas yield also increases with W/F from 0% to 4.3%. The online samples at the shortest TOS did show peaks for non-aromatic hydrocarbons, however, no higher hydrocarbon products were observed after the first sample, even at W/F= 4hr. Experiments

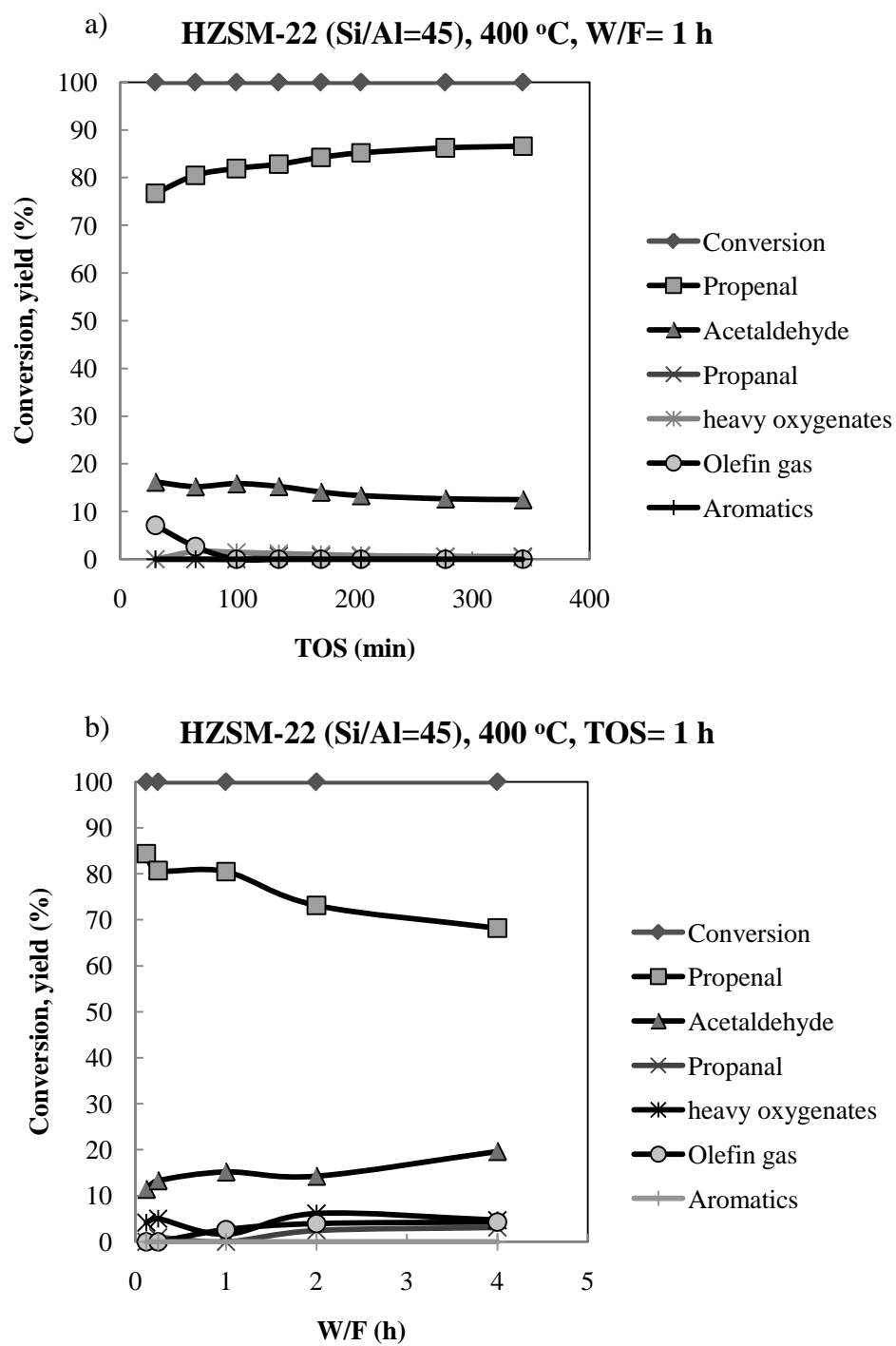


Figure 6.3. W/F (a) series and TOS (b) of glycerol conversion on HZSM-22, 400 °C, atmospheric pressure (data taken online)



operated for more than one day found continued 100 percent conversion to mostly propenal.

In order to understand the cause for the lack of hydrocarbon products on HZSM-22, an experiment with a thin bed of HZSM-5 (equivalent to W/F= 0.1 h) followed by a bed of HZSM-22 (equivalent to W/F= 2 hr) was conducted at 400 °C. In this case, the major propenal product from HZSM-5 bed is directly contacted with HZSM-22. However, the results show that no conversion to higher hydrocarbons was observed, but a lower propenal yield and increased olefin gas yield was obtained. Further investigation on HZSM-22 at W/F= 2 h was conducted with propanal, the saturated aldehyde of propenal, as the feed and high yields of isoalkenes and some aromatics were observed as the final products. Propenal is more difficult to form aromatics because of lacking alpha hydrogen for aldol condensation which is the major path of forming aromatic from propanal.

Investigation of the coke formed on HZSM-22 and HZSM-5 in these experiments shows that HZSM-5 has more coke than HZSM-22, shown in Figure 6.4 , although both zeolites have the same Si/Al of 45, it is known that HZSM-22 has somewhat less accessible acidity, 292  $\mu\text{mol/g}$  versus 350  $\mu\text{mol/g}$  determined by isopropylene amine temperature programmed desorption using the method described elsewhere[12]. The unidimensional pores opening at the ends of the needle shaped crystals suggests that a relatively small amount of coke can cause significant pore blockage that leads to significant inaccessible active sites in this channel system and limits the formation and removal of oligomers.

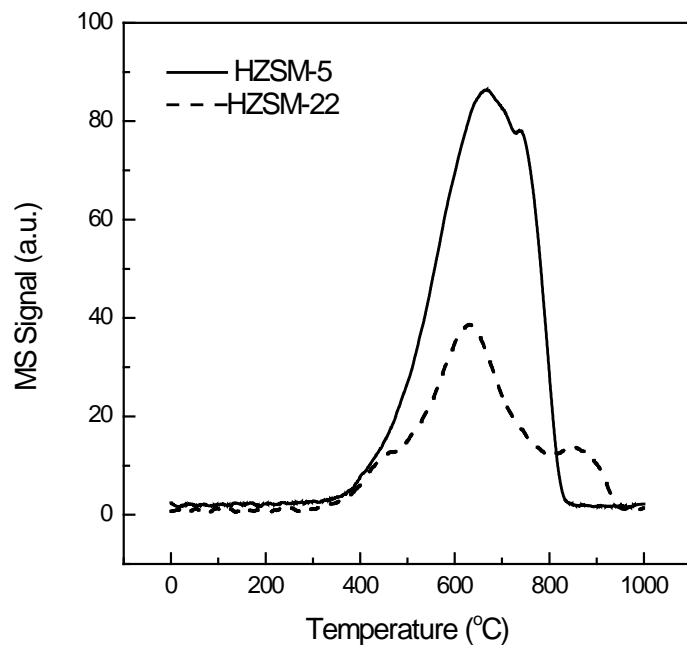


Figure 6.4. TPO of glycerol conversion on HZSM-5 & HZSM-22, 400 °C, atmospheric pressure

Table 6.5. Liquid product volume on single bed HZSM-5 and two beds PdZnO & HZSM-5, at 300 psi, T=400 °C, TOS=3 hrs, W/F= 0.5 hr

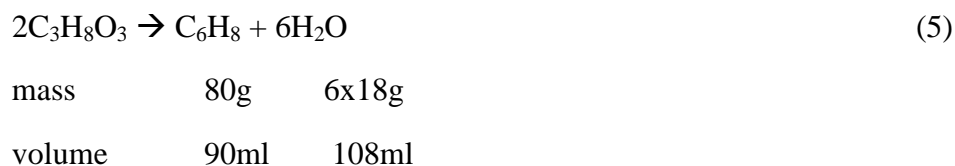
Catalysts	HZSM-5	Two Catalytic Bed Reactor (PdZnO & HZSM-5)
% Volume of Non-polar Phase (Hydrocarbon)	12	20
% Volume of Polar Phase (aqueous)	88	80
% Conversion of Glycerol	97.2	99.3

### 6.3.3. Glycerol conversion on Pd/ZnO followed by HZSM-5.

This study was made in order to separate the deoxygenation, oligomerization, and aromatization catalytic activities of the zeolite. The reaction was carried out with two catalyst beds, the first with Pd/ZnO followed by HZSM-5, operated at 300 psi.

The Pd/ZnO was placed in the first bed to partially deoxygenate the glycerol, followed by the acidic zeolite bed to oligomerize the intermediates to the final products. The products obtained from the reactions over the two beds are shown in Table 6.5. In most cases, nearly 100% of the glycerol was converted and the products formed two phases (aqueous and hydrocarbon).

These results show that the Pd/ZnO (by itself) was able to deoxygenate glycerol to partially de-oxygenated compounds, such as formaldehyde, acetaldehyde, propanal, propenal, acetone, and 1,2 propandiol, in that order. With the addition of the second bed, of HZSM-5, the oxygenate products from the first bed were able to react further to form aromatic compounds at 400 °C. There was about 20% by volume of hydrocarbon phase in the serial bed experiment while only about half of that volume was obtained from the same conditions with HZSM-5 alone. It is worth noting that the potential yield of the hydrocarbon phase by volume is a maximum of 45% (of total liquid) due to the formation of water. This is based on the stoichiometric conversion of glycerol to hydrocarbons (5).



Furthermore, at 400 °C small amounts of non-aromatic hydrocarbon products such as 2-methylbutane and 2-pentane were observed with the serial catalyst beds over HZSM-5, while no such products were found in the other experiments in this study, except the experiments with Pd/ZnO with HZSM-5 at 300 °C and the experiment with Pd/ZnO alone at 400°C. This indicates that the oligomerization function of HZSM-5 isn't active at lower temperatures, in agreement with the literature [23]. This behavior is also consistent with the results in the previous section. Hydrocarbon product distributions in the two cases of the two bed and single bed are shown in Figure 6.5. C<sub>8</sub>-C<sub>9</sub> aromatics were found as the main compounds in the hydrocarbon phase. It has been found that aromatics are predominantly produced from direct cyclization of the aldol trimer [12]. Pd/ZnO could facilitate the process by providing a fully hydrogenated monomer such as propanal that directly condenses by the aldol pathway to form the dimer and then the trimer. The conversion of glycerol and the percentages of hydrocarbon volume obtained on Pd/ZnO, HZSM-5, and Pd/ZnO with HZSM-5 as a function of time on stream are shown in Figures 6.6a and 6.6b. Compared to the single Pd/ZnO bed, glycerol conversion on HZSM-5 and Pd/ZnO with HZSM-5 did not decrease significantly with time on stream. As shown in Figure 6.6b, the hydrocarbon phase yield from the two bed experiments accounted for 20% by volume, while from the HZSM-5 only, 12% by volume was obtained over the first 3 h. The two bed experiments still provided a higher volume of hydrocarbons up to 6 h. However, no aromatics were produced after 6 h.

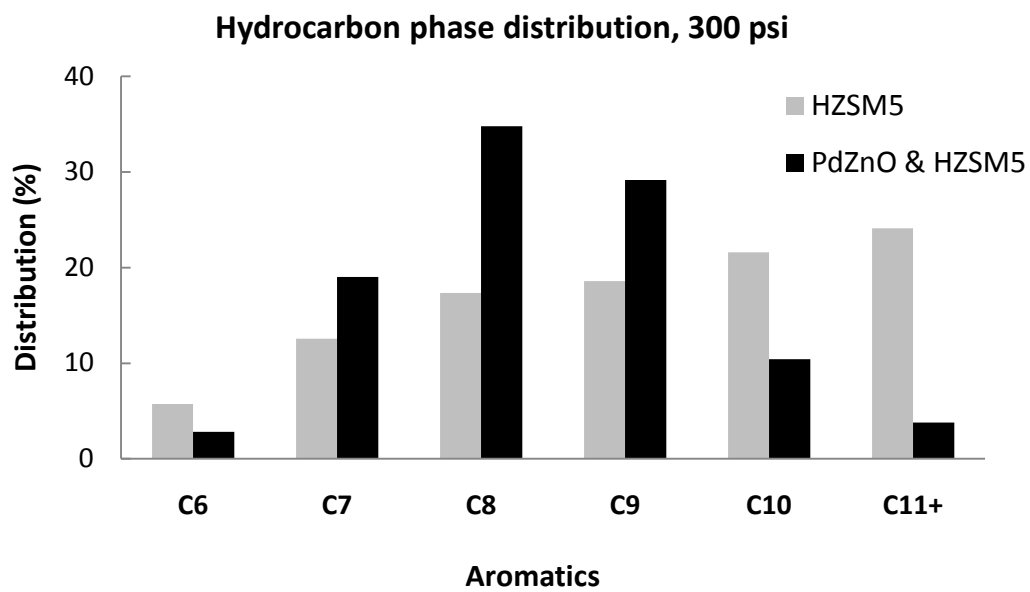


Figure 6.5. Hydrocarbon product distribution in HZSM-5 and Pd/ZnO&HZSM-5, at 400 °C, 300 psi

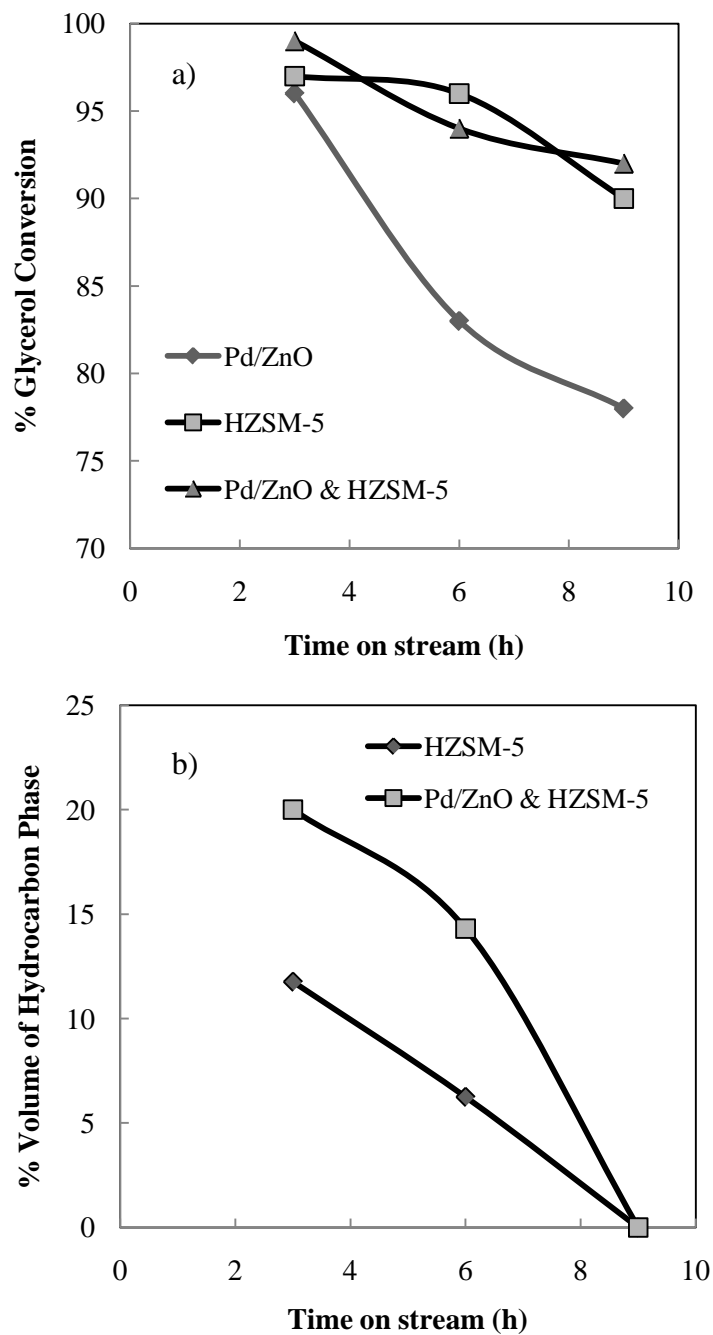


Figure 6.6– (a) Glycerol conversion at various intervals between the samples  
 (b) Percentage by volume of hydrocarbon phase at various intervals between the sample at 300 psi and 400 °C

Based on these results, it can be concluded that all of the zeolites can dehydrate glycerol. However, to make aromatic products, oligomerization of the initial products is the key reaction and this may be achieved by selection of the appropriate zeolite pore structure and reaction conditions.

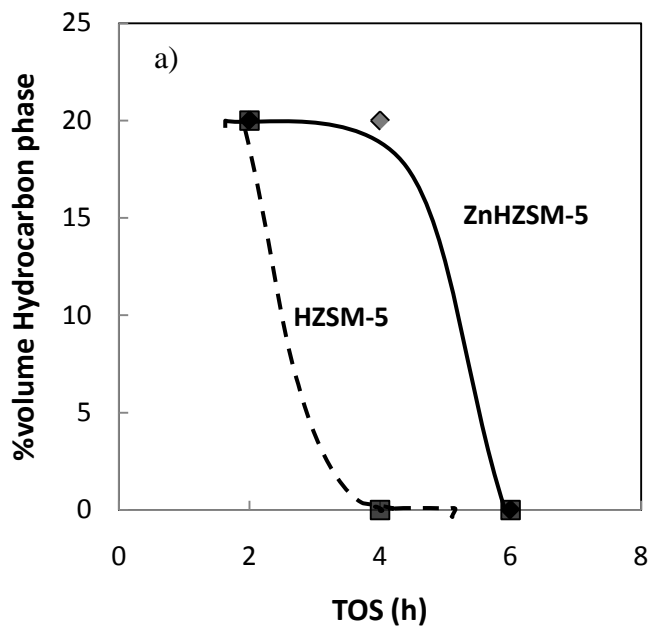
#### *6.3.4. The effect of Zn-HZSM-5.*

Zn-HZSM-5 was used to study the enhancement of aromatization activity from the conversion of glycerol. The results are shown in Figure 6.7. The role of Zn in increasing the aromatization yield was not pronounced in this case, in contrast to the work of Tanate et al [19], where aromatization via the hydrocarbon pool mechanism was significantly enhanced. However, compared to HZSM-5, it appears that the presence of Zn prolongs the catalyst lifetime for producing aromatics. The product distribution, shown in Figure 6.7, also showed lighter aromatics than when using HZSM-5.

Another experiment was conducted with 7%wt Zn-HZSM-5 with online GC product analysis. The product distribution versus TOS at W/F= 2 hr is shown in Figure 6.8. The glycerol is completely converted to aromatics (C<sub>6</sub>-C<sub>9+</sub>) at about 60% yield and olefin gas at about 40% yield.

## **6.4. Discussion**

Several possible pathways of glycerol conversion to chemicals and fuels [1] have been proposed, but three main steps have been found from the above results:



**Hydrocarbon phase distribution, atmospheric pressure**

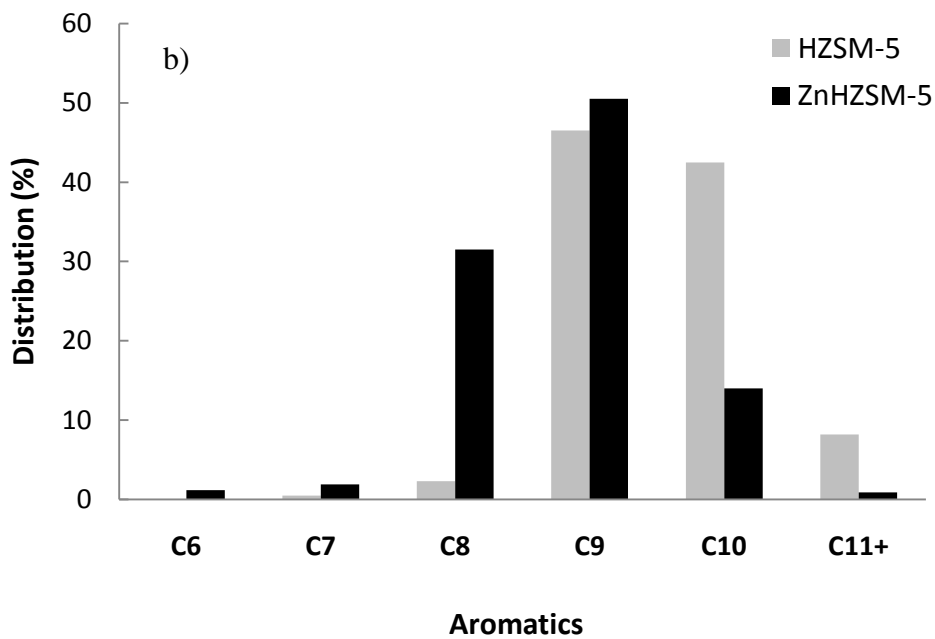


Figure 6.7. (a) Percentage by volume of aromatics product on HZSM-5 and 5% wt Zn--ZSM-5 (b) Aromatic product distribution of HZSM-5 and 5% wt Zn-HZSM-5.



(i) dehydration (ii) deoxygenation or further dehydration (iii) oligomerization (and aromatization).

#### *6.4.1. Dehydration.*

In the first step, glycerol is dehydrated to form acetol, propenal (acrolein), acetaldehyde, and formaldehyde. The potential energy plot for glycerol dehydration

has been determined by NREL using DFT calculations[24]. It has been found that decomposition of neutral glycerol requires high temperature but a substantial energy reduction occurs with addition of an acid catalyst and it is clear from these results, as well as others, that glycerol dehydration is highly active and long lived [5], even when other functions of the zeolites (oligomerization) are deactivated.

#### *6.4.2. Deoxygenation.*

In this step, oxygenates proceed through decarbonylation reactions to produce alkenes or, alternatively further dehydration, eventually producing coke and hydrogen. Acetol is subsequently dehydrated to form propenal, and can then undergo decarbonylation to produce ethylene. Internally produced hydrogen is consumed by hydrogenation or hydrogenolysis reactions. It should be pointed out that formation of large oxygenates might precede this step. Thus, larger isoalkenes could also be produced from the deoxygenation of these oxygenates, followed by oligomerization via an aldol pathway [12].

### *6.4.3. Oligomerization.*

Finally, the C<sub>2</sub>-C<sub>3</sub> alkenes as well as methanol are the precursors to produce hydrocarbons and aromatics by means of carbenium ion intermediates on the acid sites. However, this function appears to be inactive at these mild conditions [12]. It has been shown that aldol condensation of propanal forms C<sub>9</sub> aromatics via trimerization and cyclization, and that this is the predominant aromatization pathway in previous work at the mild conditions of this study [12]. However, the results from the experiments for the series of 2 beds with HZSM-5 followed by HZSM-22 has shown that propenal does not form aromatics and isoalkenes directly, in contrast to the results from propanal. This suggests that propenal cannot oligimerize via the aldol reaction pathway due to the lack of hydrogen in the alpha position.

Lastly, the point was made above that with the initial dehydration of the glycerol, substantial water is present during these reactions. Also, the production of bio-oil from biomass pyrolysis produces substantial water. Other work [21], as well as the present study, have demonstrated that water reduces the activity of the catalyst, but does not completely deactivate the initial dehydration, or the aromatization function of the catalysts.

## **6.5. Conclusions**

In summary, three main conclusions can be drawn from this study. First, the effect of pore diameter and the channel system of the zeolite plays a role in final

product distribution. Glycerol was found to be effectively converted on HZSM-5 to aromatics. Even under the limited screening regime of this study, an aromatics yield of up to 60% has been achieved. Although one dimensional zeolites were not successful in converting glycerol directly to larger hydrocarbons, HZSM-22 was able to transform glycerol to a high yield of propenal, up to 80 %, an important chemical product. Second, the presence of a Pd/ZnO catalyst bed before the HZSM-5 demonstrated a significant enhancement of liquid hydrocarbon yield by partially deoxygenating, and hydrogenating, the feed to HZSM-5. This could also be used in the same fashion with HZSM-22, to obtain good yields of higher isoalkenes. Third, addition of Zn in HZSM-5 shows promising results for enhancing catalyst life while maintaining a high yield of aromatics through a change in the nature of the acid sites. From the proposed reaction pathway, there are three main reactions that lead to production of hydrocarbons from glycerol: dehydration, deoxygenation and oligomerization. These results suggest a strategy for developing a selective catalyst for glycerol conversion to fungible fuels.

## **Acknowledgements**

The work has been financially supported by the Oklahoma Secretary of Energy and Oklahoma Center for the Advancement of Science and Technology (OCAST). One of the authors (T.D.) would like to thank Thailand Research Fund under the Royal Golden Jubilee Ph.D. Program for scholarship. The assistance of Grant Ballantyne in the synthesis of the ZSM-22 and its characterization is appreciated.

## References

- [1] B. Katryniok, S. Paul, M. Capron, and F. Dumeignil, *Chemsuschem* 2 (2009) 719-730.
- [2] A. Corma, G.W. Huber, L. Sauvanauda, and P. O'Connor, *J Catal* 257 (2008) 163-171.
- [3] K. Pathak, K.M. Reddy, N.N. Bakhshi, and A.K. Dalai, *Applied Catalysis A: General* 372 (2010) 224-238.
- [4] W. Suprun, M. Lutecki, T. Haber, and H. Papp, *Journal of Molecular Catalysis A: Chemical* 309 (2009) 71-78.
- [5] C.-J. Jia, Y. Liu, W. Schmidt, A.-H. Lu, and F. Schüth, *J Catal* 269 (2010) 71-79.
- [6] C.D. Chang, and A.J. Silvestri, *J Catal* 47 (1977) 249-259.
- [7] C.D. Chang, W.H. Lang, and R.L. Smith, *J Catal* 56 (1979) 169-173.
- [8] C.D. Chang, *Catalysis Reviews-Science and Engineering* 25 (1983) 1-118.
- [9] A.G. Gayubo, A.T. Aguayo, A. Atutxa, R. Aguado, and J. Bilbao, *Ind Eng Chem Res* 43 (2004) 2610-2618.
- [10] A.G. Gayubo, A.T. Aguayo, A. Atutxa, R. Aguado, M. Olazar, and J. Bilbao, *Ind Eng Chem Res* 43 (2004) 2619-2626.

- [11] E. Costa, J. Aguado, G. Ovejero, and P. Canizares, *Ind Eng Chem Res* 31 (1992) 1021-1025.
- [12] T. Hoang, X. Zhu, T. Sooknoi, D. Resasco, and R. Mallinson, *J Catal* (2010) (in press)
- [13] Johan A. Martens, *Angewandte Chemie International Edition* 44 (2005) 5687-5690.
- [14] P.T. Barger-UOP. 1992. Methanol conversion process using SAPO catalysts
- [15] J.A. Biscardi, E. Iglesia, *Catal Today* vol. 31, (1996) pp. 207-231.
- [16] A. Smieková, E. Rojasová, P. Hudec, and L. abo, *Applied Catalysis A: General* Volume 268 (2004) Pages 235-240
- [17] E. Rojasova, A. Smieskova, P. Hudec, Z. Zidek, *Collection of Czechoslovak Chemical Communications* 64 (1999) 168-176.
- [18] J.A. Biscardi, and E. Iglesia, *J Catal* 182 (1999) 117-128.
- [19] T. Danuthai, S. Jongpatiwut, T. Rirksomboon, S. Osuwan, and D.E. Resasco, *Catal Lett* 132 (2009) 197-204.
- [20] S. Ernst, J. Weitkamp, J.A. Martens, and P.A. Jacobs, *Applied Catalysis* 48 (1989) 137-148.
- [21] T. Hoang, X. Zhu, D. Resasco, L. Lobban, and R. Mallinson, *Cat. Comm* (2010) (Submitted)

- [22] D. Bhattacharya, and S. Sivasanker, *J Catal* 153 (1995) 353-355.
- [23] M. Stöcker, *Micropor Mesopor Mat* 29 (1999) 3-48.
- [24] M.R. Nimlos, S.J. Blanksby, X. Qian, M.E. Himmel, and D.K. Johnson, *J. Phys. Chem. A* 110 (2006) 6145-6156.

## CHAPTER 7

### CONCLUSIONS

The conversion of small oxygenates on zeolites has demonstrated promising results and significant understanding/findings. The most important finding was in Chapter 3 in which it has been shown that the predominant pathway of aromatic formation is from aldol condensation and cyclization of trimer on HZSM-5 at milder conditions. Under these conditions propylene does not produce significant aromatics and is much less reactive. This pathway for aromatics formation is much more effective than the conventional acid-catalyzed alkane/alkene conversion on zeolites. In addition, it takes place at milder conditions than those required from alkane/alkenes, with consequently lower rates of deactivation and less undesirable cracking. The practical impact of this is that highly alkylated aromatics are formed with little benzene.

Chapter 4 and 5 investigated a number of effects of the zeolite structure and properties of crystallite size and pore structure on the performance for production of aromatics. The results from these chapters strongly support what was found in Chapter 3. Significant initial C<sub>9</sub> aromatics were produced on small crystallites due to rapid removal of products from its shorter intracrystalline diffusion path length. As a result, much less deactivation, isomerization, and cracking were observed compared to the behavior over large crystallites. The results from HZSM-22 and HZSM-5 also

show that steric effects on HZSM-22, with narrower pore openings and a single dimension channel structure were important. Thus, production of aromatics on this zeolite was significantly reduced. However, much higher isoalkenes yields were observed. The effect of water was also investigated and the results show reduction in activity due to competitive adsorption. But the activity of the catalyst was regained when no added water was introduced, and the catalyst was able to perform at a lower level, operating along the same pathway

Chapter 6 gives an example of converting a highly oxygenated molecule to a high yield of aromatics. The results show a promising concept of combination two catalyst beds for further increasing aromatic yield. The importance of this idea is based on the finding in Chapter 3 that aromatics are produced more predominantly via the aldol pathway. By deoxygenation/ hydrogenation of glycerol in the first step to the hydrogenated oxygenate intermediate, more aromatics were produced.

From the results established in this work, the author hopes that conversion of small oxygenates to alkyl aromatics on zeolites has been advanced in understanding and application. Applying these findings should help in designing catalysts and reactor systems to achieve application in bio-oil refining.



## BIBLIOGRAPHY

- (1) Pathak, K.; Reddy, K. M.; Bakhshi, N. N.; Dalai, A. K. *Applied Catalysis A: General* 2010, 372, 224.
- (2) Jia, C.-J.; Liu, Y.; Schmidt, W.; Lu, A.-H.; Schüth, F. *J Catal* 2010, 269, 71.
- (3) Zilková, N.; Bejblová, M.; Gil, B.; Zones, S. I.; Burton, A. W.; Chen, C.-Y.; Musilová-Pavlacková, Z.; Kosová, G.; Cejka, J. *J Catal* 2009, 266, 79.
- (4) Zhu, X.; Lobban, L.; Resasco, D.; Mallinson, R. *J Catal* 2010 (in press).
- (5) Suprun, W.; Lutecki, M.; Haber, T.; Papp, H. *Journal of Molecular Catalysis A: Chemical* 2009, 309, 71.
- (6) Stallmach, F.; Snurr, R. Q.; Stöcker, M.; Theodorou, D. N. *Micropor Mesopor Mat* 2009, 125, 1.
- (7) Nishiyama, N.; Kawaguchi, M.; Hirota, Y.; Van Vu, D.; Egashira, Y.; Ueyama, K. *Appl Catal a-Gen* 2009, 362, 193.
- (8) Madeira, F. F.; Gnep, N. S.; Magnoux, P.; Maury, S.; Cadran, N. *Applied Catalysis A: General* 2009, 367, 39.
- (9) Kunkes, E. L.; Gürbüz, E. I.; Dumesic, J. A. *J Catal* 2009, 266, 236.
- (10) Katryniok, B.; Paul, S.; Capron, M.; Dumeignil, F. *Chemsuschem* 2009, 2, 719.
- (11) Gaertner, C. A.; Serrano-Ruiz, J. C.; Braden, D. J.; Dumesic, J. A. *J Catal* 2009, 266, 71.
- (12) Crossley, S. Dissertation, University of Oklahoma, 2009.
- (13) Carlson, T. R.; Tompsett, G. A.; Conner, W. C.; Huber, G. W. *Top Catal* 2009, 52, 241.
- (14) Bedmutha, R. J.; Ferrante, L.; Briens, C.; Berruti, F.; Inculet, I. *Chemical Engineering and Processing: Process Intensification* 2009, 48, 1112.
- (15) Balat, M.; Balat, M.; Kirtay, E.; Balat, H. *Energy Conversion and Management* 2009, 50, 3147.

- (16) Sooknoi, T.; Danuthai, T.; Lobban, L. L.; Mallinson, R. G.; Resasco, D. E. *J Catal* 2008, 258, 199.
- (17) Simonetti, D. A.; Dumesic, J. A. *Chemsuschem* 2008, 1, 725.
- (18) Neri, G.; Rizzo, G.; De Luca, L.; Corigliano, F.; Arrigo, I.; Donato, A. *Catal Commun* 2008, 9, 2085.
- (19) Corma, A.; Huber, G. W.; Sauvanauda, L.; O'Connor, P. *J Catal* 2008, 257, 163.
- (20) Dooley, K. M.; Bhat, A. K.; Plaisance, C. P.; Roy, A. D. *Appl Catal a-Gen* 2007, 320, 122.
- (21) Chheda, J. N.; Huber, G. W.; Dumesic, J. A. *Angew Chem Int Edit* 2007, 46, 7164.
- (22) Chheda, J. N.; Dumesic, J. A. *Catal Today* 2007, 123, 59.
- (23) Mohan, D.; Pittman, C. U.; Steele, P. H. *Energy & Fuels* 2006, 20, 848.
- (24) Huber, G. W.; Dumesic, J. A. *Catal Today* 2006, 111, 119.
- (25) Armaroli, T.; Simon, L. J.; Digne, M.; Montanari, T.; Bevilacqua, M.; Valtchev, V.; Patarin, J.; Busca, G. *Applied Catalysis A: General* 2006, 306, 78.
- (26) Zhang, P. Q.; Xu, J. G.; Wang, X. S.; Guo, H. C. *Chinese J Catal* 2005, 26, 216.
- (27) Yang, G.; Wang, Y.; Zhou, D.; Liu, X.; Han, X.; Bao, X. *Journal of Molecular Catalysis A: Chemical* 2005, 237, 36.
- (28) Zhang, X.; Man Lai, E. S.; Martin-Aranda, R.; Yeung, K. L. *Applied Catalysis A: General* 2004, 261, 109.
- (29) Waku, T.; Biscardi, J. A.; Iglesia, E. *J Catal* 2004, 222, 481.
- (30) Saravanamurugan, S.; Palanichamy, M.; Arabindoo, B.; Murugesan, V. *Journal of Molecular Catalysis A: Chemical* 2004, 218, 101.
- (31) Gayubo, A. G.; Aguayo, A. T.; Castilla, M.; Moran, A. L.; Bilbao, J. *Chem Eng Commun* 2004, 191, 944.
- (32) Gayubo, A. G.; Aguayo, A. T.; Atutxa, A.; Prieto, R.; Bilbao, J. *Ind Eng Chem Res* 2004, 43, 5042.
- (33) Gayubo, A. G.; Aguayo, A. T.; Atutxa, A.; Prieto, R.; Bilbao, J. *Energy & Fuels* 2004, 18, 1640.

- (34) Gayubo, A. G.; Aguayo, A. T.; Atutxa, A.; Aguado, R.; Olazar, M.; Bilbao, J. *Ind Eng Chem Res* 2004, 43, 2619.
- (35) Gayubo, A. G.; Aguayo, A. T.; Atutxa, A.; Aguado, R.; Bilbao, J. *Ind Eng Chem Res* 2004, 43, 2610.
- (36) Czernik, S.; Bridgwater, A. V. *Energy & Fuels* 2004, 18, 590.
- (37) Bai, J.; Liu, S. L.; Xie, S. J.; Xu, L. Y.; Lin, L. W. *Chinese J Catal+* 2004, 25, 70.
- (38) Waku, T.; Biscardi, J. A.; Iglesia, E. *Chem Commun* 2003, 1764.
- (39) Gayubo, A. G.; Aguayo, A. T.; Olazar, M.; Vivanco, R.; Bilbao, J. *Chem Eng Sci* 2003, 58, 5239.
- (40) Zuo, B. J.; Wang, Q. L.; Wang, Y.; Ma, Y. D. *Chinese J Catal+* 2002, 23, 555.
- (41) Yu, S. Y.; Biscardi, J. A.; Iglesia, E. *J Phys Chem B* 2002, 106, 9642.
- (42) Melo, L.; Llanos, A.; Mediavilla, M.; Moronta, D. *Journal of Molecular Catalysis A: Chemical* 2002, 177, 281.
- (43) Kareem, A.; Chand, S.; Mishra, I. M. *J Sci Ind Res India* 2001, 60, 319.
- (44) Olazar, M.; Aguado, R.; Bilbao, J.; Barona, A. *Aiche Journal* 2000, 46, 1025.
- (45) Minachev, K. M.; Isakov, Y. I.; Dmitriev, R. V.; Jaeger, N. I. *Petrol Chem+* 2000, 40, 315.
- (46) Iglesia, E.; Yu, S. Y.; Wei, L.; Biscardi, J. A. *Abstr Pap Am Chem S* 2000, 219, U249.
- (47) Stöcker, M. *Micropor Mesopor Mat* 1999, 29, 3.
- (48) Rekoske, J. E.; Barteau, M. A. *Langmuir* 1999, 15, 2061.
- (49) Möller, K. P.; Böhringer, W.; Schnitzler, A. E.; van Steen, E.; O'Connor, C. T. *Micropor Mesopor Mat* 1999, 29, 127.
- (50) Faramawy, S. *Petrol Sci Technol* 1999, 17, 249.
- (51) Chen, D.; Moljord, K.; Fuglerud, T.; Holmen, A. *Micropor Mesopor Mat* 1999, 29, 191.
- (52) Biscardi, J. A.; Iglesia, E. *J Catal* 1999, 182, 117.
- (53) Biscardi, J. A.; Iglesia, E. *Phys Chem Chem Phys* 1999, 1, 5753.

- (54) Kunkeler, P. J.; van der Waal, J. C.; Bremmer, J.; Zuurdeeg, B. J.; Downing, R. S.; van Bekkum, H. *Catal Lett* 1998, 53, 135.
- (55) Biscardi, J. A.; Meitzner, G. D.; Iglesia, E. *J Catal* 1998, 179, 192.
- (56) Biscardi, J. A.; Iglesia, E. *J Phys Chem B* 1998, 102, 9284.
- (57) Sapre, A. V. *Chem Eng Sci* 1997, 52, 4615.
- (58) Maggi, R.; Delmon, B. *Hydrotreatment and Hydrocracking of Oil Fractions* 1997, 106, 99.
- (59) Li, Y.-G.; Xie, W.-H.; Yong, S. *Applied Catalysis A: General* 1997, 150, 231.
- (60) Li, Y. G.; Xie, W. H.; Yong, S. *Appl Catal a-Gen* 1997, 150, 231.
- (61) Iglesia, E.; Barton, D. G.; Biscardi, J. A.; Gines, M. J. L.; Soled, S. L. *Catal Today* 1997, 38, 339.
- (62) Holderich, W. F.; Roseler, J.; Heitmann, G.; Liebens, A. T. *Catal Today* 1997, 37, 353.
- (63) Horne, P. A.; Williams, P. T. *Renew Energ* 1996, 7, 131.
- (64) Horne, P. A.; Williams, P. T. *Fuel* 1996, 75, 1051.
- (65) Horne, P. A.; Williams, P. T. *Fuel* 1996, 75, 1043.
- (66) Horne, P. A.; Williams, P. T. *Waste Manage* 1996, 16, 579.
- (67) Gayubo, A. G.; Benito, P. L.; Aguayo, A. T.; Castilla, M.; Bilbao, J. *Chem Eng Sci* 1996, 51, 3001.
- (68) Buchanan, J. S.; Santiesteban, J. G.; Haag, W. O. *J Catal* 1996, 158, 279.
- (69) Biscardi, J. A.; Iglesia, E. *Catal Today* 1996, 31, 207.
- (70) Adjaye, J. D.; Katikaneni, S. P. R.; Bakhshi, N. N. *Fuel Process Technol* 1996, 48, 115.
- (71) Xiong, Y. S.; Rodewald, P. G.; Chang, C. D. *J Am Chem Soc* 1995, 117, 9427.
- (72) Williams, P. T.; Horne, P. A. *J Anal Appl Pyrol* 1995, 31, 15.
- (73) Petrik, L. F.; OConnor, C. T.; Schwarz, S. *Catalysis by Microporous Materials* 1995, 94, 517.
- (74) Horne, P. A.; Williams, P. T. *J Anal Appl Pyrol* 1995, 34, 65.
- (75) Farneth, W. E.; Gorte, R. J. *Chem Rev* 1995, 95, 615.

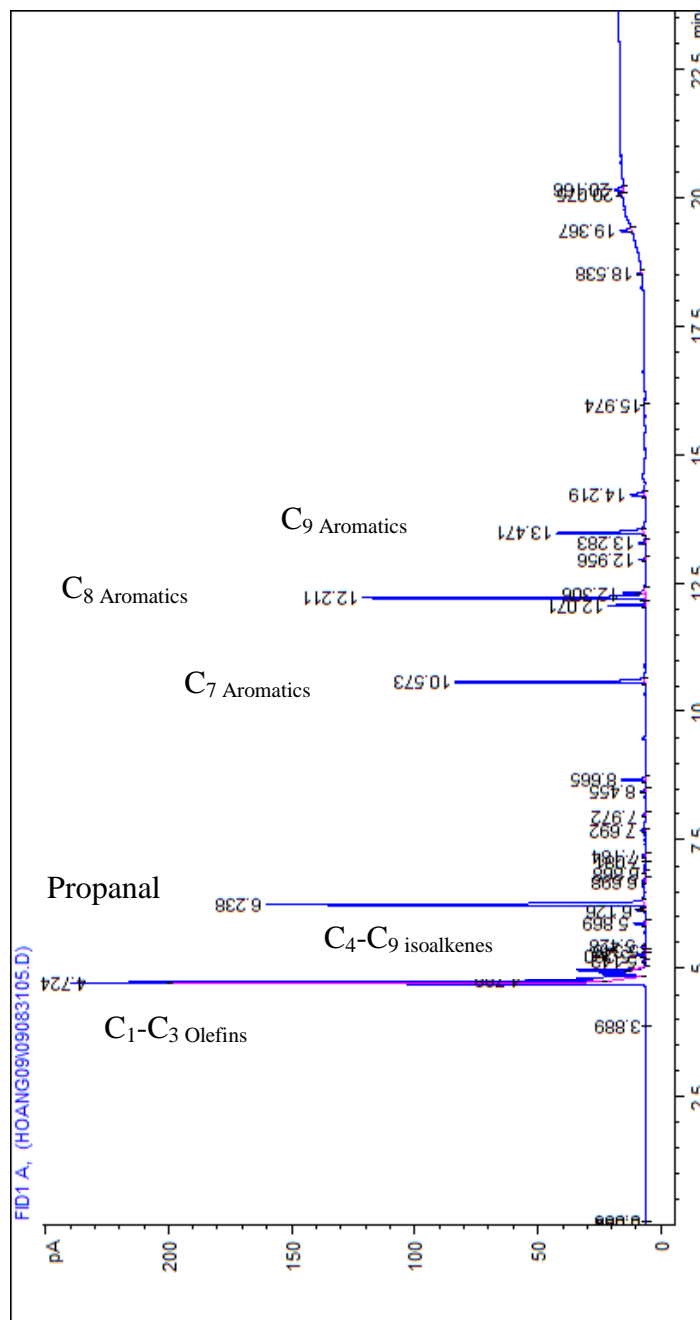
- (76) Biaglow, A. I.; Sepa, J.; Gorte, R. J.; White, D. J Catal 1995, 151, 373.
- (77) Adjaye, J. D.; Bakhshi, N. N. Biomass Bioenerg 1995, 8, 131.
- (78) Adjaye, J. D.; Bakhshi, N. N. Fuel Process Technol 1995, 45, 185.
- (79) Adjaye, J. D.; Bakhshi, N. N. Fuel Process Technol 1995, 45, 161.
- (80) Adjaye, J. D.; Bakhshi, N. N. Biomass Bioenerg 1995, 8, 265.
- (81) Williams, P. T.; Horne, P. A. Renew Energ 1994, 4, 1.
- (82) Parrillo, D. J.; Biaglow, A.; Gorte, R. J.; White, D. Zeolites and Related Microporous Materials: State of the Art 1994 1994, 84, 701.
- (83) Kurshev, V.; Kevan, L.; Parrillo, D. J.; Pereira, C.; Kokotailo, G. T.; Gorte, R. J. J Phys Chem-US 1994, 98, 10160.
- (84) Hutchings, G. J.; Johnston, P.; Lee, D. F.; Warwick, A.; Williams, C. D.; Wilkinson, M. J Catal 1994, 147, 177.
- (85) Dahl, I. M.; Kolboe, S. J Catal 1994, 149, 458.
- (86) Biaglow, A. I.; Parrillo, D. J.; Kokotailo, G. T.; Gorte, R. J. J Catal 1994, 148, 213.
- (87) Biaglow, A. I.; Gorte, R. J.; Kokotailo, G. T.; White, D. J Catal 1994, 148, 779.
- (88) Sun, Y.; Campbell, S. M.; Lunsford, J. H.; Lewis, G. E.; Palke, D.; Tau, L. M. J Catal 1993, 143, 32.
- (89) Parrillo, D. J.; Pereira, C.; Kokotailo, G. T.; Gorte, R. J. J Catal 1992, 138, 377.
- (90) Froment, G. F. In Catalysis; RSC: 1992; Vol. 9, p 1.
- (91) Walsh, D. E.; Han, S.; Palermo, R. E. J Chem Soc Chem Comm 1991, 1259.
- (92) Uguina, M. A.; Sotelo, J. L.; Serrano, D. P. Appl Catal 1991, 76, 183.
- (93) Pereira, C.; Kokotailo, G. T.; Gorte, R. J. J Phys Chem-US 1991, 95, 705.
- (94) Dehertog, W. J. H.; Froment, G. F. Appl Catal 1991, 71, 153.
- (95) Biaglow, A. I.; Adamo, A. T.; Kokotailo, G. T.; Gorte, R. J. J Catal 1991, 131, 252.
- (96) Tabak, S. A.; Bhore, N. A.; Yurchak, S. Abstr Pap Am Chem S 1990, 199, 57.

- (97) Pereira, C.; Kokotailo, G. T.; Gorte, R. J.; Farneth, W. E. *J Phys Chem-US* 1990, 94, 2063.
- (98) Parrillo, D. J.; Adamo, A. T.; Kokotailo, G. T.; Gorte, R. J. *Appl Catal* 1990, 67, 107.
- (99) Grandmaison, J. L.; Chantal, P. D.; Kaliaguine, S. C. *Fuel* 1990, 69, 1058.
- (100) Gorte, R. J.; Kofke, T. J. G.; Kokotailo, G. T. *Acs Sym Ser* 1990, 437, 88.
- (101) Kofke, T. J. G.; Gorte, R. J.; Kokotailo, G. T.; Farneth, W. E. *J Catal* 1989, 115, 265.
- (102) Kofke, T. J. G.; Gorte, R. J.; Kokotailo, G. T. *J Catal* 1989, 116, 252.
- (103) Kofke, T. J. G.; Gorte, R. J.; Kokotailo, G. T. *Appl Catal* 1989, 54, 177.
- (104) Gorte, R. J.; Kofke, T. J. G.; Kokotailo, G. T. *Abstr Pap Am Chem S* 1989, 198, 13.
- (105) Ernst, S.; Weitkamp, J.; Martens, J. A.; Jacobs, P. A. *Appl Catal* 1989, 48, 137.
- (106) Topp-Jørgensen, J. In *Studies in Surface Science and Catalysis*; D.M. Bibby, C. D. C. R. F. H., Yurchak, S., Eds.; Elsevier: 1988; Vol. Volume 36, p 293.
- (107) Meisel, S. L. In *Studies in Surface Science and Catalysis*; Bibby, D. M., Chang, C. D., Howe, R. F., Yurchak, S., Eds.; Elsevier: 1988; Vol. Volume 36, p 17.
- (108) Chen, N. Y. *J Catal* 1988, 114, 17.
- (109) Paparatto, G.; Moretti, E.; Leofanti, G.; Gatti, F. *J Catal* 1987, 105, 227.
- (110) Grandmaison, J. L.; Thibault, J.; Kaliaguine, S.; Chantal, P. D. *Anal Chem* 1987, 59, 2153.
- (111) Dessau, R. M. *J Catal* 1987, 103, 526.
- (112) Renaud, M.; Chantal, P. D.; Kaliaguine, S. *Can J Chem Eng* 1986, 64, 787.
- (113) Ratnasamy, P.; Babu, G. P.; Chandwadkar, A. J.; Kulkarni, S. B. *Zeolites* 1986, 6, 98.
- (114) Kolboe, S. *Acta Chemica Scandinavica Series a-Physical and Inorganic Chemistry* 1986, 40, 711.
- (115) Dessau, R. M. *J Catal* 1986, 99, 111.
- (116) Mole, T.; Anderson, J. R.; Creer, G. *Appl Catal* 1985, 17, 141.

- (117) Ionescu, N. I.; Albu, B.; Iosif, I.; Bozesanu, M.; Musca, G.; Pop, G. *React Kinet Catal L* 1985, 28, 437.
- (118) Grady, M. C.; Gorte, R. J. *The Journal of Physical Chemistry* 1985, 89, 1305.
- (119) Chantal, P. D.; Kaliaguine, S.; Grandmaison, J. L. *Appl Catal* 1985, 18, 133.
- (120) Chu, C. T. W.; Chang, C. D. *J Catal* 1984, 86, 297.
- (121) Chang, C. D.; Chu, C. T. W.; Socha, R. F. *J Catal* 1984, 86, 289.
- (122) Chang, C. D.; Chen, N. Y.; Koenig, L. R.; Walsh, D. E. *Abstr Pap Am Chem S* 1983, 185, 49.
- (123) Young, L. B.; Butter, S. A.; Kaeding, W. W. *J Catal* 1982, 76, 418.
- (124) Haag, W. O.; Lago, R. M.; Rodewald, P. G. *J Mol Catal* 1982, 17, 161.
- (125) Gorte, R. J. *J Catal* 1982, 75, 164.
- (126) Frillette, V. J.; Haag, W. O.; Lago, R. M. *J Catal* 1981, 67, 218.
- (127) Chang, C. D. *J Catal* 1981, 69, 244.
- (128) Rollmann, L. D.; Walsh, D. E. *J Catal* 1979, 56, 139.
- (129) Caesar, P. D.; Morrison, R. A.; Mobil Oil Corporation: U.S. , 1978; Vol. US 4 083 888.
- (130) Rollmann, L. D. *J Catal* 1977, 47, 113.
- (131) Chang, C. D.; Silvestri, A. J. *J Catal* 1977, 47, 249.
- (132) Singh, A. P.; Reddy, K. R. *Zeolites*, 14, 290.

# APPENDIX

## A.1. GC Chromatograph sample at W/F = 0.4 h (Synthesized HZSM-5 Si/Al=45)





A.2. Sample Excel data sheet at W/F = 0.4 h (Synthesized HZSM-5 Si/Al=45)

Data File F:\HOANG09\CRYSTA~1\09083105.D Sample Name: Z5S45-0.4  
 Instrument 1 9/8/2009 12:42:40 PM

H2/Propanal/ 35/0.12  
 HZSM-5-45-S 37 mg,  
 T=400 C, TOS=30 h

```

=====
Injection Date : 8/31/09 10:28:46 PM
Sample Name   : Z5S45-0.4           Location : Vial 1
Acq. Operator : Trung              Inj : 1
                                           Inj Volume : Manually
Acq. Method  : C:\HPCHEM\1\METHODS\OTG_INO.M
Last changed  : 8/31/2009 8:19:41 PM by Trung
                (modified after loading)
Analysis Method : C:\HPCHEM\1\METHODS\TRUNG.M
Last changed  : 8/22/2008 10:45:17 AM
=====
  
```

Area Percent Report

```

=====
Sorted By      : Signal
Multiplier     : 1.0000
Dilution      : 1.0000
Sample Amount  : 1.00000 [ng/ul] (not used in calc.)
=====
  
```

Signal 1: FID1 A,

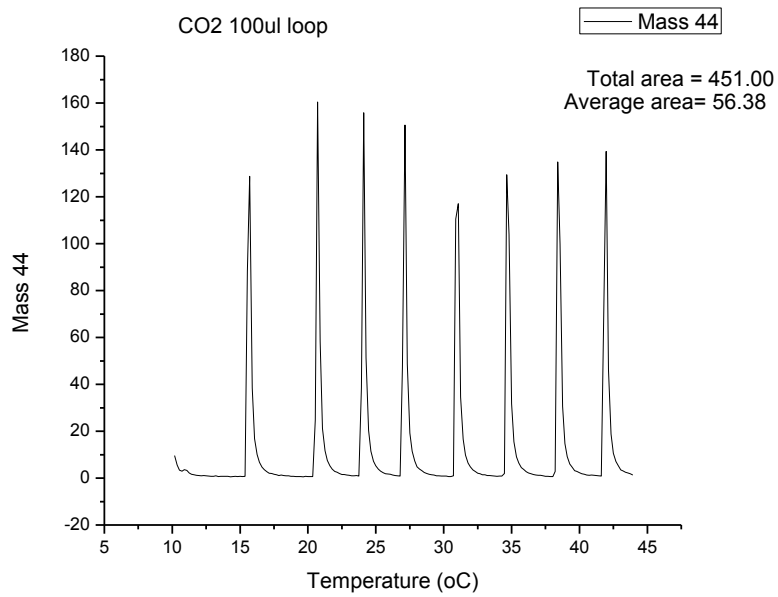
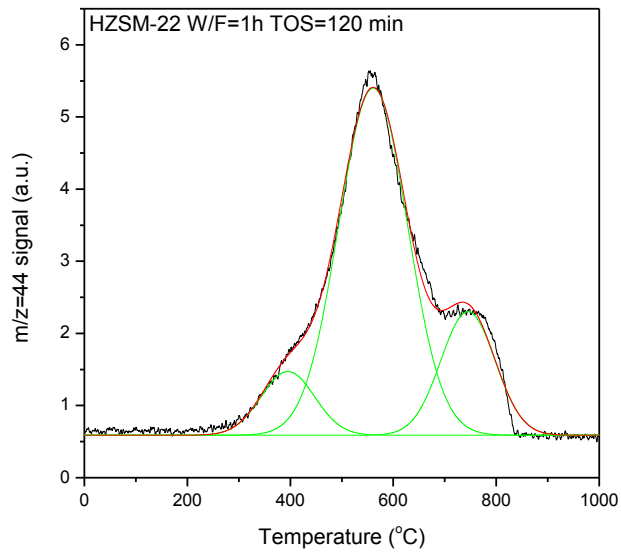
Peak #	RetTime [min]	Type	Width [min]	Area [pA*s]	Height [pA]	Area %
1	4.724	C1-C3	0.0335	543.8693	233.8208	30.33496
2	4.788	isoalkene	0.0482	158.0865	48.84602	8.81746
3	4.912	isoalkene	0.0404	52.72895	18.98212	2.94102
4	4.976	isoalkene	0.0259	52.32749	31.3075	2.91863
5	5.142	isoalkene	0.028	3.05355	1.64632	0.17032
6	5.26	isoalkene	0.0416	11.60736	4.4573	0.64741
7	5.345	isoalkene	0.028	2.15233	1.20714	0.12005

8	5.428	isoalkene	0.0409	5.88037	1.98986	0.32798
9	5.869	isoalkene	0.0311	10.11734	5.10286	0.56431
10	6.152	isoalkene	0.0483	14.77268	4.11512	0.82396
11	6.238	<i>Propanal</i>	0.0342	333.5222	153.3092	18.6026
12	6.698	isoalkene	0.0342	3.57367	1.64094	0.19933
13	7.184	isoalkene	0.0354	4.36171	1.96908	0.24328
14	7.692	isoalkene	0.0308	4.35184	2.22963	0.24273
15	7.973	isoalkene	0.0375	4.04025	1.64478	0.22535
16	8.455	isoalkene	0.0332	4.33274	1.94314	0.24166
17	8.67E+00	Benzene	3.42E-02	2.19E+01	1.00E+01	1.22177
18	1.06E+01	Toluene	2.96E-02	1.54E+02	7.72E+01	8.57764
19	12.071	Ethylbenzen	2.84E-02	2.75E+01	1.51E+01	1.53129
20	12.211	<i>p-Xylene</i>	2.91E-02	2.15E+02	1.15E+02	12.00333
21	12.306	m-Xylene	0.0318	19.25968	8.85587	1.07423
22	12.956	o-Xylene	0.0302	5.70307	2.88685	0.3181
23	13.283	C9 aromatics	0.0325	6.93448	3.19448	0.38678
24	13.471	C9 aromatics	0.0367	91.18578	36.11563	5.086
25	14.218	C9 aromatics	0.0404	17.36874	6.24691	0.96876
26	19.367	C10+	0.0345	11.62273	5.12329	0.64827
27	20.075	C10+	0.0311	4.11E+00	2.00E+00	0.22947
28	20.166	C10+	0.0417	9.56165	3.31059	0.53331
Totals				1792.879	799.0594	

=====  
 \*\*\* End of Report \*\*\*

nonArHC(C4- C8)	47.6661	GAS	30.33496
ArHC(C6- C10+)	33.7313	ISOALKENES	17.33114
Benzene	1.22177	AROMATICS	33.7313
Toluene	8.57764	BENZENE	1.22177
Ethyl- benzene	1.53129	TOLUENE	8.57764
<b>p-Xylene</b>	<b>12.00333</b>	<b>C8</b>	<b>14.92695</b>
m-Xylene	1.07423	C9	6.44154
<b>o-Xylene</b>	<b>0.3181</b>	<b>C10+</b>	<b>1.41105</b>
C9	5.47278	CONV	81.3974
Mesitylene	0.96876		
C10+	1.41105		
<b>CONV</b>	<b>81.3974</b>		

### A.3. Sample TPO HZSM-22



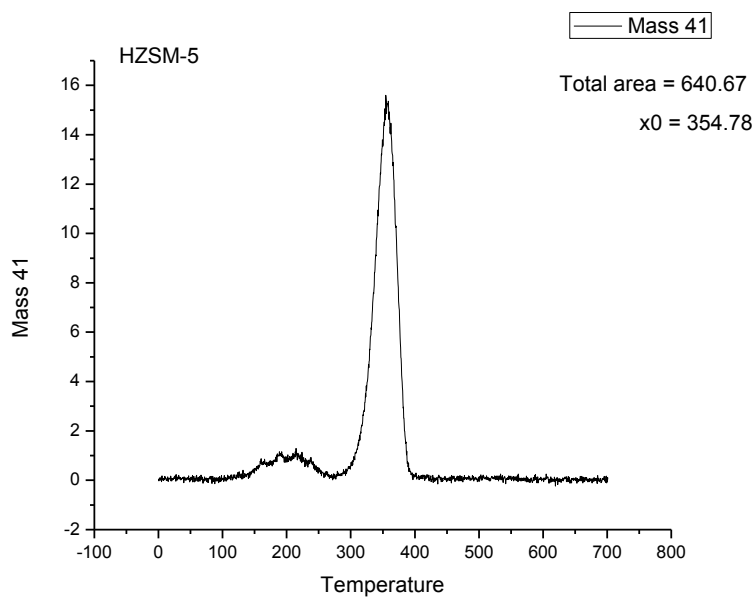
**CALCULATION TPO HZSM-22** w/f=1h  
 tos=120min

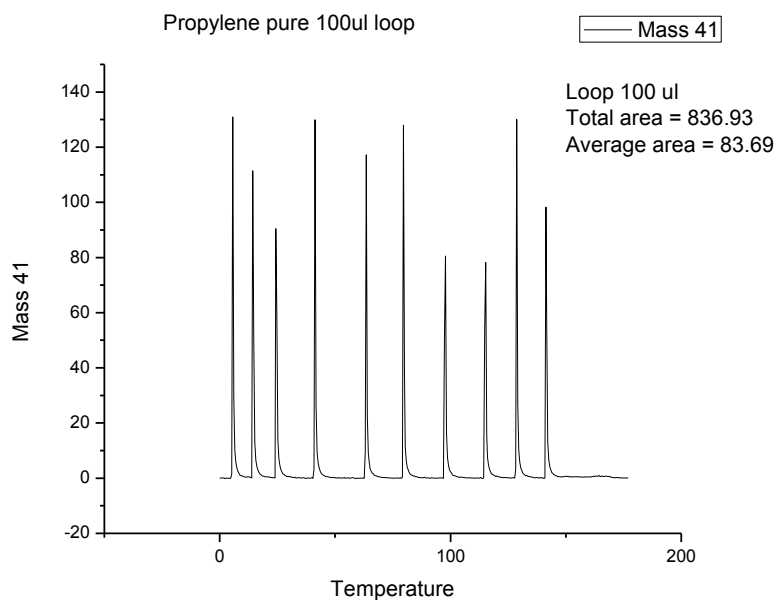
CATALYST	0.05	g
LOOP	100	ul
Propylene	0.00446	mmol
	56.38	area m/e 44

P V = n R T	
Pressure	1 atm
Gas constant	82.06 cc*atm/(mol*K)
Temperature	273 K
<b>Total product (sccm)</b>	<b>0.1</b>
<b>mmol</b>	<b>0.00446</b>

T(oC)	Acid Site	Area	mmol	umol	umol/g	g/g	%C
395		115	0.0091	9.1	<b>181.5769</b>	0.002179	<b>0.22</b>
560		805.81	0.0638	63.8	<b>1275.979</b>	0.015312	<b>1.53</b>
745		226	0.0179	17.9	<b>357.1683</b>	0.004286	<b>0.43</b>
TOTAL		1146	0.0907	90.74	1814.72	0.021777	<b>2.18</b>

#### A.4. Sample TPD IPA HZSM-22





#### CALCULATION ACID DENSITY FROM PROPYLENE

CATALYST	0.1	G
LOOP	100	UL
PROPYLENE	0.00446	MMOL
	83.69	AREA m/z 41

T(°C)	ACID SITE	AREA	MMOL	UMOL	UMOL/G
ZSM-5	BRONSTED	640	0.0341	34.1	<b>341.3597</b>

$$P V = N R T$$

PRESSURE	1	ATM
GAS		
CONSTANT	82.06	CC*ATM/(MOL*K)
TEMPERATURE	273	K

**TOTAL PRODUCT  
(SCCM)**

	<b>0.1</b>
<b>MMOL</b>	<b>0.00446</b>

## A.5. Example GCMS identification of products from glycerol

### *Oxygenate compound*

**Name**

Propanal

2-Propenal

Octane, 2-methyl-

Tetrahydrofuran, 2,2-dimethyl-

Ethanol

1,3-Dioxolane, 2-ethyl-2-methyl-

Benzene

Furan, 2,5-dimethyl-

2,3-Butanedione

1,3-Dioxane, 2-methyl-

2-Propen-1-ol

Propanal, 3-methoxy-

DL-Methyltartronic acid

2-Butanone, 3-hydroxy-

Acetol

2-Cyclopenten-1-one

Diaceone alcohol

2-Cyclopenten-1-one, 2-methyl-

1-Hydroxy-2-butanone

2-Hexanone,4-hydroxy-5-methyl-3-propyl-

CH<sub>3</sub>CH(OH)CH<sub>2</sub>C(O)CH<sub>3</sub>

Acetic acid

Ethanol, 2-(ethenyloxy)-

Pentadecane

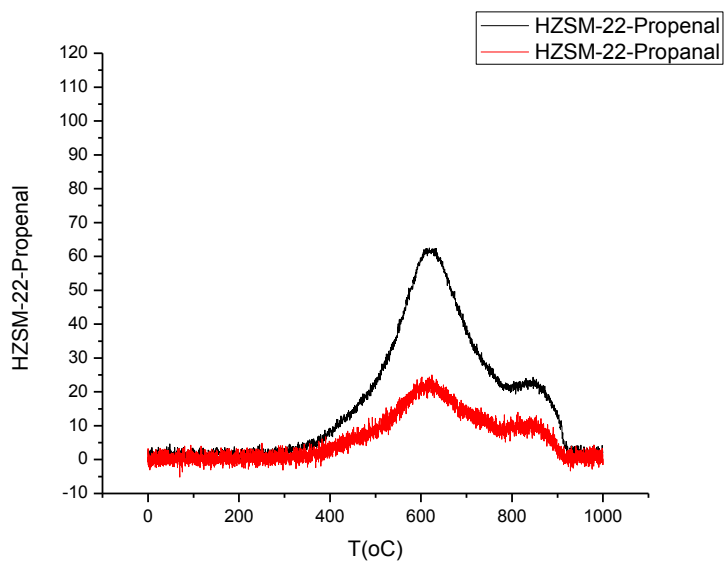
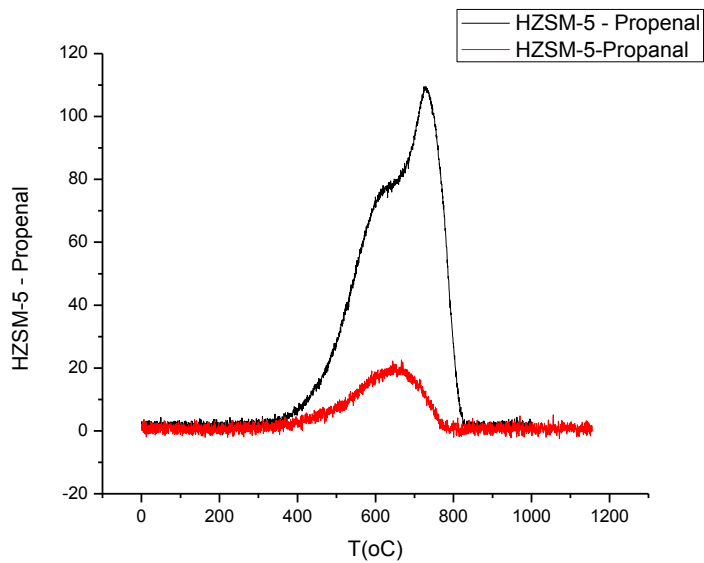
2-Cyclopenten-1-one, 3-methyl-  
Propanoic acid  
1,3-Dioxolane-4-methanol, 2-ethyl-

### *Aromatic compounds*

#### **Name**

Benzene  
Toluene  
Ethylbenzene  
Benzene, 1,3-dimethyl-  
Benzene, propyl-  
Benzene, 1-ethyl-2-methyl-  
Benzene, 1-ethyl-3-methyl-  
Benzene, 1,3,5-trimethyl-  
Styrene  
Benzene, 1-ethyl-2-methyl-  
Benzene, 1,2,3-trimethyl-  
Benzene, 1,2-diethyl-  
Benzene, 1-ethyl-3-methyl-  
Benzene, 1-ethenyl-3-methyl-  
Indane  
1H-Indene, 2,3-dihydro-2-methyl-  
Indan, 1-methyl-  
Benzene, 1-propenyl-  
Benzene, 1,2,4,5-tetramethyl-  
Benzene, 1,2,4,5-tetramethyl-  
1H-Indene, 2,3-dihydro-4-methyl-  
Indene

### A.6. TPO of Propenal and Propanal on HZSM-5 & HZSM-22

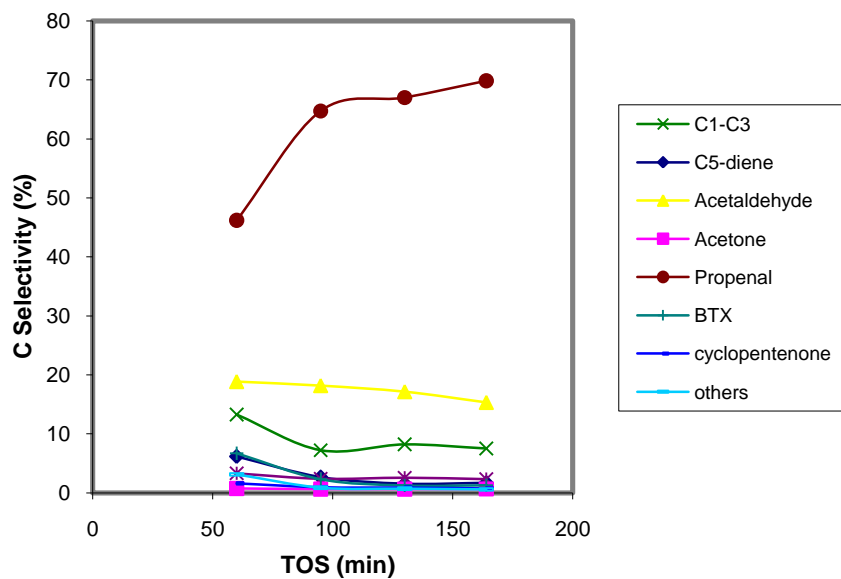




### A.7. Conversion of glycerol on HZSM-22 at higher temperature

	<b>60</b>	<b>95</b>	<b>130</b>	<b>164</b>
C1-C3	13.26	7.23	8.22	7.53
isoalkene	6.16	2.66	1.54	1.68
Acetaldehyde	18.87	18.19	17.16	15.34
Propanal	3.32	2.38	2.57	2.32
Acetone	0.73	0.65	0.65	0.66
Propenal	46.19	64.72	66.99	69.83
BTX	6.71	2.33	1.27	1.30
cyclopentenone	1.61	0.96	0.89	0.75
others	3.15	0.88	0.72	0.60
Total	100	100	100	100

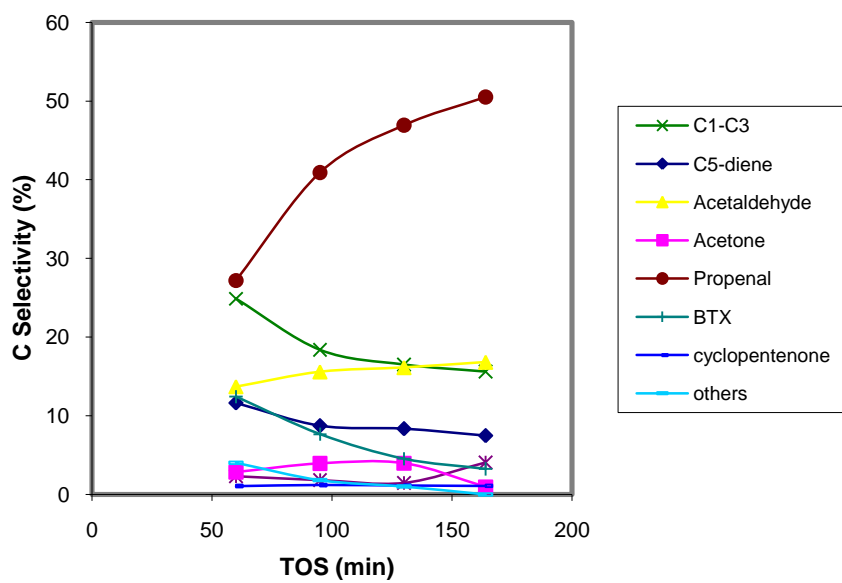
**TOS Glycerol/HZSM22/450°C/WF=2hr**



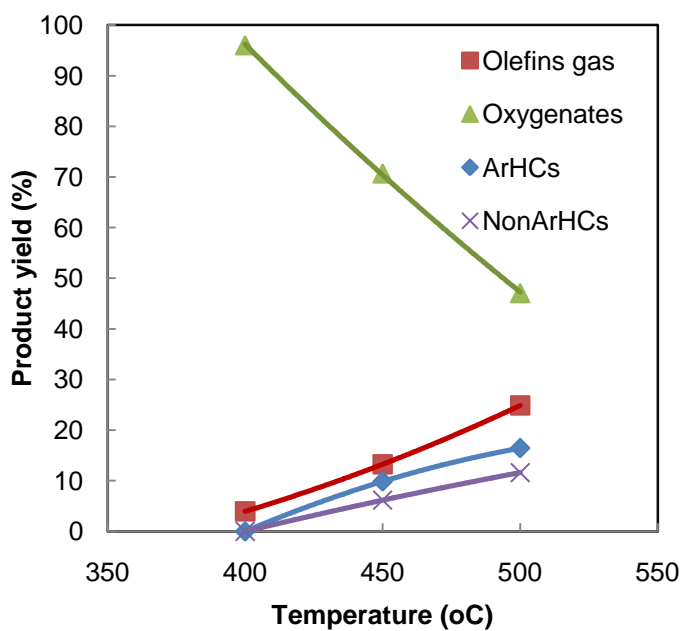
Conversion of glycerol on HZSM-22 at 500 °C

	<b>60</b>	<b>95</b>	<b>130</b>	<b>164</b>
C1-C3	24.87	18.37	16.51	15.61
isoalkene	11.62	8.73	8.35	7.47
Acetaldehyde	13.71	15.59	16.13	16.81
Propanal	2.30	1.81	1.46	4.04
Acetone	2.82	3.93	3.95	0.95
Propenal	27.19	40.92	46.94	50.51
BTX	12.42	7.65	4.53	3.24
cyclopentenone	1.07	1.19	1.13	1.09
others	4.01	1.81	1.00	0.00
Total	100	100	100	100

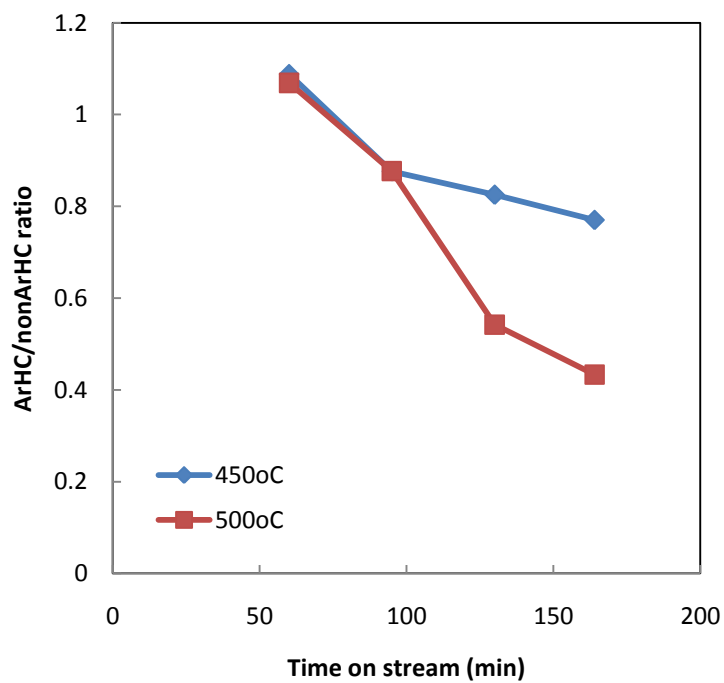
TOS Glycerol/HZSM22/500°C/WF=2hr



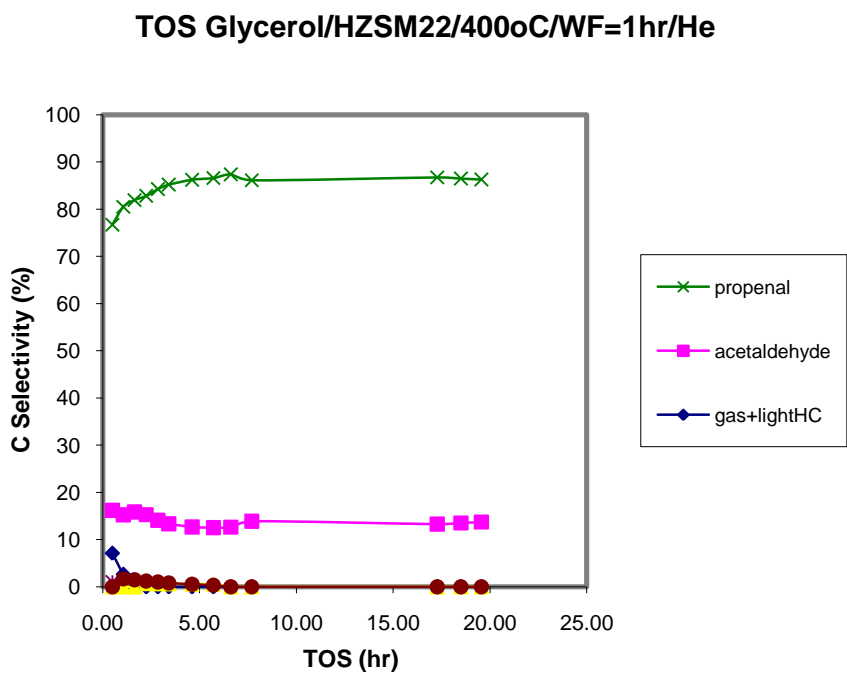
**Product yield v.s. Temperature**  
GLY Conv. HZSM-22 at W/F=2hr



**ArHC/nonArHC with TOS**

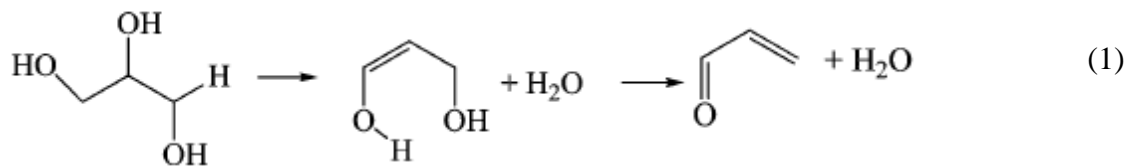


A.8. Conversion of glycerol on HZSM-22 at longer TOS (stability test)

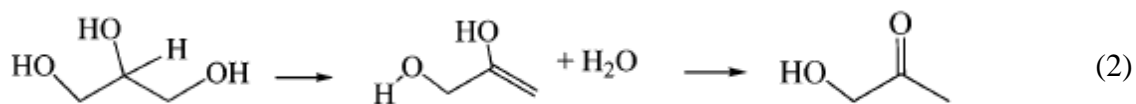


A.9. Mechanism of oxygenates formation in glycerol dehydration

a. Production of acrolein (propenal)



b. Production of acetol (acetone alcohol)



c. Production of formaldehyde and acetaldehyde

